

Cite this: *Mater. Chem. Front.*, 2020, 4, 46

## Assembling features of calixarene-based amphiphiles and supra-amphiphiles

Han-Wen Tian, Yan-Cen Liu and Dong-Sheng Guo \*

Macrocyclic amphiphiles as an emerging family of artificial amphiphiles have gained considerable attention in recent years on account of their fascinating recognition and assembly properties. Benefiting from a preorganized framework, facile modification and host–guest recognition ability, calixarenes have been widely used to fabricate self-assemblies of both amphiphiles and supra-amphiphiles. In this review, we organized hundreds of reported amphiphilic calixarenes based on their structures and systematically summarized assembling features of calixarene-based amphiphiles and supra-amphiphiles. For amphiphilic calixarenes, the size and conformation of skeletons significantly affect their assembly behaviors, such as lower critical aggregation concentration (CAC) and more diverse morphology than conventional amphiphiles. Besides, we also focus on emerging topics like uniformity, compactness, and kinetic properties of calixarene aggregation. For supra-amphiphiles, the binding affinities of calixarenes endow them with the ability to induce guest assembly. In addition, complexation of guests also improves amphiphilic calixarene aggregation. The obtained assemblies not only possess the advantages of low CAC and compact packing, but also respond to various stimuli. Finally, we pointed out several research topics of calixarene-based amphiphiles and supra-amphiphiles to be further developed in the future, such as the relationship between molecular structures and assembly properties, crosslinking, co-assembly, and utilization of cavities. We hope this review could be a guidance for studying amphiphilic assemblies based on calixarenes and other macrocyclic compounds.

Received 29th July 2019,  
Accepted 27th September 2019

DOI: 10.1039/c9qm00489k

rsc.li/frontiers-materials

### 1. Introduction

Amphiphiles are molecules that contain both a hydrophobic component and a hydrophilic component connected by covalent bonds.<sup>1</sup> Inspired by nature, synthetic amphiphilic molecules

enrich the concept of amphiphiles. Based on the number and properties of polar head(s)/hydrophobic tail(s) as well as their manner of connection, amphiphiles are classified as conventional amphiphiles (single head/single tail), bolaamphiphiles, gemini amphiphiles, double and triple chain amphiphiles, catanionic amphiphiles, amphiphilic polymers, *etc.*<sup>2</sup> Owing to their unique structures, amphiphiles can assemble into aggregates such as micelles, vesicles, lyotropic liquid crystals, 2D monolayers and 3D multilayers,<sup>1</sup> resulting in important

College of Chemistry, Key Laboratory of Functional Polymer Materials (Ministry of Education), State Key Laboratory of Elemento-Organic Chemistry, Nankai University, Tianjin 300071, China. E-mail: dshguo@nankai.edu.cn



Han-Wen Tian

Han-Wen Tian obtained his BS degree from Nankai University in 2016. Then he received his MSc degree in 2019 from Nankai University under the guidance of Prof. Dong-Sheng Guo. Currently he is a PhD candidate at Nankai University. His research interest includes the design and synthesis of calixarene-based amphiphiles and recognition and assembly properties of macrocyclic amphiphiles.



Yan-Cen Liu

Yan-Cen Liu obtained her BS and BEng degree from Nankai University and Tianjin University respectively in 2013. She received her MSc degree in 2016 from Nankai University under the guidance of Prof. Dong-Sheng Guo. Currently she is a PhD candidate at Jacobs University Bremen, Germany. Her research interest includes calixarene and cucurbituril based supramolecular chemistry.

biological functions and various applications in our daily life and industry.<sup>3</sup>

As an emerging family of artificial amphiphiles, macrocyclic amphiphiles have gained considerable attention in recent years on account of their fascinating recognition and assembly properties.<sup>3,4</sup> Just as their name implies, macrocyclic amphiphiles are obtained by introducing hydrophilic groups and lipophilic groups to the preorganized scaffold. They incorporate both bola-type and gemini-type amphiphiles into a single molecule from the viewpoint of structural characteristics. Besides, the unique advantage of macrocyclic amphiphiles is the host-guest recognition. Macrocyclic amphiphiles are deemed as “surfactants with host-guest recognition sites”,<sup>5</sup> whose macrocyclic binding sites are distributed on the surface of the amphiphilic assembly. Up to now, cyclodextrin,<sup>6</sup> calixarene<sup>7</sup> and pillararene<sup>8,9</sup> have been the commonly used compounds to construct macrocyclic amphiphiles.

On the other hand, by combining supramolecular chemistry and amphiphiles, supra-amphiphiles have attracted widespread attention of scientists.<sup>10</sup> In contrast to amphiphiles based on covalent bonds, supra-amphiphiles refer to amphiphiles constructed on the basis of noncovalent interactions or dynamic covalent bonds, which are very useful in the fabrication of nanomaterials with a high degree of structural complexity. Functional groups can be attached to supra-amphiphiles by employing various noncovalent interactions, greatly avoiding tedious covalent syntheses. Moreover, the dynamic and reversible nature of noncovalent interactions endows the resultant supramolecular architectures with excellent stimuli-responsive features. Due to their unique advantages, supra-amphiphiles are being widely and actively investigated in materials and biomedical sciences nowadays.<sup>11,12</sup>

Calixarenes are the third generation of macrocyclic compounds composed of phenolic units linked by methylene groups at the *o*-positions of phenolic hydroxyl groups. Their history dates back to the late nineteenth century, but they did not receive wide attention for a long time until Gutsche and coworkers studied calixarenes as mimic enzymes.<sup>13</sup> Calixarenes have several sites for derivation and their sizes can be adjusted.

Moreover, chemical modification, especially with water soluble groups, could significantly enhance their binding affinity. Benefiting from these properties, calixarenes have been described as macrocycles which have “(almost) unlimited possibilities”<sup>14</sup> and have been widely used to fabricate amphiphiles and supra-amphiphiles. There have been a couple of reviews about calixarene-based amphiphiles and supra-amphiphiles. In 2010, Helttunen and Shahgaldian summarized self-assembly of amphiphilic calixarenes and resorcinarenes in water, and classified aggregates by their morphology.<sup>15</sup> Later, Garcia-Rio and coworkers published a review which focuses on a promising series of calixarene, *p*-sulfonatocalixarene,<sup>16</sup> while Klymchenko and coworkers focused on amphiphilic calixarenes as gene delivery vehicles.<sup>17</sup> Recently, Guo and coworkers discussed assembly behaviors of calixarene-based amphiphiles and supra-amphiphiles, and focused on their applications in drug delivery and protein recognition.<sup>18</sup> Up to now, calixarene-based amphiphiles and supra-amphiphiles have been widely used in many fields such as sensing,<sup>19</sup> adsorption and extraction,<sup>20,21</sup> catalysis,<sup>22</sup> inorganic-organic hybrid materials,<sup>23</sup> preparation of chiral materials<sup>24</sup> and photoluminescent materials,<sup>25</sup> and biomedical applications.<sup>18,26–35</sup>

In this review, we will summarize calixarene-based amphiphiles and supra-amphiphiles reported up to now and focus our special attention on their assembling features in aqueous solution. The structure of this review will be such that we first summarize and comprehensively list chemical structures of amphiphilic calixarenes, including upper-rim hydrophilic amphiphiles, lower-rim hydrophilic amphiphiles and bola-type amphiphiles, followed by their assembling features. Next we summarize the self-assemblies of calixarene-based supra-amphiphiles and their assembling features, focusing on complexation-induced aggregation (guest-induced aggregation of host, host-induced aggregation of guest, and mutual inducement).

## 2. Calixarene-based amphiphiles

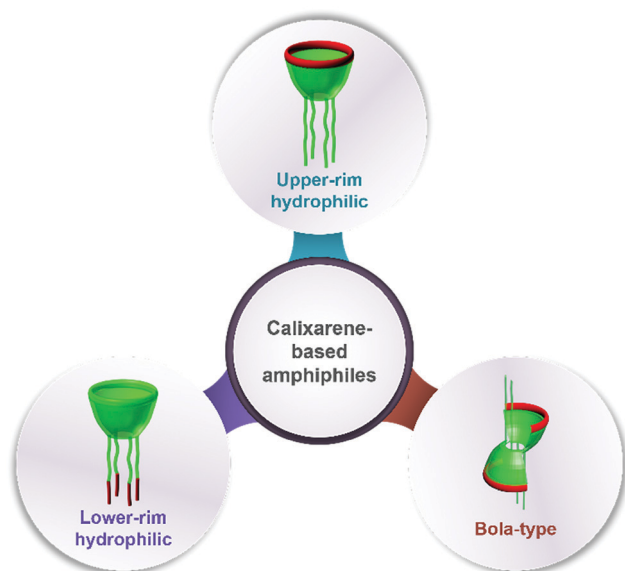
### 2.1 Fabricating amphiphilic calixarenes by covalent modification

Calixarenes possess several sites which are easily modified, such as an upper rim, lower rim, and methylene bridge. As a result, more than four hundred amphiphilic calixarenes were obtained by simply modifying hydrophilic or hydrophobic groups on scaffolds. Most works focused on amphiphilic calixarenes in the cone conformation,<sup>36</sup> in which hydrophilic and hydrophobic groups are decorated on opposite rims, resulting in upper-rim hydrophilic amphiphiles and lower-rim hydrophilic amphiphiles (Scheme 1). Moreover, the adjustable conformation of calixarenes makes it easy to modify them on the basis of an alternate conformation, or stabilize the alternate conformation after modification. The obtained compounds are bola-type amphiphiles. We comprehensively list these three classes of amphiphilic calixarenes reported up to now in Schemes 2–4 and Tables 1–3 in order to facilitate readers for following this field and further studies.



**Dong-Sheng Guo**

*Dong-Sheng Guo obtained his PhD degree from Nankai University under the guidance of Prof. Yu Liu in 2006. Then he joined Prof. Liu's group as a faculty member at the College of Chemistry, Nankai University. He was promoted as an Associate Professor in 2008, and a full Professor in 2013. Since 2014, he has begun to work independently. The current research interest of his group is in supramolecular biomedical materials based on calixarenes.*



Scheme 1 Schematic illustration of various types of calixarene-based amphiphiles.

As we can see from the schemes, most amphiphilic calixarenes are based on calix[4]arene. Calix[5]arene, calix[6]arene, calix[8]arene, calix[9]arene, and thiacalix[4]arene are also involved. For upper-rim hydrophilic amphiphiles, almost all the common substitutions which are possible for phenols have been carried out at the upper rim. For example, a sulfonate group is widely introduced because of its excellent water-solubility and convenient one-step reaction. A nitro group and a halogen (or benzyl halide) group were also attached to the upper-rim by a one-step reaction. Further derivatization from them results in numerous functional groups such as the phosphate group, guanidinium group, carboxylic group, amino group, azide group and so on. It is noteworthy that carboxylic group and amino group could involve in amide condensation, and the azide group could react with an alkynyl compound. These well-established reactions provide the possibility of decorating calixarene with almost everything, such as cyclodextrin, PEG, saccharide, and cholesterol. On the other hand, the hydrophobic moieties of most upper-rim hydrophilic amphiphiles were introduced by alkyl halides reacting with phenolic hydroxyl at the lower rim. Meanwhile, similar nucleophilic substitution has been applied for PEG chains, resulting in lower-rim hydrophilic amphiphiles. The upper-rim attached hydrophobic chain of most lower-rim hydrophilic amphiphiles were introduced at the cyclic formation step, *i.e.*, using *p*-alkylphenol as a reactant. Among them, the most popular *p*-alkylphenol is *p*-*tert*-butylphenol. In addition, the alkyl chain can be connected to the methylene, being introduced at the cyclic formation step as well. For bola-type amphiphiles, their conformations were usually controlled by template metal ions, for example, calix[4]arene tends to form alternative conformers in the presence of cesium carbonate. Since all these factors (skeleton, hydrophobic chain length, hydrophilic group, and conformation) affect the hydrophilic–hydrophobic balance,

amphiphilic calixarenes with various assembly properties have been obtained by taking advantage of convenient synthesis.

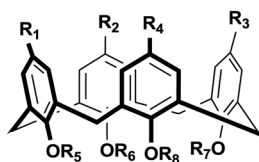
## 2.2 Assembling features of amphiphilic calixarenes

### 2.2.1 Low critical aggregation concentration (CAC).

When we study the assembly behavior of a specific amphiphile, CAC is a widely used parameter indicating self-assembling ability of amphiphiles. CAC is the concentration at which an amphiphile starts aggregating. Electrical conductivity, surface tension, light scattering and fluorescence intensity are the most commonly used parameters to determine the CAC value. Plots which show the dependence of measured physical properties on concentration of amphiphiles usually show a change of slope around CAC. CAC also relates to temperature and solvent. Under the same conditions, it is generally acknowledged that lower CAC represents stronger assembling ability, because lower CAC means lower monomer concentration in equilibrium between the monomer and assembly.<sup>3</sup>

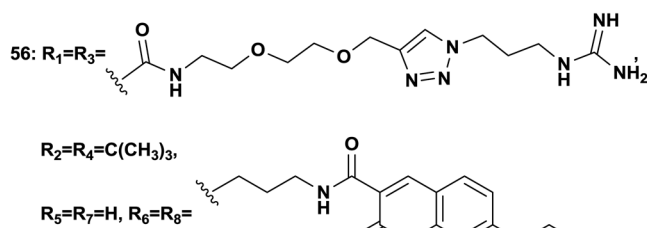
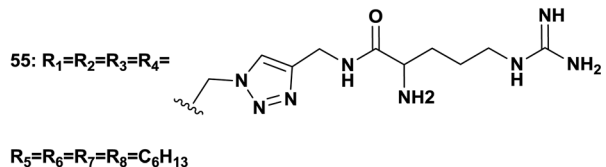
Reported CAC values of amphiphilic calixarenes are summarized in Table 4. It is easy to notice that a large proportion of amphiphilic calixarenes have quite low CACs (<1 mM) compared with common surfactants. For example, the CACs of sodium butyl benzene sulfonate, sodium hexyl benzene sulfonate, sodium octyl benzene sulfonate, and sodium dodecyl benzene sulfonate (SDBS) are 100 mM, 30 mM, 14 mM, and 1.5 mM, respectively. The CACs of the corresponding amphiphilic calix[4]arenes **3**, **6**, **8**, and **9** are 3.2 mM, 0.488 mM, 0.085 mM, and 0.02 mM, respectively. As a reference compound, the CAC of the gemini-type SDBS derivate is 0.9 mM. If we consider generalized monomer concentration, the CAC of the gemini-type SDBS derivate is 1.8 mM monomer, which is similar to SDBS, while the CAC of calix[4]arene **9** is 0.08 mM monomer, which is 19 times lower than that of SDBS. The lower CAC of calixarene undoubtedly originates from the cyclic oligomeric structure. From the viewpoint of entropy, amphiphiles in the assemblies have a lower degree of freedom than that in bulky water, so the entropy of amphiphiles (not including water molecules) decreases during the assembly process. The oligomer structure of calixarene leads to much lower entropy loss than the corresponding monomer, resulting in lower CAC as well as a more sensitive response to the structural difference.<sup>279</sup>

For example, CACs decrease more rapidly with longer alkyl chains of amphiphilic sulfonatocalix[*n*]arenes (SC*n*As) than that of sodium benzene sulfonate surfactants, as Basilio and co-workers proposed. They systematically investigated the relationship between CACs and the hydrophobic chain length of amphiphilic SC*n*As **3**, **6**, and **8** from the viewpoint of thermodynamics by ITC in detail, and obtained their free energy of micellization ( $\Delta G_M^\circ$ ).<sup>53,54</sup> They proposed that the  $\Delta G_M^\circ$  is the sum of contributions of each part of the molecule to the total free energy, such as ionic groups and counterions, aromatic rings, oxygen atoms that connect the aromatic rings to the alkyl chains, methylene group of the bridges, methylene groups of the alkyl chains, and terminal methyl groups of the chains. Among these, the free energy of transferring a methyl group from water to the micellar interior ( $\Delta G_M^\circ(\text{CH}_3)$ ) is equal to that

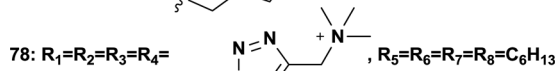
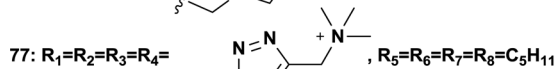
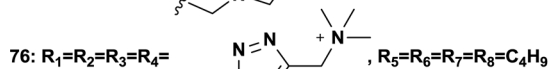
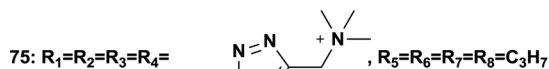
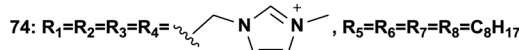
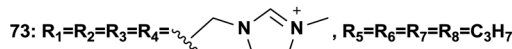


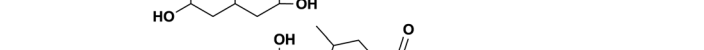
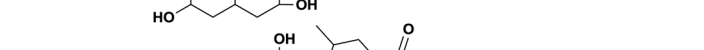
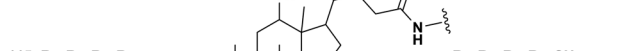
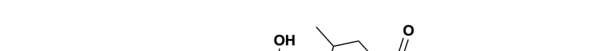
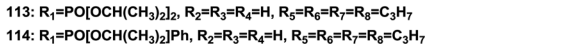
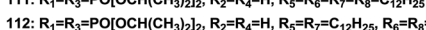
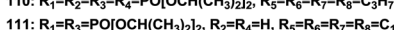
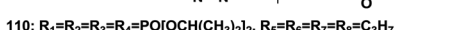
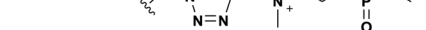
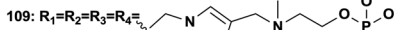
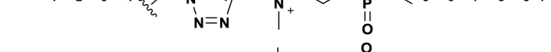
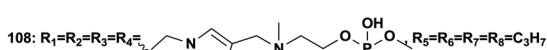
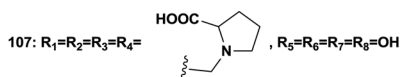
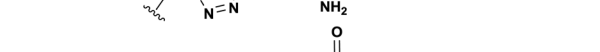
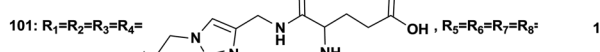
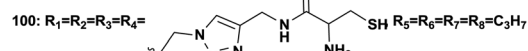
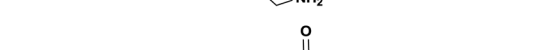
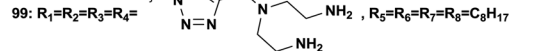
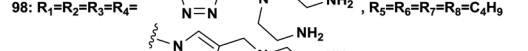
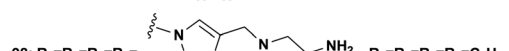
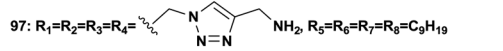
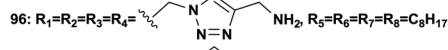
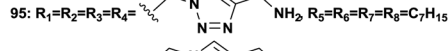
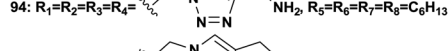
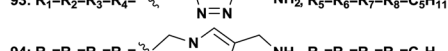
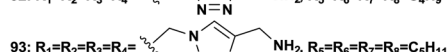
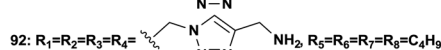
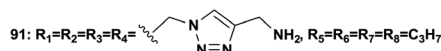
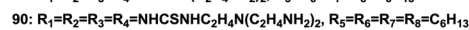
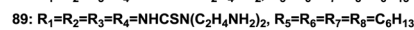
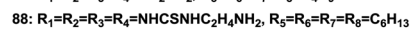
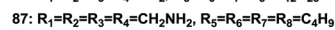
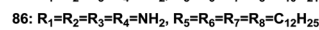
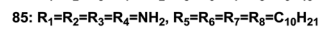
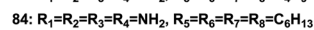
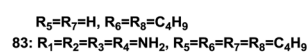
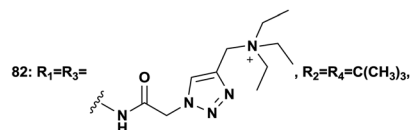
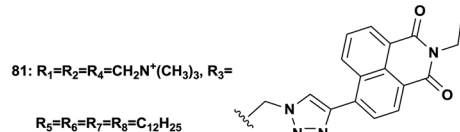
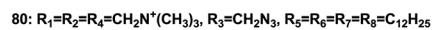
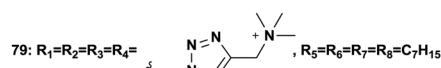
- 1:  $R_1=R_2=R_3=R_4=SO_3^-$ ,  $R_5=R_6=R_7=R_8=C_3H_7$   
 2:  $R_1=R_2=R_3=R_4=SO_3^-$ ,  $R_5=R_6=R_7=R_8=-CH_2-CH=CH_2$   
 3:  $R_1=R_2=R_3=R_4=SO_3^-$ ,  $R_5=R_6=R_7=R_8=C_4H_9$   
 4:  $R_1=R_2=R_3=R_4=SO_3^-$ ,  $R_5=R_6=R_7=R_8=C_5H_{11}$   
 5:  $R_1=R_2=R_3=R_4=SO_3^-$ ,  $R_5=R_6=R_7=R_8=CH_2CH(CH_3)C_2H_5$   
 6:  $R_1=R_2=R_3=R_4=SO_3^-$ ,  $R_5=R_6=R_7=R_8=C_6H_{13}$   
 7:  $R_1=R_2=R_3=R_4=SO_3^-$ ,  $R_5=R_6=R_7=R_8=C_7H_{15}$   
 8:  $R_1=R_2=R_3=R_4=SO_3^-$ ,  $R_5=R_6=R_7=R_8=C_8H_{17}$   
 9:  $R_1=R_2=R_3=R_4=SO_3^-$ ,  $R_5=R_6=R_7=R_8=C_{12}H_{25}$   
 10:  $R_1=R_2=R_3=R_4=PO_3H_2$ ,  $R_5=R_6=R_7=R_8=C_6H_{13}$   
 11:  $R_1=R_2=R_3=R_4=PO_3H_2$ ,  $R_5=R_6=R_7=R_8=C_8H_{17}$   
 12:  $R_1=R_2=R_3=R_4=PO_3H_2$ ,  $R_5=R_6=R_7=R_8=C_{10}H_{21}$   
 13:  $R_1=R_2=R_3=R_4=PO_3H_2$ ,  $R_5=R_6=R_7=R_8=C_{12}H_{25}$   
 14:  $R_1=R_2=R_3=R_4=PO_3H_2$ ,  $R_5=R_6=R_7=R_8=C_{14}H_{29}$   
 15:  $R_1=R_2=R_3=R_4=PO_3H_2$ ,  $R_5=R_6=R_7=R_8=C_{18}H_{37}$   
 16:  $R_1=R_2=R_3=R_4=CH_2PO_3H_2$ ,  $R_5=R_6=R_7=R_8=C_6H_{13}$   
 17:  $R_1=R_2=R_3=R_4=CH_2PO_3H_2$ ,  $R_5=R_6=R_7=R_8=C_8H_{17}$   
 18:  $R_1=R_2=R_3=R_4=CH_2PO_3H_2$ ,  $R_5=R_6=R_7=R_8=C_{12}H_{25}$   
 19:  $R_1=R_2=R_3=R_4=PO(OH)(OC_2H_5)$ ,  $R_5=R_6=R_7=R_8=C_4H_9$   
 20:  $R_1=R_2=R_3=CH_2PO_3H_2$ ,  $R_4=CH_2-N=N=N$ ,  $R_5=R_6=R_7=R_8=C_6H_{13}$   
 21:  $R_1=R_2=R_3=R_4=COOH$ ,  $R_5=R_6=R_7=R_8=C_3H_7$   
 22:  $R_1=R_2=R_3=R_4=COOH$ ,  $R_5=R_6=R_7=R_8=C_6H_{13}$   
 23:  $R_1=R_2=R_3=R_4=COOH$ ,  $R_5=R_6=R_7=R_8=C_8H_{17}$   
 24:  $R_1=R_2=R_3=R_4=COOH$ ,  $R_5=R_6=R_7=R_8=C_{12}H_{25}$   
 25:  $R_1=R_2=R_3=R_4=CH_2NHCH(CH_3)COOH$ ,  $R_5=R_6=R_7=R_8=C_{10}H_{21}$   
 26:  $R_1=R_2=R_3=R_4=NHCOC_2H_4COOH$ ,  $R_5=R_6=R_7=R_8=C_3H_7$   
 27:  $R_1=R_2=R_3=R_4=NHCOC_2H_4COOH$ ,  $R_5=R_6=R_7=R_8=C_4H_9$   
 28:  $R_1=R_2=R_3=R_4=NHCOC_2H_4COOH$ ,  $R_5=R_6=R_7=R_8=C_5H_{11}$   
 29:  $R_1=R_2=R_3=R_4=NHCOC_2H_4COOH$ ,  $R_5=R_6=R_7=R_8=C_{12}H_{25}$   
 30:  $R_1=R_2=R_3=R_4=NHCOC_3H_6COOH$ ,  $R_5=R_6=R_7=R_8=C_3H_7$   
 31:  $R_1=R_2=R_3=R_4=COOH$ ,  $R_5=R_7=C_3H_7Ph$ ,  $R_6=R_8=C_3H_7$   
 32:  $R_1=R_2=R_3=COOH$ ,  $R_4=R_5=R_7=H$ ,  $R_6=R_8=CH(CH_3)_2$   
 33:  $R_1=R_2=R_3=COOH$ ,  $R_4=R_5=R_7=H$ ,  $R_6=R_8=C_3H_7$   
 34:  $R_1=R_2=R_3=CH_2COOH$ ,  $R_4=R_5=R_6=R_7=H$ ,  $R_8=CH_3$   
 35:  $R_1=R_2=R_3=CH_2COOH$ ,  $R_4=R_5=R_6=R_7=H$ ,  $R_8=C_2H_5$   
 36:  $R_1=R_2=R_3=CH_2COOH$ ,  $R_4=R_5=R_6=R_7=H$ ,  $R_8=C_3H_7$   
 37:  $R_1=R_2=R_3=CH_2COOH$ ,  $R_4=R_5=R_6=R_7=H$ ,  $R_8=C_4H_9$   
 38:  $R_1=R_2=R_3=CH_2COOH$ ,  $R_4=R_5=R_6=R_7=H$ ,  $R_8=C_5H_{11}$   
 39:  $R_1=R_2=R_3=CH_2COOH$ ,  $R_4=R_5=R_6=R_7=H$ ,  $R_8=C_6H_{13}$   
 40:  $R_1=R_2=R_3=CH_2COOH$ ,  $R_4=R_5=R_6=R_7=H$ ,  $R_8=C_7H_{15}$   
 41:  $R_1=R_2=R_3=CH_2COOH$ ,  $R_4=R_5=R_6=R_7=H$ ,  $R_8=C_8H_{17}$   
 42:  $R_1=R_2=R_3=CH_2COOH$ ,  $R_4=R_5=R_6=R_7=H$ ,  $R_8=C_9H_{19}$   
 43:  $R_1=R_2=R_3=CH_2COOH$ ,  $R_4=R_5=R_6=R_7=H$ ,  $R_8=C_{10}H_{21}$   
 44:  $R_1=R_2=R_3=CH_2COOH$ ,  $R_4=R_5=R_6=R_7=H$ ,  $R_8=C_{12}H_{25}$   
 45:  $R_1=R_2=R_3=CH_2COOH$ ,  $R_4=R_5=R_6=R_7=H$ ,  $R_8=C_{10}H_{21}$   
 46:  $R_1=R_2=R_3=R_4=NHCOPHCONHC(C_2H_4COOH)_3$ ,  
 $R_5=R_6=R_7=R_8=C_{12}H_{25}$   
 47:  $R_1=R_3=NHCOCH_2CONHC(C_2H_4COOH)_3$ ,  
 $R_2=R_4=C(CH_3)_3$ ,  $R_5=R_6=R_7=R_8=C_{12}H_{25}$

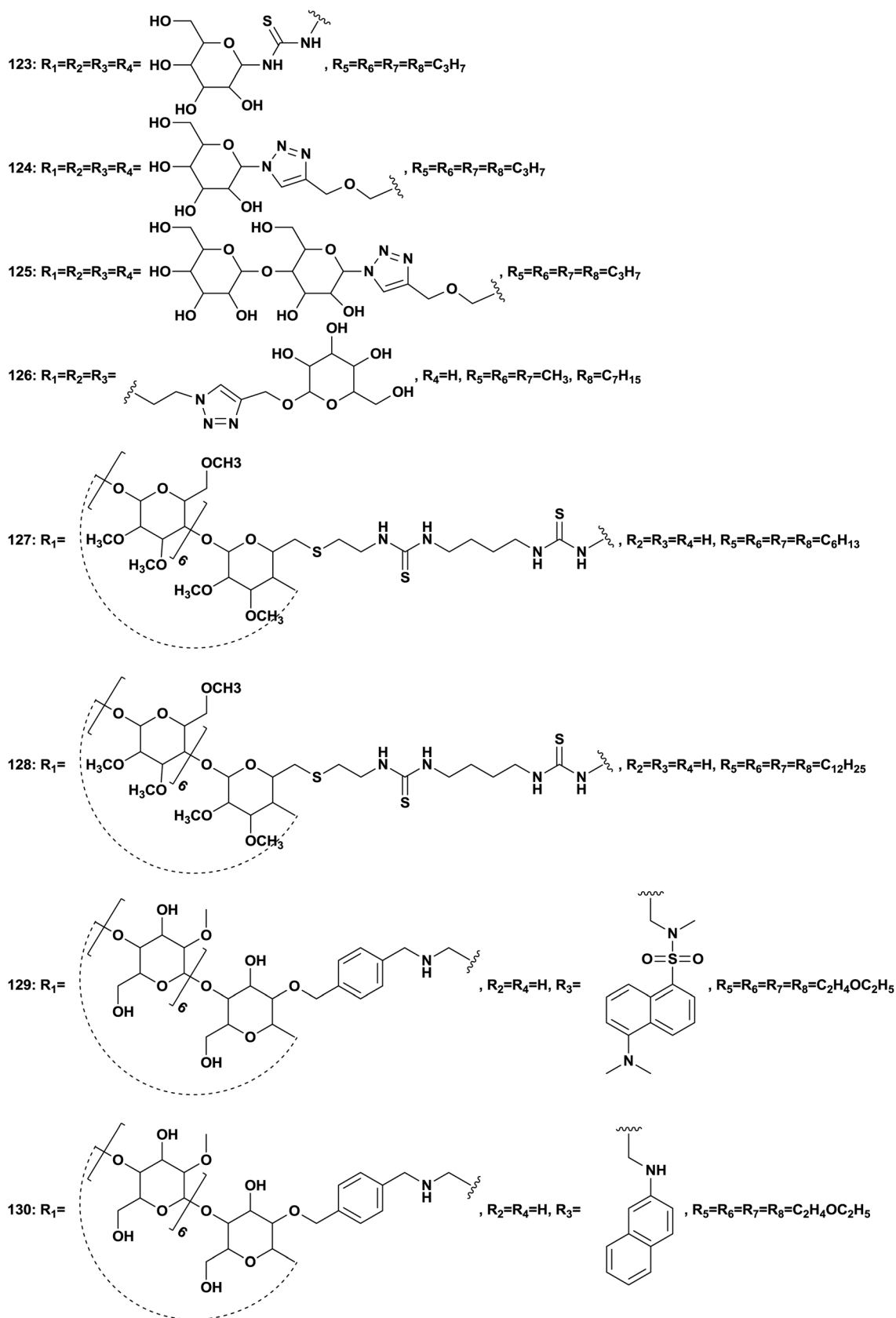
- 48:  $R_1=R_2=R_3=R_4=NHC(NH_2)_2^+$ ,  $R_5=R_6=R_7=R_8=C_4H_7$   
 49:  $R_1=R_2=R_3=R_4=NHC(NH_2)_2^+$ ,  $R_5=R_6=R_7=R_8=C_6H_{13}$   
 50:  $R_1=R_2=R_3=R_4=NHC(NH_2)_2^+$ ,  $R_5=R_6=R_7=R_8=C_8H_{17}$   
 51:  $R_1=R_2=R_3=R_4=NHC(NH_2)_2^+$ ,  $R_5=R_6=R_7=R_8=C_{12}H_{25}$   
 52:  $R_1=R_2=R_3=R_4=CH_2NHC(NH_2)_2^+$ ,  $R_5=R_6=R_7=R_8=C_6H_{13}$   
 53:  $R_1=R_2=R_3=R_4=NHC(NH_2)_2^+$ ,  $R_5=R_6=R_7=R_8=C_2H_4OC_2H_5$   
 54:  $R_1=R_2=R_3=R_4=NHCOCH(NH_2)C_3H_6NHC(NH_2)_2^+$ ,  $R_5=R_6=R_7=R_8=C_6H_{13}$

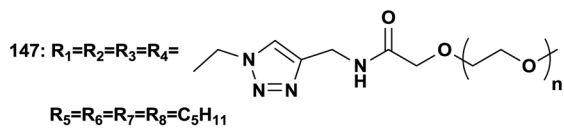
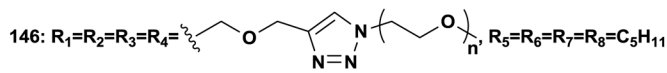
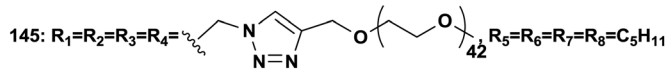
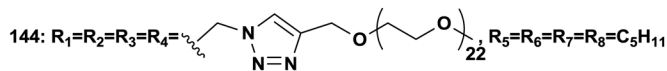
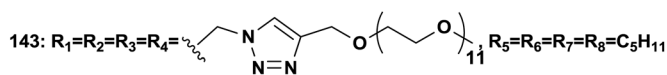
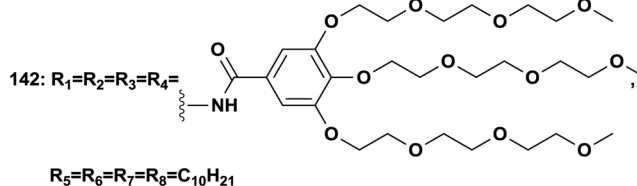
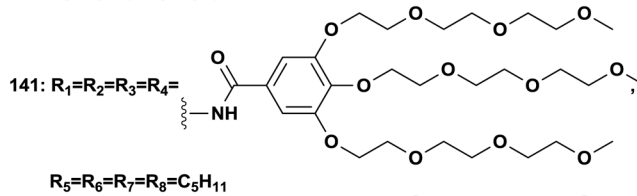
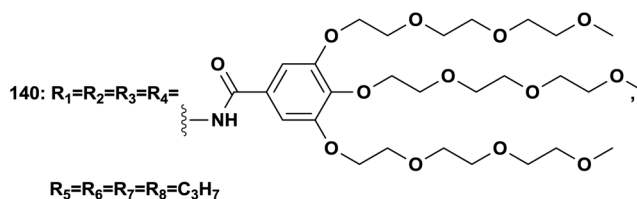
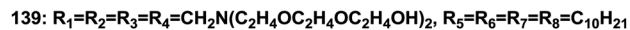
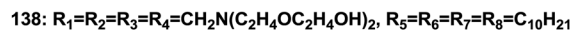
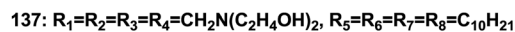
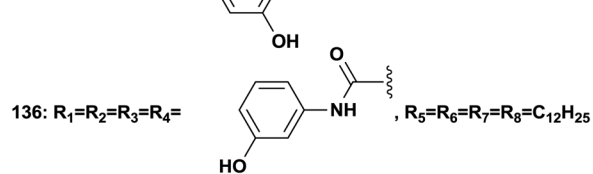
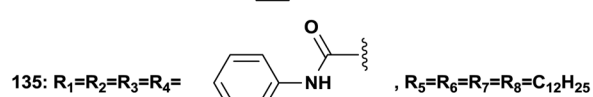
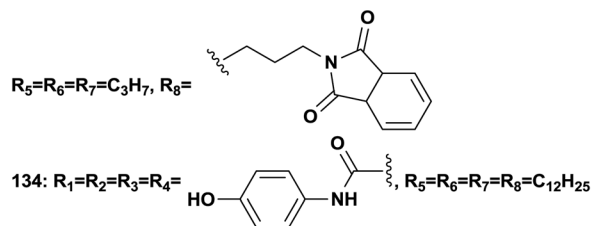
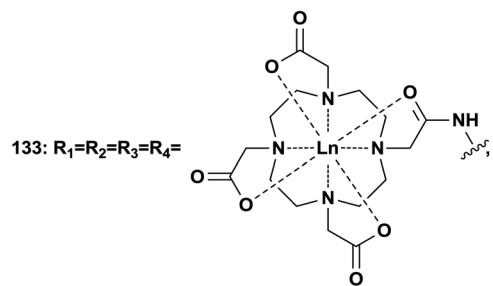
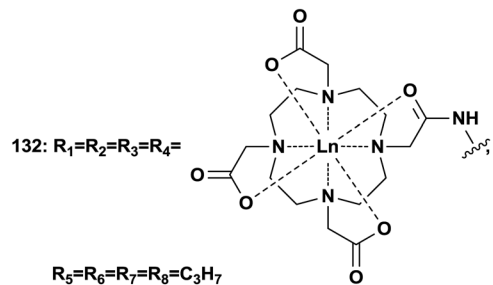
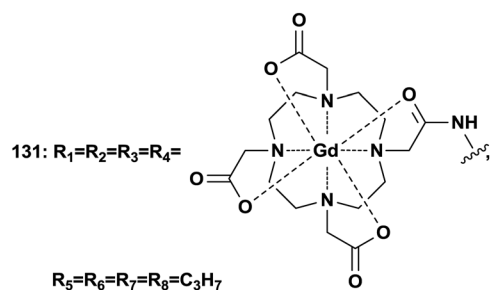


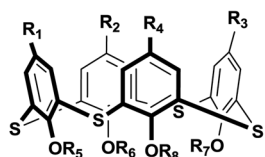
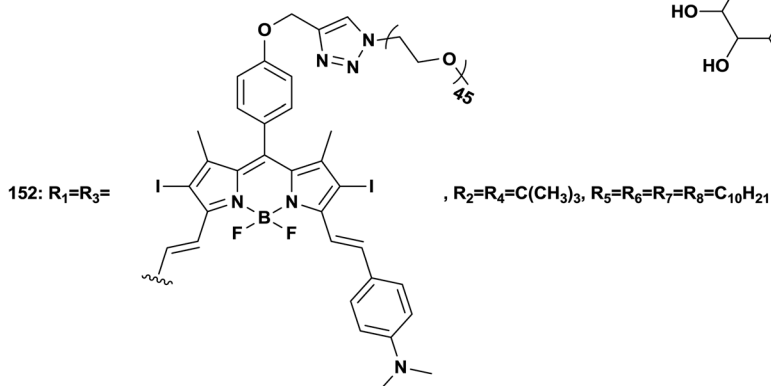
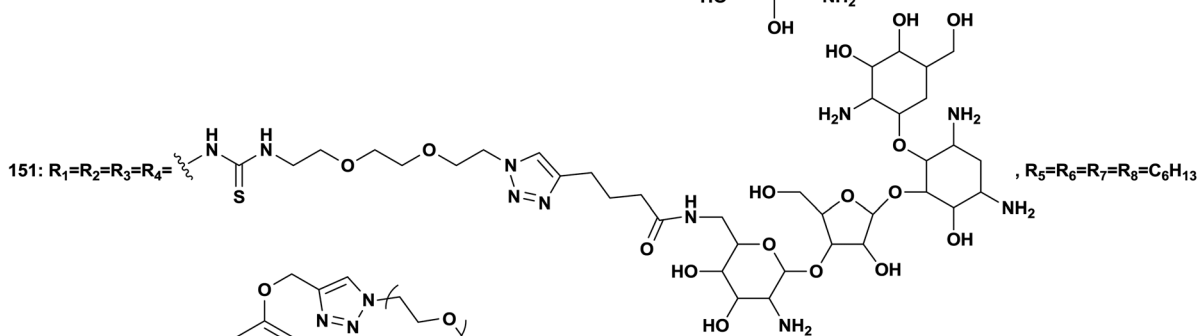
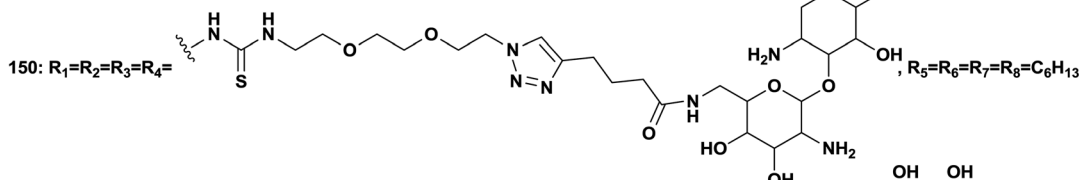
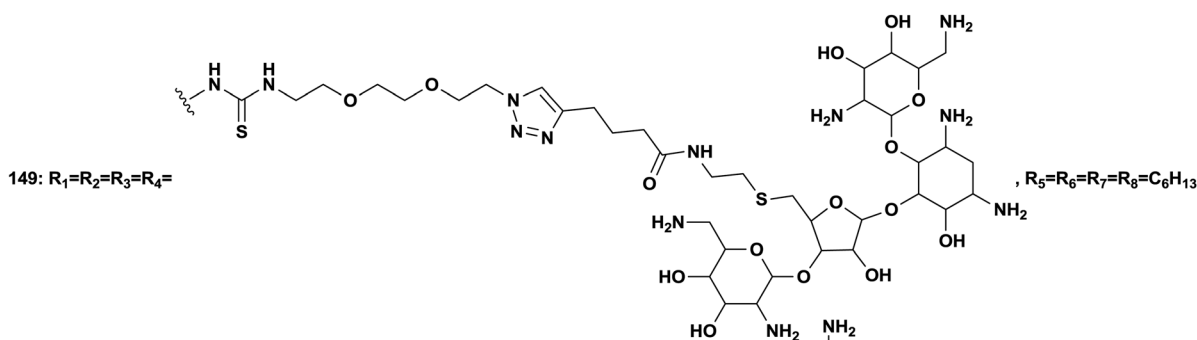
- 57:  $R_1=R_2=R_3=R_4=N^+(CH_3)_3$ ,  $R_5=R_6=R_7=R_8=C_3H_7$   
 58:  $R_1=R_2=R_3=R_4=CH_2N^+(CH_3)_3$ ,  $R_5=R_6=R_7=R_8=C_3H_7$   
 59:  $R_1=R_2=R_3=R_4=CH_2N^+(CH_3)_3$ ,  $R_5=R_6=R_7=R_8=C_6H_{13}$   
 60:  $R_1=R_2=R_3=R_4=CH_2N^+(CH_3)_3$ ,  $R_5=R_6=R_7=R_8=C_8H_{17}$   
 61:  $R_1=R_2=R_3=R_4=CH_2N^+(CH_3)_3$ ,  $R_5=R_6=R_7=R_8=C_{12}H_{25}$   
 62:  $R_1=R_2=R_3=R_4=COOC_2H_4N^+(CH_3)_3$ ,  $R_5=R_6=R_7=R_8=C_{12}H_{25}$   
 63:  $R_1=R_2=R_3=R_4=CH_2N^+(CH_3)_2CH_2C\equiv CH$ ,  $R_5=R_6=R_7=R_8=C_8H_{17}$   
 64:  $R_1=R_2=R_3=R_4=CH_2N^+(CH_3)_2C_2H_4OH$ ,  $R_5=R_6=R_7=R_8=C_3H_7$   
 65:  $R_1=R_2=R_3=R_4=CH_2N^+(CH_3)_2C_2H_4OH$ ,  $R_5=R_6=R_7=R_8=C_6H_{13}$   
 66:  $R_1=R_2=R_3=R_4=CH_2N^+(CH_3)_2C_2H_4OH$ ,  $R_5=R_6=R_7=R_8=C_8H_{17}$   
 67:  $R_1=R_2=R_3=R_4=CH_2N^+(CH_3)_2C_2H_4OH$ ,  $R_5=R_6=R_7=R_8=C_{12}H_{25}$   
 68:  $R_1=R_2=R_3=R_4=CH_2N^+(CH_3)_2C_2H_4OH$ ,  $R_5=R_6=R_7=R_8=C_{16}H_{33}$   
 69:  $R_1=R_2=R_3=R_4=CH_2N^+(CH_3)_2C_2H_4OH$ ,  $R_5=R_7=C_3H_7$ ,  $R_6=R_8=C_{16}H_{33}$   
 70:  $R_1=R_2=R_3=R_4=CH_2N^+(CH_3)(C_2H_4OH)_2$ ,  $R_5=R_6=R_7=R_8=C_3H_7$   
 71:  $R_1=R_2=R_3=R_4=CH_2N^+(CH_3)_2C_2H_4NH_2$ ,  $R_5=R_6=R_7=R_8=C_3H_7$   
 72:  $R_1=R_2=R_3=R_4=CH_2N^+(CH_3)_2C_2H_4NH_2$ ,  $R_5=R_6=R_7=R_8=C_8H_{17}$



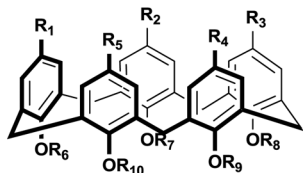








153:  $R_1=R_2=R_3=PO(OC_2H_5)_2$ ,  $R_4=R_5=R_6=R_7=H$ ,  $R_8=C_{10}H_{21}$



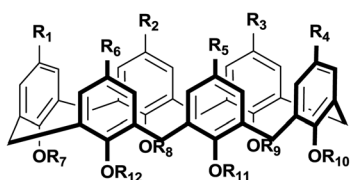
154:  $R_1=R_2=R_3=R_4=R_5=COOH$ ,  $R_6=R_7=R_8=R_9=R_{10}=C_{12}H_{25}$

155:  $R_1=R_2=R_3=R_4=R_5=NHC(NH_2)_2^+$ ,  $R_6=R_7=R_8=R_9=R_{10}=C_3H_6CH(CH_3)_2$

156:  $R_1=R_2=R_3=R_4=R_5=NHC(NH_2)_2^+$ ,  $R_6=R_7=R_8=R_9=R_{10}=C_{12}H_{25}$

157:  $R_1=R_2=R_3=R_4=R_5=N^+(CH_3)_3$ ,  $R_6=R_7=R_8=R_9=R_{10}=C_3H_6CH(CH_3)_2$

158:  $R_1=R_2=R_3=R_4=R_5=COOC_2H_4N^+(CH_3)_3$ ,  $R_6=R_7=R_8=R_9=R_{10}=C_{12}H_{25}$



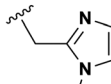
159:  $R_1=R_2=R_3=R_4=R_5=R_6=SO_3^-$ ,  $R_7=R_8=R_9=R_{10}=R_{11}=R_{12}=C_3H_7$

160:  $R_1=R_2=R_3=R_4=R_5=R_6=SO_3^-$ ,  $R_7=R_8=R_9=R_{10}=R_{11}=R_{12}=C_4H_9$

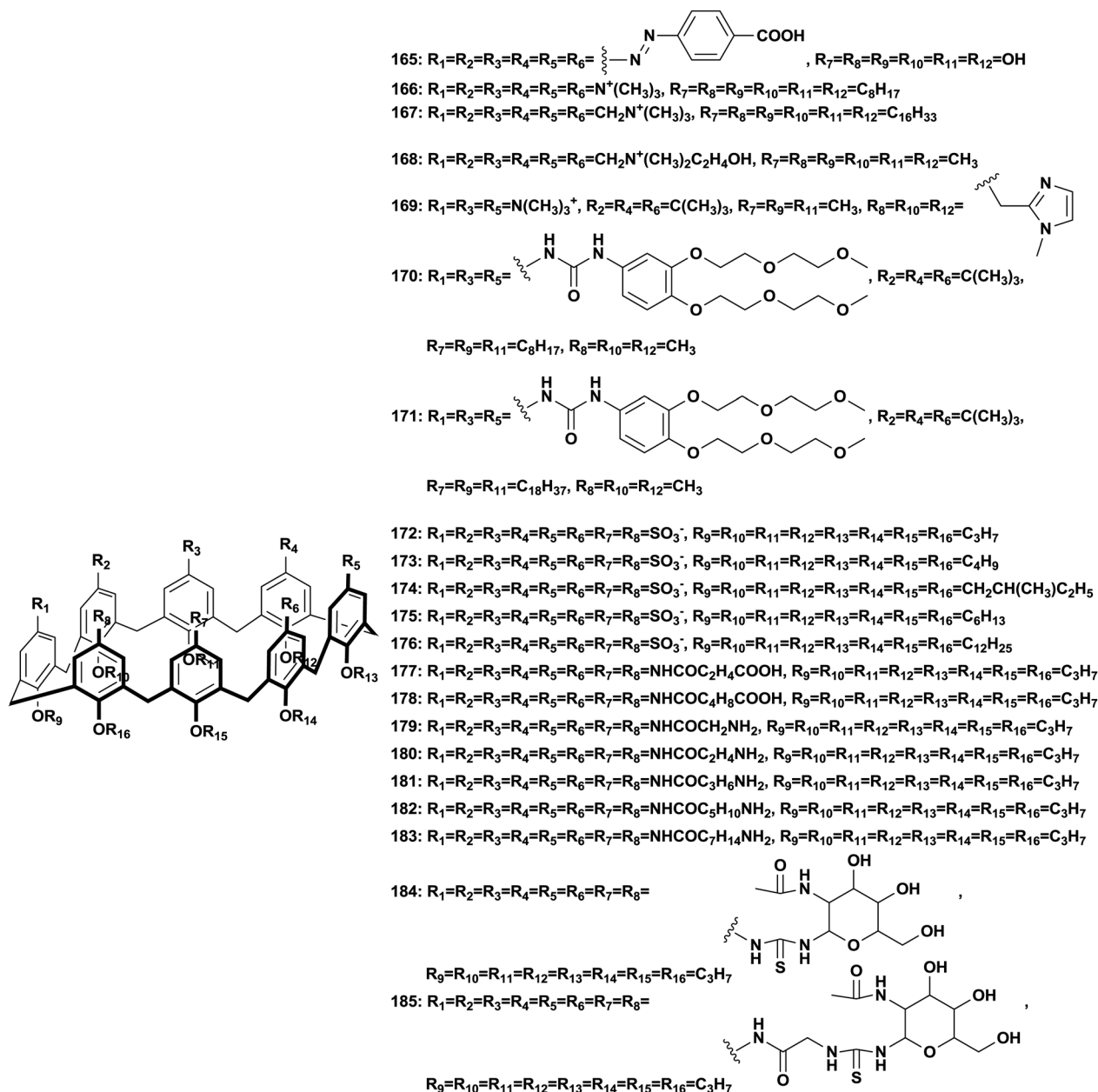
161:  $R_1=R_2=R_3=R_4=R_5=R_6=SO_3^-$ ,  $R_7=R_8=R_9=R_{10}=R_{11}=R_{12}=CH_2CH(CH_3)C_2H_5$

162:  $R_1=R_2=R_3=R_4=R_5=R_6=SO_3^-$ ,  $R_7=R_8=R_9=R_{10}=R_{11}=R_{12}=C_6H_{13}$

163:  $R_1=R_2=R_3=R_4=R_5=R_6=SO_3^-$ ,  $R_7=R_8=R_9=R_{10}=R_{11}=R_{12}=C_{12}H_{25}$

164:  $R_1=R_3=R_5=SO_3^-$ ,  $R_2=R_4=R_6=C(CH_3)_3$ ,  $R_7=R_9=R_{11}=CH_3$ ,  $R_8=R_{10}=R_{12}=$  





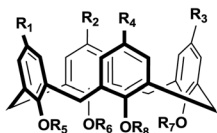
Scheme 2 Structures of upper-rim hydrophilic amphiphilic calixarenes.

of methylene groups ( $\Delta G_M^\circ(\text{CH}_2)$ ) add a constant (which can be represented by  $\Delta G_M^\circ(\text{CH}_3) = \Delta G_M^\circ(\text{CH}_2) + k$ , in which  $k$  is a constant). Therefore, the overall contribution of alkyl chains equals the free energy change for transferring one  $\text{CH}_2$  unit from the aqueous medium to the micellar interior ( $\Delta G_M^\circ(\text{CH}_2)$ ) multiplied by the carbon number of the alkyl chain, while other parts remain constant despite the change in carbon number. So the slope of  $\Delta G_M^\circ$  against carbon number is ( $\Delta G_M^\circ(\text{CH}_2)$ ).<sup>53,54</sup>

Since  $\Delta G_M^\circ$  is proportional to  $\log \text{CAC}$ , we plotted  $\log 4\text{CAC}$  of four amphiphilic SC4As with 4, 6, 8, 12 carbons and  $\log \text{CAC}$  of the corresponding monomer, *versus* the number of carbon atoms in the hydrophobic chain (Fig. 1), and the slope of linear

fitting is proportional to ( $\Delta G_M^\circ(\text{CH}_2)$ ). Results show a negative slope which reflects that the hydrophobic interaction contributes more favourably to the micellization process in the presence of longer alkyl chains. More importantly, the slope of calixarenes ( $-0.27$ ) is lower than the value generally observed for single-chain surfactants ( $-0.22$ ), which means  $\Delta G_M^\circ$  decreases more rapidly with longer alkyl chains of amphiphilic SCnAs than that of sodium sulfonate surfactants. This may be due to the existence of intramolecular interactions between the alkyl chains of the free monomers.<sup>53</sup>

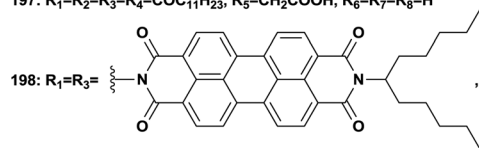
Similar to the difference between monomers and oligomers, in general, larger size of the skeleton results in a lower degree of entropic cost,<sup>279</sup> thus should lead to lower CAC, which is



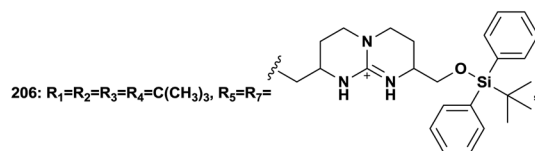
186:  $R_1=R_2=R_3=R_4=C(CH_3)_3$ ,  $R_5=R_6=R_7=R_8=C_3H_6SO_3^-$   
 187:  $R_1=R_2=R_3=R_4=H$ ,  $R_5=R_6=R_7=R_8=C_3H_6SO_3^-$

188:  $R_1=R_2=R_3=R_4=C(CH_3)_3$ ,  $R_5=R_6=R_7=R_8=C_2H_4PO_4H_2$   
 189:  $R_1=R_2=R_3=R_4=COC_9H_{11}$ ,  $R_5=R_6=R_7=R_8=H$   
 190:  $R_1=R_2=R_3=R_4=COC_7H_{15}$ ,  $R_5=R_6=R_7=R_8=H$   
 191:  $R_1=R_2=R_3=R_4=COC_9H_{19}$ ,  $R_5=R_6=R_7=R_8=H$   
 192:  $R_1=R_2=R_3=R_4=COC_{11}H_{23}$ ,  $R_5=R_6=R_7=R_8=H$   
 193:  $R_1=R_2=R_3=R_4=C_3H_6C_8F_{17}$ ,  $R_5=R_6=R_7=R_8=CH_2CONH(C_2H_4O)_3C_2H_4PO_4H_2$

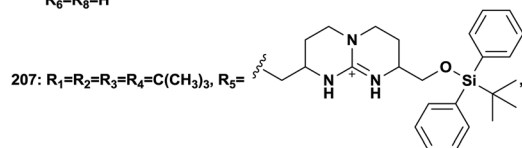
194:  $R_1=R_2=R_3=R_4=C(CH_3)_3$ ,  $R_5=R_6=R_7=R_8=CH_2COOH$   
 195:  $R_1=R_2=R_3=R_4=C(CH_3)_2CH_2C(CH_3)_3$ ,  $R_5=R_6=R_7=R_8=CH_2COOH$   
 196:  $R_1=R_2=R_3=R_4=C_3H_6C_8F_{17}$ ,  
 $R_5=R_6=R_7=R_8=CH_2CONH(C_2H_4O)_3C_2H_4N(CH_2COOH)_2$   
 197:  $R_1=R_2=R_3=R_4=COC_{11}H_{23}$ ,  $R_5=R_6=R_7=R_8=CH_2COOH$ ,  $R_9=R_{10}=R_{11}=H$



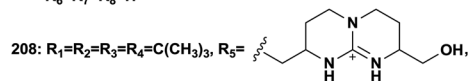
$R_2=R_4=R_5=R_7=H$ ,  $R_6=R_8=C_3H_6CONHC(C_2H_4COOH)_3$   
 199:  $R_1=R_2=R_3=R_4=H$ ,  $R_5=R_6=R_7=R_8=C_3H_6NHC(NH_2)_2^+$   
 200:  $R_1=R_2=R_3=R_4=H$ ,  $R_5=R_6=R_7=R_8=C_6H_{12}NHC(NH_2)_2^+$   
 201:  $R_1=R_2=R_3=R_4=C_3H_7$ ,  $R_5=R_6=R_7=R_8=C_3H_6NHC(NH_2)_2^+$   
 202:  $R_1=R_2=R_3=R_4=C(CH_3)_3$ ,  $R_5=R_6=R_7=R_8=C_3H_6NHC(NH_2)_2^+$   
 203:  $R_1=R_2=R_3=R_4=C(CH_3)_3$ ,  $R_5=R_6=R_7=R_8=C_4H_8NHC(NH_2)_2^+$   
 204:  $R_1=R_2=R_3=R_4=C_6H_{13}$ ,  $R_5=R_6=R_7=R_8=C_3H_6NHC(NH_2)_2^+$   
 205:  $R_1=R_2=R_3=R_4=C(CH_3)_3$ ,  $R_5=R_6=R_7=R_8=C_2H_4NHC(NH_2)_2^+$ ,  $R_9=R_{10}=H$



$R_6=R_8=H$



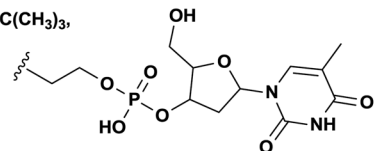
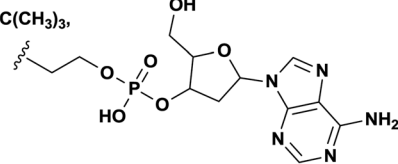
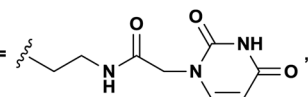
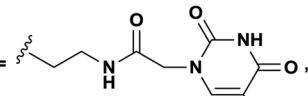
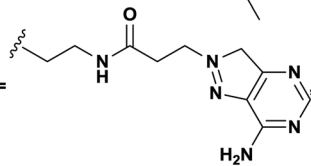
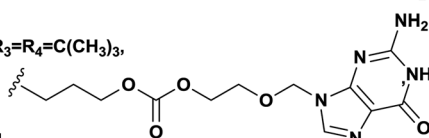
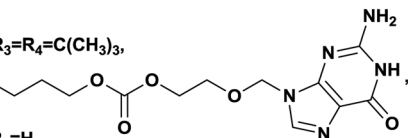
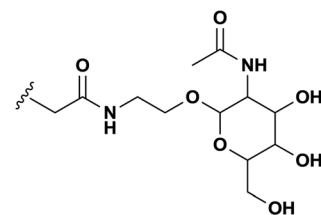
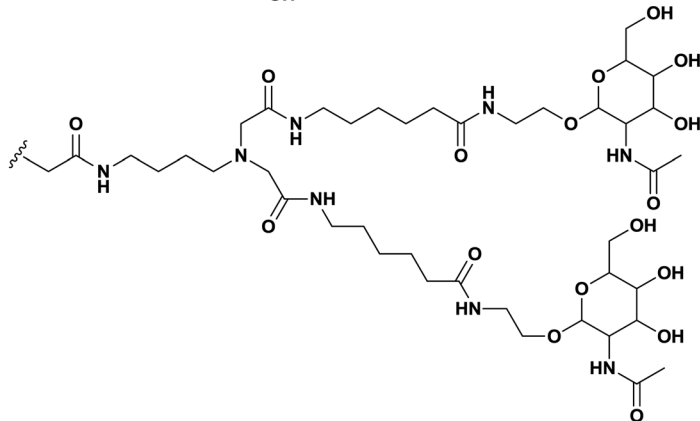
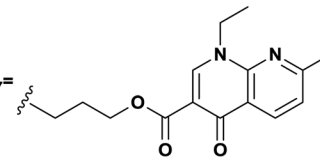
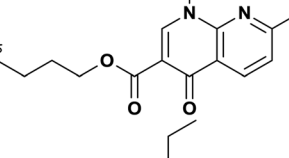
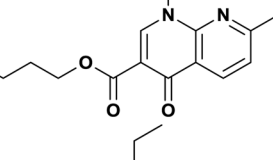
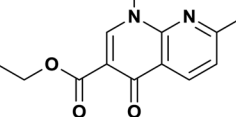
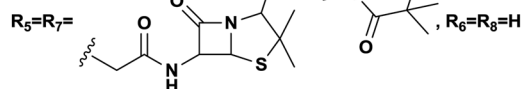
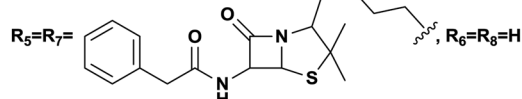
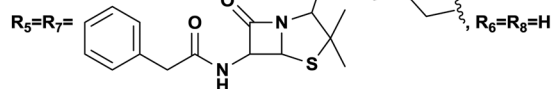
$R_6=R_7=R_8=H$

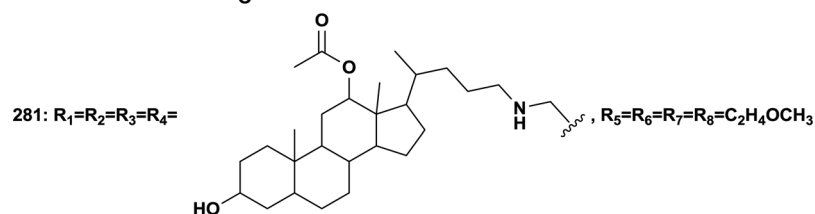
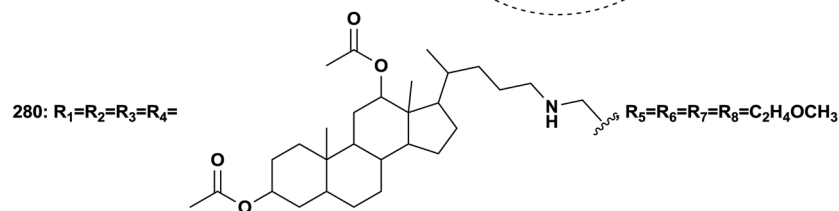
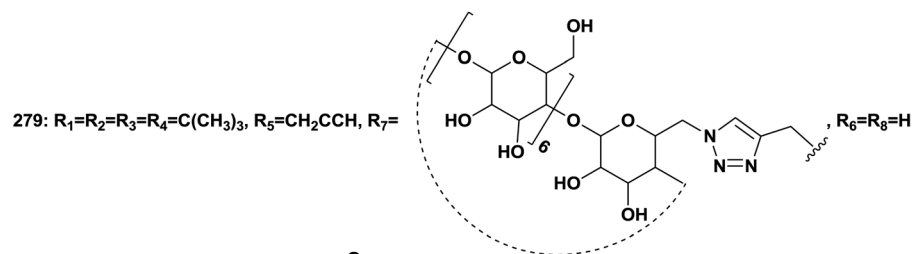
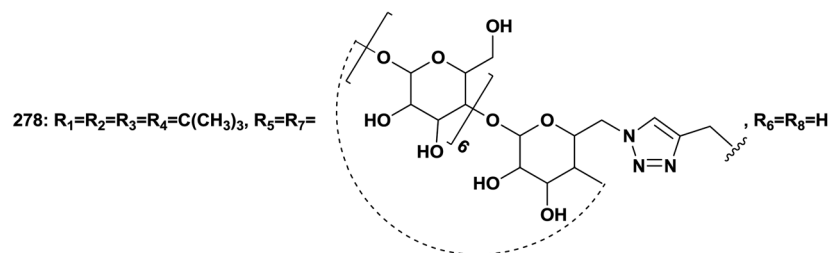
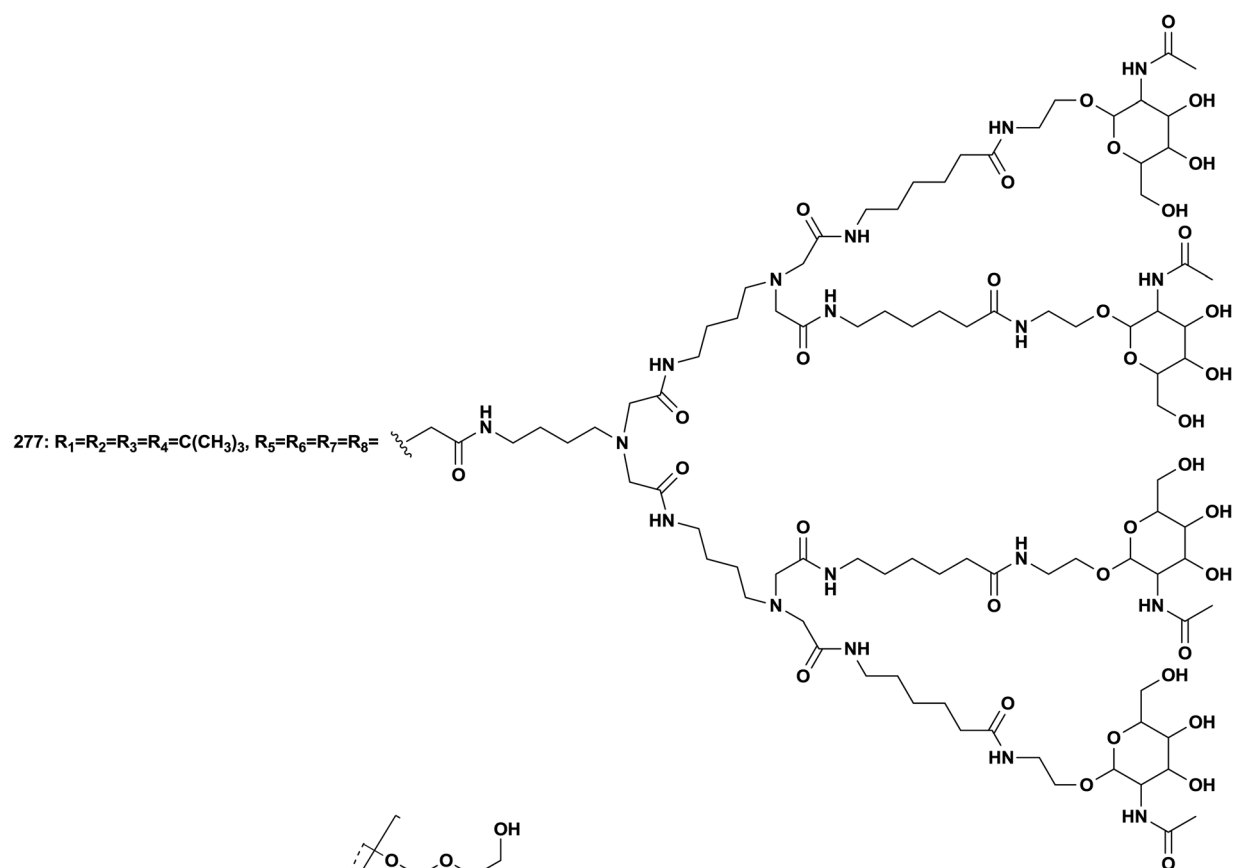


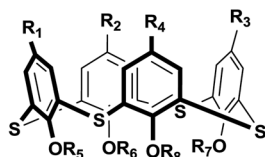
$R_6=R_7=R_8=H$

209:  $R_1=R_2=R_3=R_4=H$ ,  $R_5=R_6=R_7=R_8=C_3H_6N^+(CH_3)_3$   
 210:  $R_1=R_2=R_3=R_4=H$ ,  $R_5=R_6=R_7=R_8=C_6H_{12}N^+(CH_3)_2C_2H_4OH$   
 211:  $R_1=R_2=R_3=R_4=H$ ,  $R_5=R_6=R_7=R_8=C_3H_6NH_2$   
 212:  $R_1=R_2=R_3=R_4=C_3H_6C_8F_{17}$ ,  
 $R_5=R_6=R_7=R_8=CH_2CONH(C_2H_4O)_3C_2H_4NH_2$   
 213:  $R_1=R_2=R_3=R_4=C_2H_5$ ,  $R_5=R_6=R_7=R_8=H$   
 214:  $R_1=R_2=R_3=R_4=C_4H_9$ ,  $R_5=R_6=R_7=R_8=H$   
 215:  $R_1=R_2=R_3=R_4=C_6H_{13}$ ,  $R_5=R_6=R_7=R_8=H$

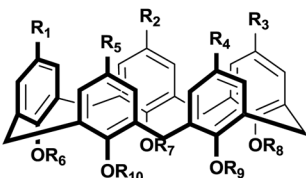
216:  $R_1=R_2=R_3=R_4=COC_9H_{11}$ ,  $R_5=R_6=R_7=R_8=H$   
 217:  $R_1=R_2=R_3=R_4=COC_7H_{15}$ ,  $R_5=R_6=R_7=R_8=H$   
 218:  $R_1=R_2=R_3=R_4=COC_9H_{19}$ ,  $R_5=R_6=R_7=R_8=H$   
 219:  $R_1=R_2=R_3=R_4=COC_{11}H_{23}$ ,  $R_5=R_6=R_7=R_8=H$   
 220:  $R_1=R_2=R_3=R_4=COC_{13}H_{27}$ ,  $R_5=R_6=R_7=R_8=H$   
 221:  $R_1=R_2=R_3=R_4=COC_{15}H_{31}$ ,  $R_5=R_6=R_7=R_8=H$   
 222:  $R_1=R_2=R_3=R_4=N_2PhCH_3$ ,  $R_5=R_6=R_7=R_8=H$   
 223:  $R_1=R_2=R_3=R_4=C_3H_6C_8F_{17}$ ,  $R_5=R_6=R_7=R_8=H$   
 224:  $R_1=R_2=R_3=R_4=N_2PhCl$ ,  $R_5=R_6=R_7=R_8=H$   
 225:  $R_1=R_3=COC_{17}H_{35}$ ,  $R_2=R_4=H$ ,  $R_5=R_6=R_7=R_8=H$   
 226:  $R_1=R_2=R_3=R_4=COC_{11}H_{23}$ ,  $R_5=R_6=PO(OC_2H_5)_2$ ,  $R_7=R_8=H$   
 227:  $R_1=R_2=R_3=R_4=COC_{11}H_{23}$ ,  $R_5=CH_2COOC_2H_5$ ,  $R_6=R_7=R_8=H$   
 228:  $R_1=R_2=R_3=R_4=C(CH_3)_3$ ,  $R_5=R_6=R_7=R_8=CH_2COOC_2H_5$   
 229:  $R_1=R_2=R_3=R_4=C(CH_3)_2CH_2C(CH_3)_3$ ,  $R_5=R_6=R_7=R_8=C_2H_4OH$   
 230:  $R_1=R_2=R_3=R_4=C(CH_3)_3$ ,  $R_5=R_6=R_7=R_8=(C_2H_4O)_6H$   
 231:  $R_1=R_2=R_3=R_4=C(CH_3)_3$ ,  $R_5=R_6=R_7=R_8=(C_2H_4O)_{10}H$   
 232:  $R_1=R_2=R_3=R_4=C(CH_3)_3$ ,  $R_5=R_6=R_7=R_8=(C_2H_4O)_{16}H$   
 233:  $R_1=R_2=R_3=R_4=C_4H_9$ ,  $R_5=R_6=R_7=R_8=(C_2H_4O)_{16}H$   
 234:  $R_1=R_2=R_3=R_4=C_9H_{19}$ ,  $R_5=R_6=R_7=R_8=(C_2H_4O)_8H$   
 235:  $R_1=R_2=R_3=R_4=C_9H_{19}$ ,  $R_5=R_6=R_7=R_8=(C_2H_4O)_{12}H$   
 236:  $R_1=R_2=R_3=R_4=C_9H_{19}$ ,  $R_5=R_6=R_7=R_8=(C_2H_4O)_{16}H$   
 237:  $R_1=R_2=R_3=R_4=C_6H_{12}CH(CH_3)_2$ ,  $R_5=R_6=R_7=R_8=(C_2H_4O)_4H$   
 238:  $R_1=R_2=R_3=R_4=C_6H_{12}CH(CH_3)_2$ ,  $R_5=R_6=R_7=R_8=(C_2H_4O)_8H$   
 239:  $R_1=R_2=R_3=R_4=C_6H_{12}CH(CH_3)_2$ ,  $R_5=R_6=R_7=R_8=(C_2H_4O)_9H$   
 240:  $R_1=R_2=R_3=R_4=C_6H_{12}CH(CH_3)_2$ ,  $R_5=R_6=R_7=R_8=(C_2H_4O)_{12}H$   
 241:  $R_1=R_2=R_3=R_4=C_6H_{12}CH(CH_3)_2$ ,  $R_5=R_6=R_7=R_8=(C_2H_4O)_{16}H$   
 242:  $R_1=R_2=R_3=R_4=C_6H_{12}CH(CH_3)_2$ ,  $R_5=R_6=R_7=R_8=(C_2H_4O)_{20}H$   
 243:  $R_1=R_2=R_3=R_4=C(CH_3)_3$ ,  $R_5=R_6=R_7=R_8=(C_2H_4O)_{14}H$   
 244:  $R_1=R_2=R_3=R_4=C(CH_3)_3$ ,  $R_5=R_6=R_7=R_8=(C_2H_4O)_{18}H$   
 245:  $R_1=R_2=R_3=R_4=C(CH_3)_3$ ,  $R_5=R_6=R_7=R_8=(C_2H_4O)_{34}H$   
 246:  $R_1=R_2=R_3=R_4=C(CH_3)_3$ ,  $R_5=R_6=R_7=R_8=(C_2H_4O)_{45}H$   
 247:  $R_1=R_2=R_3=R_4=C(CH_3)_3$ ,  $R_5=R_6=R_7=R_8=(C_2H_4O)_{56}H$   
 248:  $R_1=R_2=R_3=R_4=C(CH_3)_3$ ,  $R_5=R_6=R_7=R_8=(C_2H_4O)_{67}H$   
 249:  $R_1=R_2=R_3=R_4=C(CH_3)_3$ ,  $R_5=R_6=R_7=R_8=(C_2H_4O)_{110}H$   
 250:  $R_1=R_2=R_3=R_4=C(CH_3)_3$ ,  $R_5=R_6=R_7=R_8=(C_2H_4O)_{150}H$   
 251:  $R_1=R_2=R_3=R_4=C(CH_3)_3$ ,  $R_5=R_6=R_7=R_8=(C_2H_4O)_{200}H$   
 252:  $R_1=R_2=R_3=R_4=C(CH_3)_3$ ,  $R_5=R_6=R_7=R_8=(C_2H_4O)_{250}H$   
 253:  $R_1=R_2=R_3=R_4=C(CH_3)_3$ ,  $R_5=R_6=R_7=R_8=CH_2COO(C_2H_4O)_{20}C_{16}H_{33}$   
 254:  $R_1=R_2=R_3=R_4=C(CH_3)_3$ ,  $R_5=R_6=C_2H_4(OC_2H_4)_{12}OCH_3$ ,  $R_7=R_8=H$   
 255:  $R_1=R_2=R_3=R_4=C(CH_3)_3$ ,  $R_5=R_7=$   
 $R_6=R_8=C_2H_4O(COC_5H_{10})_{11}OH$   
 256:  $R_1=R_2=R_3=R_4=C(CH_3)_3$ ,  $R_5=R_7=$   
 $R_6=R_8=C_2H_4O(COC_5H_{10})_{11}OH$   
 257:  $R_1=R_2=R_3=R_4=C(CH_3)_3$ ,  $R_5=R_7=$   
 $R_6=R_8=C_2H_4O(COC_5H_{10})_{22}OH$   
 258:  $R_1=R_2=R_3=R_4=C(CH_3)_3$ ,  $R_5=R_7=$   
 $R_6=R_8=C_2H_4O(COC_5H_{10})_{22}OH$   
 259:  $R_1=R_2=R_3=R_4=C(CH_3)_3$ ,  $R_5=R_7=$   
 $R_6=R_8=C_2H_4O(COC_5H_{10})_{40}OH$   
 260:  $R_1=R_2=R_3=R_4=C(CH_3)_3$ ,  $R_5=R_7=$   
 $R_6=R_8=C_2H_4O(COC_5H_{10})_{40}OH$

261:  $R_1=R_2=R_3=R_4=C(CH_3)_3$ , $R_5=R_6=R_7=R_8=$ 262:  $R_1=R_2=R_3=R_4=C(CH_3)_3$ , $R_5=R_6=R_7=R_8=$ 263:  $R_1=R_2=R_3=R_4=C(CH_3)_3$ ,  $R_5=R_7=$  $R_6=R_8=H$ 264:  $R_1=R_2=R_3=R_4=C(CH_3)_3$ ,  $R_5=R_7=$  $R_6=R_8=H$ 265:  $R_1=R_2=R_3=R_4=C(CH_3)_3$ ,  $R_5=R_7=$  $R_6=R_8=H$ 266:  $R_1=R_2=R_3=R_4=C(CH_3)_3$ , $R_5=R_7=$  $R_6=R_8=H$ 267:  $R_1=R_2=R_3=R_4=C(CH_3)_3$ , $R_5=$  $R_6=R_7=R_8=H$ 275:  $R_1=R_2=R_3=R_4=C(CH_3)_3$ ,  $R_5=R_6=R_7=R_8=$ 276:  $R_1=R_2=R_3=R_4=C(CH_3)_3$ ,  $R_5=R_6=R_7=R_8=$ 268:  $R_1=R_2=R_3=R_4=C(CH_3)_3$ ,  $R_5=R_7=$  $R_6=R_8=H$ 269:  $R_1=R_2=R_3=R_4=C(CH_3)_3$ ,  $R_5=$  $R_6=R_7=R_8=H$ 270:  $R_1=R_2=R_3=R_4=H$ ,  $R_5=R_7=$  $R_6=R_8=H$ 271:  $R_1=R_2=R_3=R_4=H$ ,  $R_5=$  $R_6=R_7=R_8=H$ 272:  $R_1=R_2=R_3=R_4=C(CH_3)_3$ , $R_5=R_7=$ 273:  $R_1=R_2=R_3=R_4=C(CH_3)_3$ , $R_5=R_7=$ 274:  $R_1=R_2=R_3=R_4=C(CH_3)_3$ , $R_5=R_7=$ 

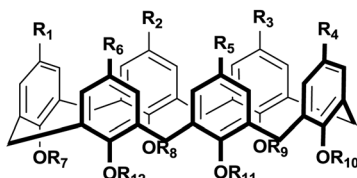




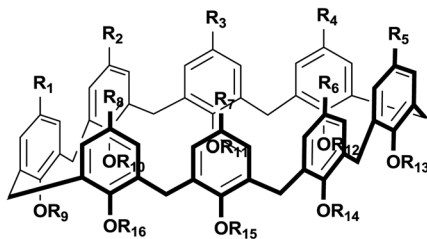
- 282:  $R_1=R_2=R_3=R_4=C(CH_3)_3$ ,  $R_5=R_6=R_7=R_8=C_3H_6SO_3^-$   
 283:  $R_1=R_2=R_3=R_4=C(CH_3)_3$ ,  $R_5=R_6=R_7=R_8=CH_2CONHC_3H_6N^+(CH_3)_3$   
 284:  $R_1=R_2=R_3=R_4=C(CH_3)_3$ ,  $R_5=R_6=R_7=R_8=CH_2CONHC_3H_6N^+(CH_3)_2CH_2Ph$   
 285:  $R_1=R_2=R_3=R_4=C(CH_3)_3$ ,  $R_5=R_6=R_7=R_8=CH_2CONHC_3H_6N^+(CH_3)_2C_2H_5$   
 286:  $R_1=R_2=R_3=R_4=C(CH_3)_3$ ,  $R_5=R_6=R_7=R_8=CH_2CONHC_3H_6N^+(CH_3)_2C_3H_6Ph$   
 287:  $R_1=R_2=R_3=R_4=C(CH_3)_3$ ,  $R_5=R_6=R_7=R_8=CH_2CONHC_3H_6N^+(CH_3)_2CH_2COOC_2H_5$   
 288:  $R_1=R_2=R_3=R_4=C(CH_3)_3$ ,  $R_5=R_6=R_7=R_8=CH_2CONHC_3H_6N^+(C_2H_5)_2CH_3$   
 289:  $R_1=R_2=R_3=R_4=C(CH_3)_3$ ,  $R_5=R_6=R_7=R_8=CH_2CONHC_2H_4N^+(C_2H_5)_2CH_2CONHCH_2COOC_2H_5$   
 290:  $R_1=R_2=R_3=R_4=C(CH_3)_3$ ,  $R_5=R_6=R_7=R_8=CH_2CONHC_3H_6N^+(CH_3)_2CH_2CONHCH_2COOC_2H_5$   
 291:  $R_1=R_2=R_3=R_4=C(CH_3)_3$ ,  $R_5=(C_2H_4O)_{14}CH_3$ ,  $R_6=R_7=R_8=H$   
 292:  $R_1=R_2=R_3=R_4=C(CH_3)_3$ ,  $R_5=R_6=R_7=R_8=CH_2CONHC_3H_6N^+(CH_3)_2C_3H_6SO_3^-$   
 293:  $R_1=R_2=R_3=R_4=C(CH_3)_3$ ,  $R_5=R_6=R_7=R_8=CH_2CONHC_3H_6N^+(CH_3)_2C_4H_8SO_3^-$



- 294:  $R_1=R_2=R_3=R_4=R_5=C(CH_3)_3$ ,  $R_6=R_7=R_8=R_9=R_{10}=C_4H_8SO_3^-$   
 295:  $R_1=R_2=R_3=R_4=R_5=C(CH_3)_3$ ,  $R_6=R_7=R_8=R_9=R_{10}=(C_2H_4O)_{12}CH_3$   
 296:  $R_1=R_2=R_3=R_4=R_5=CH_3$ ,  $R_6=R_7=R_8=R_9=R_{10}=(C_2H_4O)_{12}CH_3$

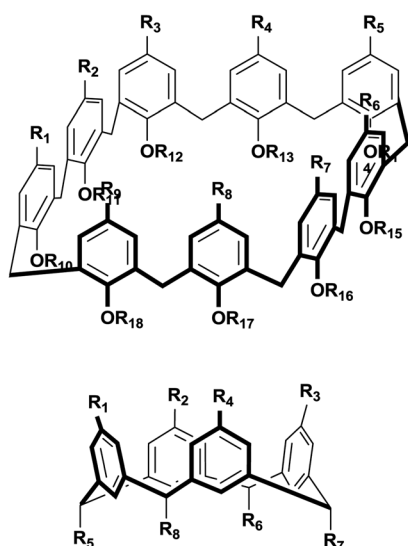


- 297:  $R_1=R_2=R_3=R_4=R_5=R_6=H$ ,  $R_7=R_8=R_9=R_{10}=R_{11}=R_{12}=C_3H_6SO_3^-$   
 298:  $R_1=R_2=R_3=R_4=R_5=R_6=C_4H_9$ ,  $R_7=R_8=R_9=R_{10}=R_{11}=R_{12}=C_3H_6SO_3^-$   
 299:  $R_1=R_2=R_3=R_4=R_5=R_6=C(CH_3)_3$ ,  $R_7=R_8=R_9=R_{10}=R_{11}=R_{12}=C_3H_6SO_3^-$   
 300:  $R_1=R_2=R_3=R_4=R_5=R_6=C_6H_{13}$ ,  $R_7=R_8=R_9=R_{10}=R_{11}=R_{12}=C_3H_6SO_3^-$   
 301:  $R_1=R_2=R_3=R_4=R_5=R_6=C_{12}H_{25}$ ,  $R_7=R_8=R_9=R_{10}=R_{11}=R_{12}=C_3H_6SO_3^-$   
 302:  $R_1=R_2=R_3=R_4=R_5=R_6=COC_3H_7$ ,  $R_7=R_8=R_9=R_{10}=R_{11}=R_{12}=C_4H_8SO_3^-$   
 303:  $R_1=R_2=R_3=R_4=R_5=R_6=COC_5H_{11}$ ,  $R_7=R_8=R_9=R_{10}=R_{11}=R_{12}=C_4H_8SO_3^-$   
 304:  $R_1=R_2=R_3=R_4=R_5=R_6=COC_7H_{15}$ ,  $R_7=R_8=R_9=R_{10}=R_{11}=R_{12}=C_4H_8SO_3^-$   
 305:  $R_1=R_2=R_3=R_4=R_5=R_6=H$ ,  $R_7=R_8=R_9=R_{10}=R_{11}=R_{12}=CH_2COOH$   
 306:  $R_1=R_2=R_3=R_4=R_5=R_6=COC_3H_7$ ,  $R_7=R_8=R_9=R_{10}=R_{11}=R_{12}=CH_2COOH$   
 307:  $R_1=R_2=R_3=R_4=R_5=R_6=COC_5H_{11}$ ,  $R_7=R_8=R_9=R_{10}=R_{11}=R_{12}=CH_2COOH$   
 308:  $R_1=R_2=R_3=R_4=R_5=R_6=COC_7H_{15}$ ,  $R_7=R_8=R_9=R_{10}=R_{11}=R_{12}=CH_2COOH$   
 309:  $R_1=R_2=R_3=R_4=R_5=R_6=C(CH_3)_3$ ,  $R_7=C_3H_6COOH$ ,  $R_8=R_9=R_{10}=R_{11}=R_{12}=H$   
 310:  $R_1=R_2=R_3=R_4=R_5=R_6=C(CH_3)_3$ ,  $R_7=R_9=R_{11}=C_2H_4NH_2$ ,  $R_8=R_{10}=R_{12}=CH_3$   
 311:  $R_1=R_2=R_3=R_4=R_5=R_6=C(CH_3)_3$ ,  $R_7=R_{10}=CH_2CONHC_3H_6NH_2$ ,  $R_8=R_9=R_{11}=R_{12}=H$   
 312:  $R_1=R_2=R_3=R_4=R_5=R_6=COC_3H_7$ ,  $R_7=R_8=R_9=R_{10}=R_{11}=R_{12}=CH_2COOC_2H_5$   
 313:  $R_1=R_2=R_3=R_4=R_5=R_6=COC_5H_{11}$ ,  $R_7=R_8=R_9=R_{10}=R_{11}=R_{12}=CH_2COOC_2H_5$   
 314:  $R_1=R_2=R_3=R_4=R_5=R_6=COC_7H_{15}$ ,  $R_7=R_8=R_9=R_{10}=R_{11}=R_{12}=CH_2COOC_2H_5$   
 315:  $R_1=R_2=R_3=R_4=R_5=R_6=COC_3H_7$ ,  $R_7=R_8=R_9=R_{10}=R_{11}=R_{12}=(C_2H_4O)_2CH_3$   
 316:  $R_1=R_2=R_3=R_4=R_5=R_6=COC_5H_{11}$ ,  $R_7=R_8=R_9=R_{10}=R_{11}=R_{12}=(C_2H_4O)_2CH_3$   
 317:  $R_1=R_2=R_3=R_4=R_5=R_6=COC_7H_{15}$ ,  $R_7=R_8=R_9=R_{10}=R_{11}=R_{12}=(C_2H_4O)_2CH_3$   
 318:  $R_1=R_2=R_3=R_4=R_5=R_6=C(CH_3)_3$ ,  $R_7=R_8=R_9=R_{10}=R_{11}=R_{12}=COCH_3$   
 319:  $R_1=R_2=R_3=R_4=R_5=R_6=C(CH_3)_3$ ,  $R_7=R_8=R_9=R_{10}=R_{11}=R_{12}=[CH_2CH(CH_3)O]_xH$   
 320:  $R_1=R_2=R_3=R_4=R_5=R_6=C(CH_3)_3$ ,  $R_7=R_8=R_9=R_{10}=R_{11}=R_{12}=[CH_2CH(CH_3)O]_x[COOCH_2C(CH_3)_2CH_2O]_yH$   
 321:  $R_1=R_2=R_3=R_4=R_5=R_6=R_7=R_8=H$ ,  $R_9=R_{10}=R_{11}=R_{12}=R_{13}=R_{14}=R_{15}=R_{16}=C_3H_6SO_3^-$   
 322:  $R_1=R_2=R_3=R_4=R_5=R_6=R_7=R_8=C(CH_3)_3$ ,  $R_9=R_{10}=R_{11}=R_{12}=R_{13}=R_{14}=R_{15}=R_{16}=C_3H_6SO_3^-$   
 323:  $R_1=R_2=R_3=R_4=R_5=R_6=R_7=R_8=COC_7H_{15}$ ,  $R_9=R_{10}=R_{11}=R_{12}=R_{13}=R_{14}=R_{15}=R_{16}=C_4H_8SO_3^-$   
 324:  $R_1=R_2=R_3=R_4=R_5=R_6=R_7=R_8=COC_{15}H_{31}$ ,  $R_9=R_{10}=R_{11}=R_{12}=R_{13}=R_{14}=R_{15}=R_{16}=C_4H_8SO_3^-$   
 325:  $R_1=R_2=R_3=R_4=R_5=R_6=R_7=R_8=H$ ,  $R_9=R_{10}=R_{11}=R_{12}=R_{13}=R_{14}=R_{15}=R_{16}=CH_2COOH$   
 326:  $R_1=R_2=R_3=R_4=R_5=R_6=R_7=R_8=C(CH_3)_3$ ,  $R_9=R_{10}=R_{11}=R_{12}=R_{13}=R_{14}=R_{15}=R_{16}=C_3H_6COOH$   
 327:  $R_1=R_2=R_3=R_4=R_5=R_6=R_7=R_8=COC_7H_{15}$ ,  $R_9=R_{10}=R_{11}=R_{12}=R_{13}=R_{14}=R_{15}=R_{16}=CH_2COOH$   
 328:  $R_1=R_2=R_3=R_4=R_5=R_6=R_7=R_8=COC_{15}H_{31}$ ,  $R_9=R_{10}=R_{11}=R_{12}=R_{13}=R_{14}=R_{15}=R_{16}=CH_2COOH$   
 329:  $R_1=R_2=R_3=R_4=R_5=R_6=R_7=R_8=COC_7H_{15}$ ,  $R_9=R_{10}=R_{11}=R_{12}=R_{13}=R_{14}=R_{15}=R_{16}=C_3H_6COOH$   
 330:  $R_1=R_2=R_3=R_4=R_5=R_6=R_7=R_8=COC_{15}H_{31}$ ,  $R_9=R_{10}=R_{11}=R_{12}=R_{13}=R_{14}=R_{15}=R_{16}=C_3H_6COOH$   
 331:  $R_1=R_2=R_3=R_4=R_5=R_6=R_7=R_8=C(CH_3)_2CH_2C(CH_3)_3$ ,  
 $R_9=R_{10}=R_{11}=R_{12}=R_{13}=R_{14}=R_{15}=R_{16}=CH_2COOH$



- 332:  $R_1=R_2=R_3=R_4=R_5=R_6=R_7=R_8=H$ ,  $R_9=R_{10}=R_{11}=R_{12}=R_{13}=R_{14}=R_{15}=R_{16}=C_3H_6NHC(NH_2)_2^+$
- 333:  $R_1=R_2=R_3=R_4=R_5=R_6=R_7=R_8=COC_7H_{15}$ ,  $R_9=R_{10}=R_{11}=R_{12}=R_{13}=R_{14}=R_{15}=R_{16}=H$
- 334:  $R_1=R_2=R_3=R_4=R_5=R_6=R_7=R_8=COC_9H_{19}$ ,  $R_9=R_{10}=R_{11}=R_{12}=R_{13}=R_{14}=R_{15}=R_{16}=H$
- 335:  $R_1=R_2=R_3=R_4=R_5=R_6=R_7=R_8=COC_{11}H_{23}$ ,  $R_9=R_{10}=R_{11}=R_{12}=R_{13}=R_{14}=R_{15}=R_{16}=H$
- 336:  $R_1=R_2=R_3=R_4=R_5=R_6=R_7=R_8=COC_{13}H_{27}$ ,  $R_9=R_{10}=R_{11}=R_{12}=R_{13}=R_{14}=R_{15}=R_{16}=H$
- 337:  $R_1=R_2=R_3=R_4=R_5=R_6=R_7=R_8=COC_{15}H_{31}$ ,  $R_9=R_{10}=R_{11}=R_{12}=R_{13}=R_{14}=R_{15}=R_{16}=H$
- 338:  $R_1=R_2=R_3=R_4=R_5=R_6=R_7=R_8=COC_7H_{15}$ ,  $R_9=R_{10}=R_{11}=R_{12}=R_{13}=R_{14}=R_{15}=R_{16}=C_3H_6CN$
- 339:  $R_1=R_2=R_3=R_4=R_5=R_6=R_7=R_8=COC_{15}H_{31}$ ,  $R_9=R_{10}=R_{11}=R_{12}=R_{13}=R_{14}=R_{15}=R_{16}=C_3H_6CN$
- 340:  $R_1=R_2=R_3=R_4=R_5=R_6=R_7=R_8=C(CH_3)_2CH_2C(CH_3)_3$ ,  
 $R_9=R_{10}=R_{11}=R_{12}=R_{13}=R_{14}=R_{15}=R_{16}=CH_2COOC_2H_5$
- 341:  $R_1=R_2=R_3=R_4=R_5=R_6=R_7=R_8=COC_7H_{15}$ ,  $R_9=R_{10}=R_{11}=R_{12}=R_{13}=R_{14}=R_{15}=R_{16}=CH_2COOC_2H_5$
- 342:  $R_1=R_2=R_3=R_4=R_5=R_6=R_7=R_8=COC_{15}H_{31}$ ,  $R_9=R_{10}=R_{11}=R_{12}=R_{13}=R_{14}=R_{15}=R_{16}=CH_2COOC_2H_5$
- 343:  $R_1=R_2=R_3=R_4=R_5=R_6=R_7=R_8=COC_7H_{15}$ ,  $R_9=R_{10}=R_{11}=R_{12}=R_{13}=R_{14}=R_{15}=R_{16}=C_3H_6COOC_2H_5$
- 344:  $R_1=R_2=R_3=R_4=R_5=R_6=R_7=R_8=COC_{15}H_{31}$ ,  $R_9=R_{10}=R_{11}=R_{12}=R_{13}=R_{14}=R_{15}=R_{16}=C_3H_6COOC_2H_5$
- 345:  $R_1=R_2=R_3=R_4=R_5=R_6=R_7=R_8=H$ ,  $R_9=R_{10}=R_{11}=R_{12}=R_{13}=R_{14}=R_{15}=R_{16}=(C_2H_4O)_3H$
- 346:  $R_1=R_2=R_3=R_4=R_5=R_6=R_7=R_8=C(CH_3)_3$ ,  $R_9=R_{10}=R_{11}=R_{12}=R_{13}=R_{14}=R_{15}=R_{16}=(C_2H_4O)_3H$
- 347:  $R_1=R_2=R_3=R_4=R_5=R_6=R_7=R_8=C(CH_3)_2CH_2C(CH_3)_3$ ,  
 $R_9=R_{10}=R_{11}=R_{12}=R_{13}=R_{14}=R_{15}=R_{16}=(C_2H_4O)_3H$
- 348:  $R_1=R_2=R_3=R_4=R_5=R_6=R_7=R_8=OCH_2Ph$ ,  $R_9=R_{10}=R_{11}=R_{12}=R_{13}=R_{14}=R_{15}=R_{16}=(C_2H_4O)_3H$
- 349:  $R_1=R_2=R_3=R_4=R_5=R_6=R_7=R_8=H$ ,  $R_9=R_{10}=R_{11}=R_{12}=R_{13}=R_{14}=R_{15}=R_{16}=(C_2H_4O)_6H$
- 350:  $R_1=R_2=R_3=R_4=R_5=R_6=R_7=R_8=C(CH_3)_3$ ,  $R_9=R_{10}=R_{11}=R_{12}=R_{13}=R_{14}=R_{15}=R_{16}=(C_2H_4O)_6H$
- 351:  $R_1=R_2=R_3=R_4=R_5=R_6=R_7=R_8=C(CH_3)_2CH_2C(CH_3)_3$ ,  
 $R_9=R_{10}=R_{11}=R_{12}=R_{13}=R_{14}=R_{15}=R_{16}=(C_2H_4O)_6H$
- 352:  $R_1=R_2=R_3=R_4=R_5=R_6=R_7=R_8=OCH_2Ph$ ,  $R_9=R_{10}=R_{11}=R_{12}=R_{13}=R_{14}=R_{15}=R_{16}=(C_2H_4O)_6H$
- 353:  $R_1=R_2=R_3=R_4=R_5=R_6=R_7=R_8=H$ ,  $R_9=R_{10}=R_{11}=R_{12}=R_{13}=R_{14}=R_{15}=R_{16}=(C_2H_4O)_9H$
- 354:  $R_1=R_2=R_3=R_4=R_5=R_6=R_7=R_8=OH$ ,  $R_9=R_{10}=R_{11}=R_{12}=R_{13}=R_{14}=R_{15}=R_{16}=(C_2H_4O)_9H$
- 355:  $R_1=R_2=R_3=R_4=R_5=R_6=R_7=R_8=C(CH_3)_3$ ,  $R_9=R_{10}=R_{11}=R_{12}=R_{13}=R_{14}=R_{15}=R_{16}=(C_2H_4O)_9H$
- 356:  $R_1=R_2=R_3=R_4=R_5=R_6=R_7=R_8=C(CH_3)_2CH_2C(CH_3)_3$ ,  
 $R_9=R_{10}=R_{11}=R_{12}=R_{13}=R_{14}=R_{15}=R_{16}=(C_2H_4O)_9H$
- 357:  $R_1=R_2=R_3=R_4=R_5=R_6=R_7=R_8=OCH_2Ph$ ,  $R_9=R_{10}=R_{11}=R_{12}=R_{13}=R_{14}=R_{15}=R_{16}=(C_2H_4O)_9H$
- 358:  $R_1=R_2=R_3=R_4=R_5=R_6=R_7=R_8=C(CH_3)_3$ ,  $R_9=R_{10}=R_{11}=R_{12}=R_{13}=R_{14}=R_{15}=R_{16}=(C_2H_4O)_{12}H$
- 359:  $R_1=R_2=R_3=R_4=R_5=R_6=R_7=R_8=OCH_2Ph$ ,  $R_9=R_{10}=R_{11}=R_{12}=R_{13}=R_{14}=R_{15}=R_{16}=(C_2H_4O)_{12}H$
- 360:  $R_1=R_2=R_3=R_4=R_5=R_6=R_7=R_8=OCH_2Ph$ ,  $R_9=R_{10}=R_{11}=R_{12}=R_{13}=R_{14}=R_{15}=R_{16}=(C_2H_4O)_{18}H$
- 361:  $R_1=R_2=R_3=R_4=R_5=R_6=R_7=R_8=COC_7H_{15}$ ,  $R_9=R_{10}=R_{11}=R_{12}=R_{13}=R_{14}=R_{15}=R_{16}=C_2H_4OCH_3$
- 362:  $R_1=R_2=R_3=R_4=R_5=R_6=R_7=R_8=COC_{15}H_{31}$ ,  $R_9=R_{10}=R_{11}=R_{12}=R_{13}=R_{14}=R_{15}=R_{16}=C_2H_4OCH_3$
- 363:  $R_1=R_2=R_3=R_4=R_5=R_6=R_7=R_8=COC_7H_{15}$ ,  $R_9=R_{10}=R_{11}=R_{12}=R_{13}=R_{14}=R_{15}=R_{16}=(C_2H_4O)_2CH_3$
- 364:  $R_1=R_2=R_3=R_4=R_5=R_6=R_7=R_8=COC_{15}H_{31}$ ,  $R_9=R_{10}=R_{11}=R_{12}=R_{13}=R_{14}=R_{15}=R_{16}=(C_2H_4O)_2CH_3$
- 365:  $R_1=R_2=R_3=R_4=R_5=R_6=R_7=R_8=H$ ,  $R_9=R_{10}=R_{11}=R_{12}=R_{13}=R_{14}=R_{15}=R_{16}=(C_2H_4O)_3CH_3$
- 366:  $R_1=R_2=R_3=R_4=R_5=R_6=R_7=R_8=C(CH_3)_3$ ,  $R_9=R_{10}=R_{11}=R_{12}=R_{13}=R_{14}=R_{15}=R_{16}=(C_2H_4O)_3CH_3$
- 367:  $R_1=R_2=R_3=R_4=R_5=R_6=R_7=R_8=C(CH_3)_2CH_2C(CH_3)_3$ ,  
 $R_9=R_{10}=R_{11}=R_{12}=R_{13}=R_{14}=R_{15}=R_{16}=(C_2H_4O)_3CH_3$
- 368:  $R_1=R_2=R_3=R_4=R_5=R_6=R_7=R_8=OCH_2Ph$ ,  $R_9=R_{10}=R_{11}=R_{12}=R_{13}=R_{14}=R_{15}=R_{16}=(C_2H_4O)_3CH_3$
- 369:  $R_1=R_2=R_3=R_4=R_5=R_6=R_7=R_8=C(CH_3)_3$ ,  
 $R_9=R_{10}=R_{11}=R_{12}=R_{13}=R_{14}=R_{15}=R_{16}=CH_2COO(C_2H_4O)_{20}C_{16}H_{33}$
- 370:  $R_1=R_2=R_3=R_4=R_5=R_6=R_7=R_8=C(CH_3)_3$ ,  
 $R_9=R_{10}=R_{11}=R_{12}=R_{13}=R_{14}=R_{15}=R_{16}=CH_2COO(C_2H_4O)_{22}C_{16}H_{33}$
- 371:  $R_1=R_2=R_3=R_4=R_5=R_6=R_7=R_8=C(CH_3)_3$ ,  
 $R_9=R_{10}=R_{11}=R_{12}=R_{13}=R_{14}=R_{15}=R_{16}=C_{10}H_{21}COO(OC_2H_4)_2OCH_3$

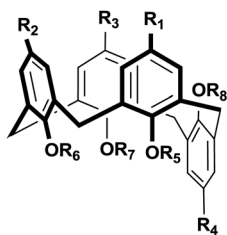
- 372:  $R_1=R_2=R_3=R_4=R_5=R_6=R_7=R_8=H$ ,  $R_9=R_{10}=R_{11}=R_{12}=R_{13}=R_{14}=R_{15}=R_{16}=(C_2H_4O)_3THP$   
 373:  $R_1=R_2=R_3=R_4=R_5=R_6=R_7=R_8=C(CH_3)_3$ ,  $R_9=R_{10}=R_{11}=R_{12}=R_{13}=R_{14}=R_{15}=R_{16}=(C_2H_4O)_3THP$   
 374:  $R_1=R_2=R_3=R_4=R_5=R_6=R_7=R_8=C(CH_3)_2CH_2C(CH_3)_3$ ,  
 $R_9=R_{10}=R_{11}=R_{12}=R_{13}=R_{14}=R_{15}=R_{16}=(C_2H_4O)_3THP$   
 375:  $R_1=R_2=R_3=R_4=R_5=R_6=R_7=R_8=OCH_2Ph$ ,  $R_9=R_{10}=R_{11}=R_{12}=R_{13}=R_{14}=R_{15}=R_{16}=(C_2H_4O)_3THP$   
 376:  $R_1=R_2=R_3=R_4=R_5=R_6=R_7=R_8=H$ ,  $R_9=R_{10}=R_{11}=R_{12}=R_{13}=R_{14}=R_{15}=R_{16}=(C_2H_4O)_6THP$   
 377:  $R_1=R_2=R_3=R_4=R_5=R_6=R_7=R_8=C(CH_3)_3$ ,  $R_9=R_{10}=R_{11}=R_{12}=R_{13}=R_{14}=R_{15}=R_{16}=(C_2H_4O)_6THP$   
 378:  $R_1=R_2=R_3=R_4=R_5=R_6=R_7=R_8=C(CH_3)_2CH_2C(CH_3)_3$ ,  
 $R_9=R_{10}=R_{11}=R_{12}=R_{13}=R_{14}=R_{15}=R_{16}=(C_2H_4O)_6THP$   
 379:  $R_1=R_2=R_3=R_4=R_5=R_6=R_7=R_8=OCH_2Ph$ ,  $R_9=R_{10}=R_{11}=R_{12}=R_{13}=R_{14}=R_{15}=R_{16}=(C_2H_4O)_6THP$   
 380:  $R_1=R_2=R_3=R_4=R_5=R_6=R_7=R_8=OCH_2Ph$ ,  $R_9=R_{10}=R_{11}=R_{12}=R_{13}=R_{14}=R_{15}=R_{16}=(C_2H_4O)_6PMB$   
 381:  $R_1=R_2=R_3=R_4=R_5=R_6=R_7=R_8=H$ ,  $R_9=R_{10}=R_{11}=R_{12}=R_{13}=R_{14}=R_{15}=R_{16}=(C_2H_4O)_9PMB$   
 382:  $R_1=R_2=R_3=R_4=R_5=R_6=R_7=R_8=C(CH_3)_3$ ,  $R_9=R_{10}=R_{11}=R_{12}=R_{13}=R_{14}=R_{15}=R_{16}=(C_2H_4O)_9PMB$   
 383:  $R_1=R_2=R_3=R_4=R_5=R_6=R_7=R_8=C(CH_3)_2CH_2C(CH_3)_3$ ,  
 $R_9=R_{10}=R_{11}=R_{12}=R_{13}=R_{14}=R_{15}=R_{16}=(C_2H_4O)_9PMB$   
 384:  $R_1=R_2=R_3=R_4=R_5=R_6=R_7=R_8=OCH_2Ph$ ,  $R_9=R_{10}=R_{11}=R_{12}=R_{13}=R_{14}=R_{15}=R_{16}=(C_2H_4O)_9PMB$   
 385:  $R_1=R_2=R_3=R_4=R_5=R_6=R_7=R_8=C(CH_3)_3$ ,  $R_9=R_{10}=R_{11}=R_{12}=R_{13}=R_{14}=R_{15}=R_{16}=(C_2H_4O)_{12}PMB$   
 386:  $R_1=R_2=R_3=R_4=R_5=R_6=R_7=R_8=OCH_2Ph$ ,  $R_9=R_{10}=R_{11}=R_{12}=R_{13}=R_{14}=R_{15}=R_{16}=(C_2H_4O)_{12}PMB$   
 387:  $R_1=R_2=R_3=R_4=R_5=R_6=R_7=R_8=OCH_2Ph$ ,  $R_9=R_{10}=R_{11}=R_{12}=R_{13}=R_{14}=R_{15}=R_{16}=(C_2H_4O)_{18}PMB$   
 388:  $R_1=R_2=R_3=R_4=R_5=R_6=R_7=R_8=OCH_2Ph$ ,  $R_9=R_{10}=R_{11}=R_{12}=R_{13}=R_{14}=R_{15}=R_{16}=(C_2H_4O)_6CH_2Ph$   
 389:  $R_1=R_2=R_3=R_4=R_5=R_6=R_7=R_8=OCH_2Ph$ ,  $R_9=R_{10}=R_{11}=R_{12}=R_{13}=R_{14}=R_{15}=R_{16}=(C_2H_4O)_9CH_2Ph$   
 390:  $R_1=R_2=R_3=R_4=R_5=R_6=R_7=R_8=H$ ,  $R_9=R_{10}=R_{11}=R_{12}=R_{13}=R_{14}=R_{15}=R_{16}=(C_2H_4O)_{12}CH_2Ph$   
 391:  $R_1=R_2=R_3=R_4=R_5=R_6=R_7=R_8=C(CH_3)_3$ ,  $R_9=R_{10}=R_{11}=R_{12}=R_{13}=R_{14}=R_{15}=R_{16}=(C_2H_4O)_{12}CH_2Ph$   
 392:  $R_1=R_2=R_3=R_4=R_5=R_6=R_7=R_8=C(CH_3)_2CH_2C(CH_3)_3$ ,  
 $R_9=R_{10}=R_{11}=R_{12}=R_{13}=R_{14}=R_{15}=R_{16}=(C_2H_4O)_{12}CH_2Ph$   
 393:  $R_1=R_2=R_3=R_4=R_5=R_6=R_7=R_8=OCH_2Ph$ ,  $R_9=R_{10}=R_{11}=R_{12}=R_{13}=R_{14}=R_{15}=R_{16}=(C_2H_4O)_{12}CH_2Ph$   
 394:  $R_1=R_2=R_3=R_4=R_5=R_6=R_7=R_8=H$ ,  $R_9=R_{10}=R_{11}=R_{12}=R_{13}=R_{14}=R_{15}=R_{16}=(C_2H_4O)_{18}CH_2Ph$   
 395:  $R_1=R_2=R_3=R_4=R_5=R_6=R_7=R_8=C(CH_3)_3$ ,  $R_9=R_{10}=R_{11}=R_{12}=R_{13}=R_{14}=R_{15}=R_{16}=(C_2H_4O)_{18}CH_2Ph$   
 396:  $R_1=R_2=R_3=R_4=R_5=R_6=R_7=R_8=C(CH_3)_2CH_2C(CH_3)_3$ ,  
 $R_9=R_{10}=R_{11}=R_{12}=R_{13}=R_{14}=R_{15}=R_{16}=(C_2H_4O)_{18}CH_2Ph$   
 397:  $R_1=R_2=R_3=R_4=R_5=R_6=R_7=R_8=OCH_2Ph$ ,  $R_9=R_{10}=R_{11}=R_{12}=R_{13}=R_{14}=R_{15}=R_{16}=(C_2H_4O)_{18}CH_2Ph$   
 398:  $R_1=R_2=R_3=R_4=R_5=R_6=R_7=R_8=H$ ,  $R_9=R_{10}=R_{11}=R_{12}=R_{13}=R_{14}=R_{15}=R_{16}=(C_2H_4O)_{24}CH_2Ph$   
 399:  $R_1=R_2=R_3=R_4=R_5=R_6=R_7=R_8=C(CH_3)_3$ ,  $R_9=R_{10}=R_{11}=R_{12}=R_{13}=R_{14}=R_{15}=R_{16}=(C_2H_4O)_{24}CH_2Ph$   
 400:  $R_1=R_2=R_3=R_4=R_5=R_6=R_7=R_8=C(CH_3)_2CH_2C(CH_3)_3$ ,  
 $R_9=R_{10}=R_{11}=R_{12}=R_{13}=R_{14}=R_{15}=R_{16}=(C_2H_4O)_{24}CH_2Ph$   
 401:  $R_1=R_2=R_3=R_4=R_5=R_6=R_7=R_8=OCH_2Ph$ ,  $R_9=R_{10}=R_{11}=R_{12}=R_{13}=R_{14}=R_{15}=R_{16}=(C_2H_4O)_{24}CH_2Ph$   
 402:  $R_1=R_2=R_3=R_4=R_5=R_6=R_7=R_8=R_9=COC_5H_{11}$ ,  $R_{10}=R_{11}=R_{12}=R_{13}=R_{14}=R_{15}=R_{16}=R_{17}=R_{18}=H$   
 403:  $R_1=R_2=R_3=R_4=R_5=R_6=R_7=R_8=R_9=COC_7H_{15}$ ,  $R_{10}=R_{11}=R_{12}=R_{13}=R_{14}=R_{15}=R_{16}=R_{17}=R_{18}=H$   
 404:  $R_1=R_2=R_3=R_4=R_5=R_6=R_7=R_8=R_9=COC_9H_{19}$ ,  $R_{10}=R_{11}=R_{12}=R_{13}=R_{14}=R_{15}=R_{16}=R_{17}=R_{18}=H$   
 405:  $R_1=R_2=R_3=R_4=R_5=R_6=R_7=R_8=R_9=COC_{11}H_{23}$ ,  $R_{10}=R_{11}=R_{12}=R_{13}=R_{14}=R_{15}=R_{16}=R_{17}=R_{18}=H$   
 406:  $R_1=R_2=R_3=R_4=R_5=R_6=R_7=R_8=R_9=COC_{13}H_{27}$ ,  $R_{10}=R_{11}=R_{12}=R_{13}=R_{14}=R_{15}=R_{16}=R_{17}=R_{18}=H$



Scheme 3 Structures of lower-rim hydrophilic amphiphilic calixarenes.

indeed supported by some reported values. For example, Shinkai and co-workers reported that in amphiphilic SCnAs **3**, **160**, **173**, which have 4, 6, and 8 repeat units respectively, the

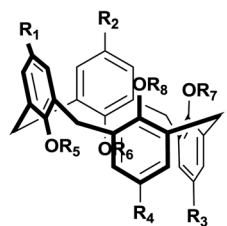
CAC values decrease from 2.5 mM to 1.0 mM and then to 0.7 mM with increasing ring size.<sup>49</sup> Zhao and co-workers synthesized amphiphilic calix[6]arene **305** and calix[8]arene **325** by



408:  $R_1=R_3=R_6=R_8=H$ ,  $R_2=R_4=COOH$ ,  $R_5=R_7=COPh$

409:  $R_1=R_3=R_6=R_7=H$ ,  $R_2=R_4=COOH$ ,  $R_5=R_8=COPh$

410:  $R_1=R_2=R_3=R_4=C(CH_3)_3$ ,  $R_5=R_6=R_7=R_8=C_3H_6NHC(NH_2)_2^+$



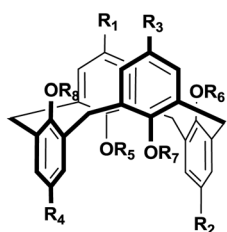
411:  $R_1=R_2=R_3=R_4=C(CH_3)_3$ ,  $R_5=R_6=R_7=R_8=C_3H_6NHC(NH_2)_2^+$

412:  $R_1=R_2=R_3=R_4=COOH$ ,  $R_5=R_6=R_7=R_8=C_3H_7$

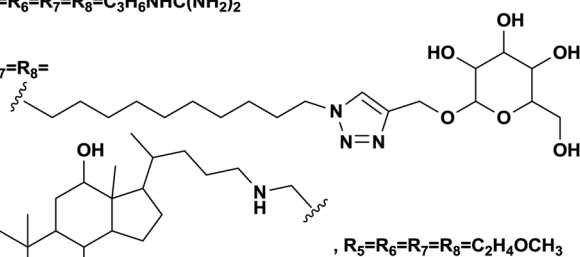
413:  $R_1=R_2=R_3=R_4=COOH$ ,  $R_5=R_6=R_7=R_8=CH(CH_3)_2$

414:  $R_1=R_2=R_3=COOH$ ,  $R_4=H$ ,  $R_5=R_6=R_7=R_8=CH(CH_3)_2$

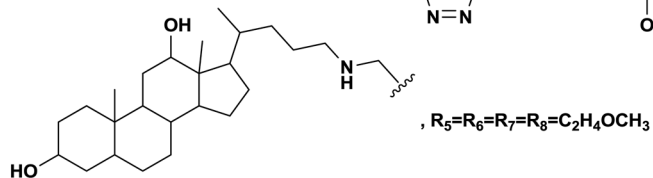
415:  $R_1=R_2=R_3=R_4=C(CH_3)_3$ ,  $R_5=R_6=R_7=R_8=C_3H_6NHC(NH_2)_2^+$



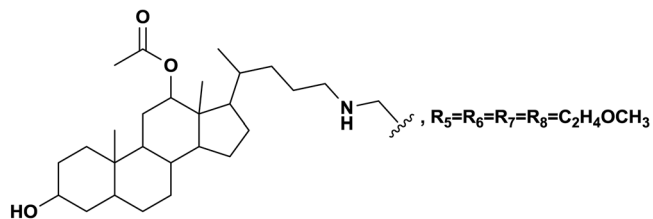
416:  $R_1=R_2=R_3=R_4=H$ ,  $R_5=R_6=R_7=R_8=$



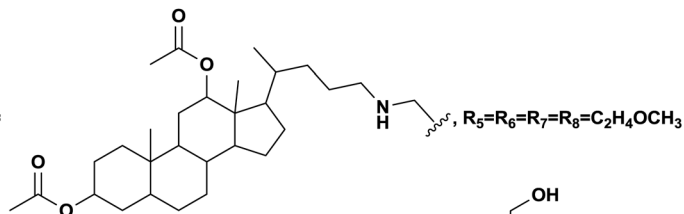
417:  $R_1=R_2=R_3=R_4=$



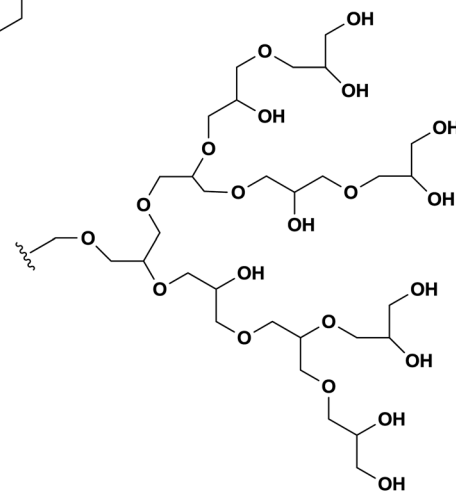
418:  $R_1=R_2=R_3=R_4=$



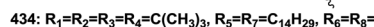
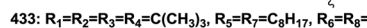
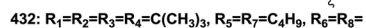
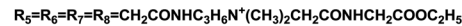
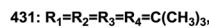
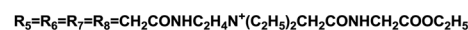
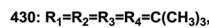
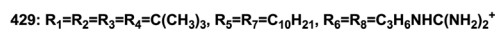
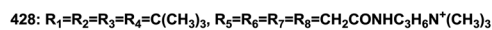
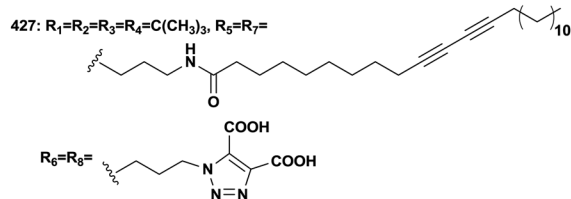
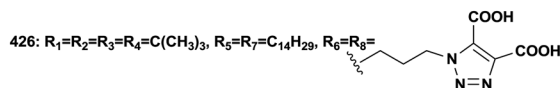
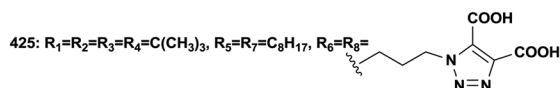
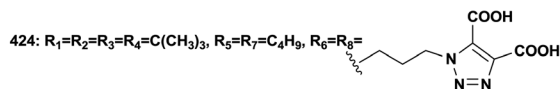
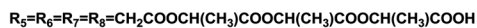
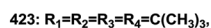
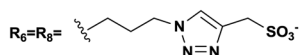
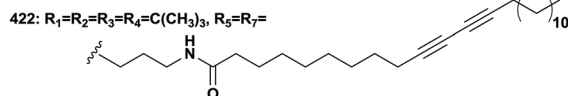
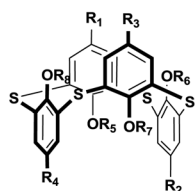
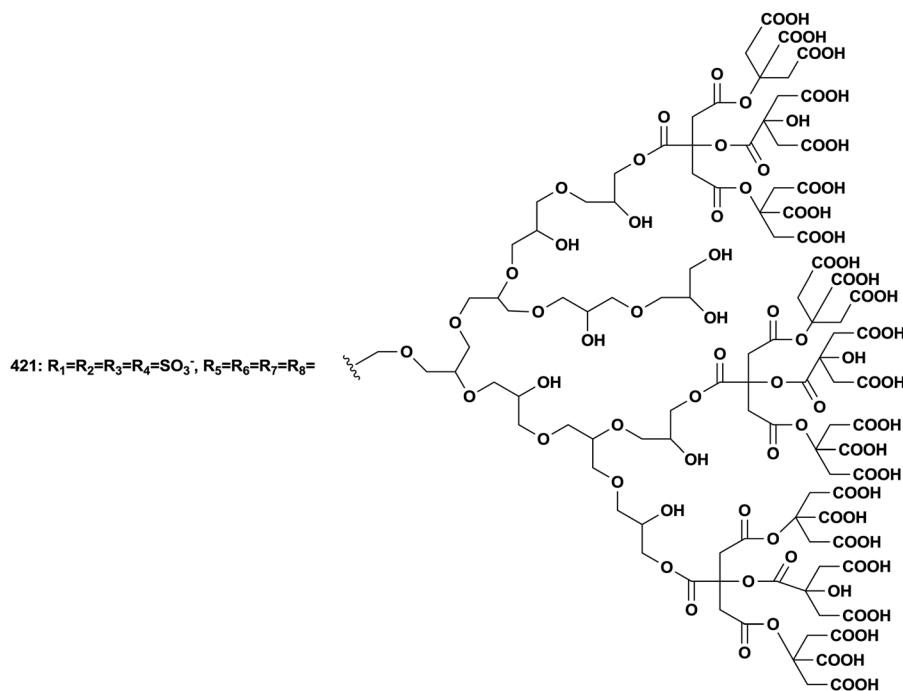
419:  $R_1=R_2=R_3=R_4=$

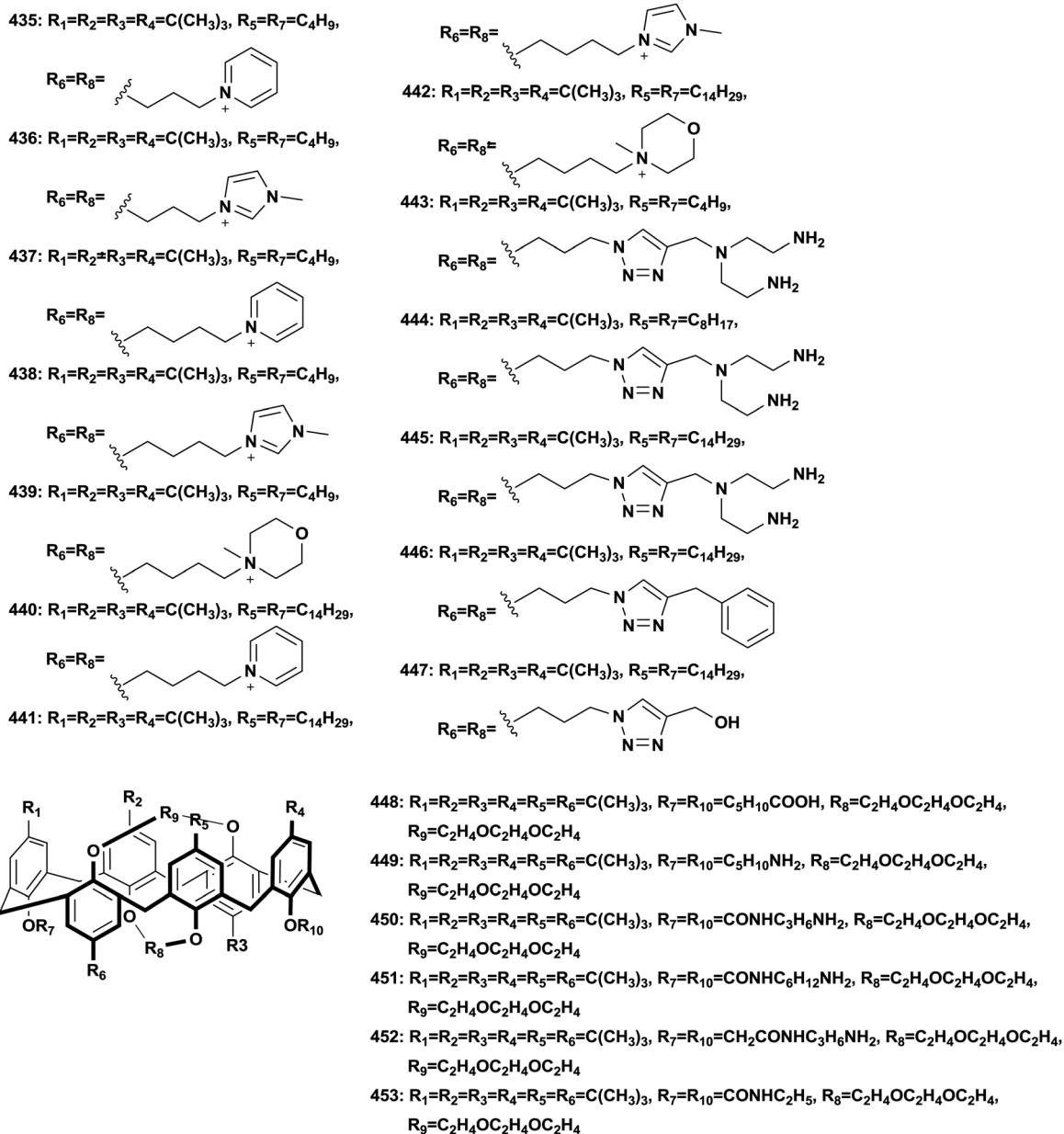


420:  $R_1=R_2=R_3=R_4=SO_3^-$ ,  $R_5=R_6=R_7=R_8=$









Scheme 4 Structures of bola-type amphiphilic calixarenes.

introducing acetoxy groups into the hydroxyls of calixarenes.<sup>259</sup> They interpreted the decrease in CAC (5.79–3.05  $\mu\text{M}$ ) with increasing phenyl groups (6–8) as strengthening of the hydrophobic interactions. However, other examples didn't show any significant trend. For instance, Xu and coworkers found the CAC of choline-modified calix[5]arene **158** (5.5  $\mu\text{M}$ ) is slightly higher than that of the corresponding calix[4]arene, **62** (5.2  $\mu\text{M}$ ).<sup>46</sup> Shinkai and coworkers reported that the CACs of lower-rim sulfonic group modified **186**, **299** and **322** are 0.55 mM, 0.58 mM and 0.40 mM by conductivity at 30  $^{\circ}\text{C}$ , respectively.<sup>49</sup> These unexpected phenomena may be explained by the shape of the skeleton and the conformation in bulk solution. As an example of conformation influencing CAC, Basilio and co-workers studied amphiphilic SCnAs **6**, **162** and **175**. The CAC values increase

(from 0.488 to 0.750 mM) with increasing number of monomeric units (from 4 to 8).<sup>54</sup> The calix[4]arene derivative, which is preorganized into the cone conformation, is favourable for the formation of globular aggregates. The calix[6]arene and calix[8]arene derivatives do not adopt cone conformations in bulk solution. Further thermodynamic studies show that changing these conformations to the more favourable cone conformer in the aggregates implied an energetic cost that contributed to making the micellization Gibbs free energy ( $\Delta G_M^{\circ}$ ) less efficient. The other example related to conformations was reported by Arimori and coworkers.<sup>132</sup> CAC of amphiphilic calix[4]arene **412** in a cone conformation is 10  $\mu\text{M}$  whereas in a 1,3-alternate conformation, **412** could not aggregate at a concentration of even up to 10 mM. This difference implies that the conformation of calixarene is a critical factor of CAC.

Table 1 References of upper-rim hydrophilic amphiphilic calixarenes in Scheme 2

Compound	Ref.	Compound	Ref.	Compound	Ref.	Compound	Ref.
1	37	48	107	94	122 and 124	140	142 and 143
2	44	49	45, 112 and 113	95	124	141	142 and 143
3	49–59	50	45, 112 and 113	96	124	142	142, 143 and 146
4	62–66	51	117–121	97	122	143	63 and 150
5	79	52	45	98	136	144	63 and 150
6	52–54, 58, 64 and 82–89	53	108	99	136	145	150
7	64 and 95	54	108 and 128	100	139	146	63
8	53, 54, 64 and 106	55	108	101	63 and 140	147	63
9	56, 62, 82, 86, 109 and 110	56	131	102	63	148	168
10	114	57	127 and 132	103	94	149	170
11	114 and 116	58	74, 75, 127, 134 and 135	104	94	150	170
12	114 and 126	59	138	105	136	151	170
13	114 and 126	60	42 and 116	106	136	152	176
14	114	61	42 and 43	107	161 and 162	153	177
15	129	62	46 and 47	108	167	154	25 and 179
16	130	63	60	109	167	155	180 and 181
17	116	64	71–77	110	172	156	180
18	43	65	77	111	174	157	107
19	61, 104, 105 and 137	66	72 and 74–77	112	174	158	46
20	130	67	77 and 100–103	113	172	159	37
21	38–40	68	77	114	172	160	49, 59, 82, 106, 148 and 186
22	45	69	77	115	141	161	79
23	45	70	115	116	141 and 182–184	162	5, 49, 53, 54, 82, 86, 147 and 148
24	42, 45, 67–70	71	76	117	145 and 182	163	5, 37, 86, 106, 147 and 151–154
25	23	72	76 and 77	118	141	164	155
26	90	73	76 and 127	119	183	165	158
27	90	74	72 and 76	120	141	166	49 and 160
28	90	75	63	121	141	167	165 and 166
29	111	76	63	122	145	168	73
30	90	77	133	123	149	169	171
31	38	78	63	124	123	170	173
32	40	79	66 and 95	125	157	171	173
33	40	80	43	126	159	172	37
34	41	81	43	127	163 and 164	173	49
35	41	82	48	128	163 and 164	174	79
36	41	83	61	129	169	175	53 and 54
37	41	84	78	130	169	176	37 and 153
38	41	85	81	131	127	177	144
39	41	86	93 and 94	132	175	178	144
40	41	87	61, 104 and 105	133	175	179	144
41	41	88	108	134	178	180	144
42	41	89	108	135	178	181	144
43	41	90	108	136	178	182	144
44	41	91	122–125	137	185	183	144
45	80	92	124	138	185	184	156
46	91 and 92	93	124	139	185	185	156
47	92 and 96–99						

On the other hand, similar to conventional surfactants, CACs of amphiphilic calixarenes are directly related to their hydrophobic/hydrophilic groups and affected by environments (temperature, pH, ionic strength and solvent).

For example, Rodik and co-workers synthesized a series of choline modified amphiphilic calixarenes **64–66** and **69** bearing various lengths of alkyl chains at the lower rim.<sup>77</sup> They found that CACs decreased (390–0.75  $\mu\text{M}$ ) with the increase in the chain length (3–16  $\text{CH}_2$  units). And we have already discussed before that CACs decrease more rapidly with longer alkyl chains.

Introducing extra interactions such as hydrogen bonds is an efficient way to enhance assembly, decreasing the CAC. Consoli and co-workers synthesized two amphiphilic calix[4]arenes **261** and **262** decorated with nucleotides at the lower rim.<sup>229</sup>

The CAC of **262** bearing adenine nucleotides (0.22 mM) is lower than that of **261** bearing thymine nucleotides (0.51 mM), which is consistent with the capacity of adenine to establish stronger stacking interactions with respect to thymine nucleobase.

High salt concentration could reduce electrostatic repulsion of like charges at the hydrophilic head group, resulting in a lower CAC value. Rodik and co-workers synthesized amphiphilic calix[4]arenes **64** and **66** bearing cationic choline groups at the upper rim and alkyl chains at the lower rim.<sup>72</sup> Their CACs were found to be decreased from pure water (0.37 mM for **64** and 0.048 mM for **66**) to 20 mM Tris buffer (0.067 mM for **64** and 0.0062 mM for **66**). Mchedlov-Petrosyan and co-workers found that the CAC of **64** decreased (4–0.12 mM) with increasing concentration of NaCl as well.<sup>73</sup>

Table 2 References of lower-rim hydrophilic amphiphilic calixarenes in Scheme 3

Compound	Ref.	Compound	Ref.	Compound	Ref.	Compound	Ref.	Compound	Ref.
186	49, 187 and 188	236	208	286	235 and 236	336	243	386	245
187	37 and 49	237	200	287	235 and 236	337	243 and 244	387	245
188	194	238	200, 204 and 223	288	237	338	244	388	245
189	197	239	204 and 227	289	247	339	244	389	245
190	197	240	200	290	247	340	248	390	245
191	197	241	200 and 223	291	249	341	244	391	245
192	190, 197 and 201	242	200	292	232 and 250	342	244	392	245
193	203	243	191	293	250	343	244	393	245
194	210	244	191	294	251–254	344	244	394	245
195	199 and 212	245	191	295	257	345	245	395	245
196	203	246	191	296	257	346	245	396	245
197	193	247	191	297	49	347	245	397	245
198	92	248	191	298	49	348	245	398	245
199	113 and 198	249	191	299	49	349	245	399	245
200	198	250	191	300	49	350	245	400	245
201	113	251	191	301	49	351	245	401	245
202	45, 198 and 230	252	191	302	246	352	245	402	262
203	45	253	209	303	246	353	245	403	262
204	113 and 198	254	211	304	246	354	245	404	262
205	238	255	213	305	259	355	245	405	262
206	189	256	213	306	246	356	245	406	262
207	189	257	213	307	246	357	245	407	22
208	189	258	213	308	246	358	245		
209	198	259	213	309	263	359	245		
210	102	260	213	310	264	360	245		
211	198	261	194 and 229	311	242	361	244		
212	202 and 203	262	194 and 229	312	246	362	244		
213	207	263	234	313	246	363	244		
214	207	264	234	314	246	364	244		
215	207	265	234 and 241	315	246	365	245		
216	190, 207 and 215–220	266	192	316	246	366	245		
217	190, 207, 215, 216, 219, 221 and 222	267	192	317	246	367	245		
218	190, 207 and 215–219	268	196	318	195	368	245		
219	190, 193, 201, 207, 215, 216, 225 and 226	269	196	319	255	369	256		
220	207 and 216	270	196	320	255	370	258		
221	207 and 216	271	196	321	49	371	258		
222	231	272	206	322	49	372	245		
223	233	273	206	323	244	373	245		
224	231	274	206	324	244	374	245		
225	239 and 240	275	214	325	259	375	245		
226	190	276	214	326	260 and 261	376	245		
227	193	277	214	327	244	377	245		
228	195	278	224	328	244	378	245		
229	199	279	224	329	244	379	245		
230	200	280	228	330	244	380	245		
231	200	281	228	331	248	381	245		
232	200, 204 and 205	282	188 and 232	332	198	382	245		
233	208	283	235–237	333	243 and 244	383	245		
234	208	284	235–237	334	243	384	245		
235	208	285	235 and 236	335	243	385	245		

Similarly, the pH value could change the protonation states of hydrophilic heads, influencing charge interactions, resulting in a CAC change. Fujii and co-workers synthesized a new amphiphilic calix[4]arene **91** with hydrophilic amino end groups.<sup>122</sup> With pH increasing from 3 (below the  $pK_a$  of amino group) to 8 (above the  $pK_a$  of amino group), the CAC decreased (from 0.11 to 0.042 mM). Further, they prepared a new calix[4]arene-based lipid **101** containing glutamic acid as the hydrophilic group.<sup>63,140</sup> The  $\alpha$ -amine and the  $\gamma$ -carboxylic acid groups of the glutamic acid moiety allowed a continuous change in the state of the head group from cationic to zwitterionic and then to anionic with increasing pH. The CAC at pH 7.5 (1.0  $\mu$ M) was

lower than that obtained under other pH conditions (4.4  $\mu$ M at pH 3.2 and 1.8  $\mu$ M at pH 10) because the intermolecular electrostatic repulsions are cancelled by the zwitterionic nature.

**2.2.2 Diverse morphology.** Besides CAC, morphology is another important property of amphiphilic assembly. It is not only an interesting topic in fundamental research, but also related to potential applications. NMR, DOSY, small-angle X-ray scattering (SAXS), and photo correlation spectroscopy (PCS) are methods that could be used to measure the size and shape of aggregates, while transmission electron microscopy (TEM), scanning electron microscopy (SEM), and AFM could provide us with more intuitional pictures. We summarize self-assembling

Table 3 References of bola-type amphiphilic calixarenes in Scheme 4

Compound	Ref.	Compound	Ref.	Compound	Ref.	Compound	Ref.
408	40	420	265	432	266	444	267
409	40	421	265	433	266	445	267
410	230	422	268	434	266	446	269
411	230	423	270	435	271	447	269
412	40	424	272	436	271	448	273
413	40	425	272	437	271	449	273
414	40	426	269	438	271	450	273
			and				
			272				
415	230	427	268	439	271	451	273
416	274	428	232	440	271	452	242
							and
							275–
							277
417	228	429	120	441	271	453	273
418	228	430	247	442	271	—	—
419	228	431	247	443	267	—	—

morphologies of all reported amphiphilic calixarenes in aqueous solution in Table 5, which does not include Langmuir–Blodgett films formed at the air–water interface.

Compared with corresponding conventional surfactants, self-assemblies of amphiphilic calixarenes show diverse morphologies. For example, sodium dodecyl sulphate (SDS) forms spherical micelles with an average radius of 2.09 nm.<sup>280</sup> Its corresponding calixarene, amphiphilic sulfonatocalix[4]arene **9**, forms micelles with an average radius of 6.9 nm<sup>109</sup> and the hexameric derivative **163** forms aggregates with various sizes (radii from about 70 nm to 195 nm) depending on the concentration.<sup>154</sup> For positively charged surfactants, dodecylguanidine hydrochloride forms micelles as well,<sup>281</sup> while the amphiphilic guanidinium-modified calix[4]arene **51** is able to form SLN with an average radius of 73 nm.<sup>117</sup> Such great differences mainly come from their unique skeletons. It is well known that the critical packing parameter (CPP) proposed by Israelachvili and coworkers is a parameter to estimate the morphology of an amphiphilic assembly.<sup>282</sup> Definition of the CPP value is  $P = V_H/(a_0l_c)$ , where  $V_H$  is the volume occupied by hydrophobic groups in the assembly core,  $a_0$  is cross-sectional area occupied by the hydrophilic group at the assembly–solution interface, and  $l_c$  is the chain length of the hydrophobic group in the assembly core. However, the CPP is hard to precisely apply in the case of macrocyclic amphiphiles. Various sizes and conformations of skeletons result in complicated, unpredictable, and diverse morphologies.

For example, Zhao and coworkers reported fully carboxylic acid modified amphiphilic calix[6]arene **305** and calix[8]arene **325**.<sup>259</sup> The mean radius of aggregates of **305** ( $111.2 \pm 17.4$  nm) is larger than that of **325** ( $89.8 \pm 14.8$  nm). Similarly, Xu and coworkers investigated choline modified amphiphilic calix[4]arene **62** and calix[5]arene **158**.<sup>46</sup> Despite their similar CAC values, the average radius of vesicles of **62** (75 nm) is almost two fold that of **158** (40 nm) (Fig. 2). The explanation of decreasing diameter with a larger skeleton is controversial; it may be related to an enhanced hydrophobic effect, different symmetry, or lower entropy loss. Exceptionally, Basilio and coworkers reported that an ellipsoidal micelle of amphiphilic sulfonatocalix[8]arene **175**

has a longer main semiaxis (7.3 nm) than that of calix[6]arene **162** (6.6 nm), which is the result of a more flexible conformation of calix[8]arene.<sup>54</sup>

Conformation is also an important factor. Stoikov's group reported a series of quaternary ammonium-modified amphiphilic calix[4]arenes which have the same decoration and different conformations (**283**, **289** and **290** in cone conformation and **428**, **430** and **431** in 1,3-alternate conformation).<sup>232,247</sup> At a concentration of 0.3 mM, the radius of assembly of **283** (227 nm) is larger than that of **428** (71 nm). At a concentration of 1 mM, the radius of assembly of **289** (70.8 nm) is larger than that of **430** (49.9 nm) while the radius of assembly of **290** (37.7 nm) is smaller than that of **431** (46.4 nm). We assume that conformations of skeletons in assemblies affect the curvature and sizes of assemblies due to different aggregation modes.

Certainly, the length of hydrophobic chains and the structure of hydrophilic head groups could affect the morphologies of aggregates. For instance, increasing the hydrophobic chain from 6 carbons to 9 carbons causes different morphologies of amphiphilic aminocalix[4]arenes **94** and **97** assemblies, which are micelle and cylinder respectively (Fig. 2).<sup>122</sup> For a series of amphiphilic calixarenes that show similar aggregation morphologies, some of them present a trend in size. Jebors and coworkers reported several SLNs assembled by acylcalix[9]arenes with different lengths of the carbon chain (**402–406**). The sizes of their aggregates decrease with increasing carbon atoms (radii decrease from 108 nm to 41 nm).<sup>262</sup> Similarly, Burirov and coworkers studied two kinds of amine modified amphiphilic calixarenes with 4 carbons (**98** and **105**) and 8 carbons (**99** and **106**) as the hydrophobic chain, respectively.<sup>136</sup> **98** and **99** are completely modified whereas **105** and **106** are partially modified. Aggregates of **98** and **105** show larger radii (88 nm and 97 nm, respectively) than those of **99** and **106** (70 nm and 77 nm, respectively), respectively. In principle, more and longer hydrophobic chains lead to a stronger hydrophobic effect, resulting in more compact packing, which leads to smaller aggregates. However, there are contrary examples such as a series of cyclodextrin modified amphiphilic calixarenes **127** and **128**, whose aggregate size increases with increasing carbon chain (radii increase from 65 nm to 95 nm).<sup>163,164</sup> This phenomenon may be related to the large volume of cyclodextrin. Besides, the aggregates of bola-type amphiphilic calixarenes **432–434** are of the same size, although they bear 4-carbon chains, 8-carbon chains, and 14-carbon chains, respectively.<sup>266</sup> In brief, we just find limited examples of hydrophobic chains affecting the morphology with a certain trend, while in many cases, morphologies vary irregularly with chain length.

Hydrophilic head affecting the aggregation morphology is an even more complicated topic. Factors such as volume, hydration energy, and interactions between hydrophilic head groups may give us a clue, but it is still difficult to predict aggregate morphologies from their structure. Here we just name several examples that may provide some ideas. Stoikov and coworkers<sup>235–237,247</sup> synthesized several amphiphilic butylthiacalix[4]arenes with quaternary ammonium, as well as amide (**289**, **290**), ester (**287**), benzene (**284**), or phthalimide

Table 4 CACs of amphiphilic calixarenes

Compound	CAC (mM)	Condition <sup>a</sup>	Method <sup>b</sup>	Ref.
3	2.5	30 °C	Conductivity	49
3	3.05	15 °C	ITC	53
3	3.20		ITC	53
3	3.40	35 °C	ITC	53
3	3.73	45 °C	ITC	53
3	4.16	55 °C	ITC	53
3	3.18		Conductivity	54
4	$(8.98 \pm 2.69) \times 10^{-2}$	10 mM NaCl	Fluorescence	65
4	$(5.84 \pm 4.49) \times 10^{-2}$	15 mM NaCl	Fluorescence	65
4	0.566	50 mM NaCl	Fluorescence	66
6	0.54		Fluorescence	84
6	0.32	D <sub>2</sub> O	DOSY	84
6	0.450	15 °C	ITC	53
6	0.488		ITC	53
6	0.520	35 °C	ITC	53
6	0.600	45 °C	ITC	53
6	0.689	55 °C	ITC	53
6	0.491		Conductivity	54
6	0.040	10 mM NaCl	Fluorescence	64
7	0.020	10 mM NaCl	Fluorescence	64
8	0.0700	15 °C	ITC	53
8	0.0850		ITC	53
8	0.0940	35 °C	ITC	53
8	0.112	45 °C	ITC	53
8	0.150	55 °C	ITC	53
8	0.0911		Conductivity	54
9	0.02		Fluorescence	109
15	0.0285		AFM	129
21	0.65	pH 10 NaHCO <sub>3</sub> , <i>I</i> = 0.123 M	UV-vis	38
31	0.045	pH 10 NaHCO <sub>3</sub> , <i>I</i> = 0.123 M	UV-vis	38
31	0.035	pH 10 NaHCO <sub>3</sub> , <i>I</i> = 0.123 M	UV-vis	38
34	1	pH 6, 20 °C	Surface tension	41
34	1.3	pH 8, 20 °C	Surface tension	41
35	1.6	pH 6, 20 °C	Surface tension	41
35	1.3	pH 8, 20 °C	Surface tension	41
36	1.3	pH 6, 20 °C	Surface tension	41
36	1	pH 8, 20 °C	Surface tension	41
37	1.2	pH 6, 20 °C	Surface tension	41
37	1.1	pH 8, 20 °C	Surface tension	41
38	1.3	pH 6, 20 °C	Surface tension	41
38	1.2	pH 8, 20 °C	Surface tension	41
39	1.2	pH 6, 20 °C	Surface tension	41
39	1	pH 8, 20 °C	Surface tension	41
40	1.2	pH 6, 20 °C	Surface tension	41
40	1.1	pH 8, 20 °C	Surface tension	41
41	1.2	pH 6, 20 °C	Surface tension	41
41	0.2	pH 8, 20 °C	Surface tension	41
42	0.1	pH 6, 20 °C	Surface tension	41
42	0.4	pH 8, 20 °C	Surface tension	41
43	0.5	pH 6, 20 °C	Surface tension	41
43	0.1	pH 8, 20 °C	Surface tension	41
44	0.1	pH 6, 20 °C	Surface tension	41
44	0.1	pH 8, 20 °C	Surface tension	41
46	0.023		Conductivity	91
46	0.056	pH 7 Na <sup>+</sup> /K <sup>+</sup> PB	Fluorescence	91
46	0.037	pH 9 Na <sup>+</sup> borate	Fluorescence	91
46	0.041	pH 7 Na <sup>+</sup> /K <sup>+</sup> PB	Fluorescence	91
46	0.0021	pH 9 Na <sup>+</sup> borate	Fluorescence	91
46	0.073	pH 7 Na <sup>+</sup> /K <sup>+</sup> PB	Fluorescence	91
46	0.052	pH 9 Na <sup>+</sup> borate	Fluorescence	91
46	0.04	pH 7 Na <sup>+</sup> /K <sup>+</sup> PB	Fluorescence	91
46	0.043	pH 9 Na <sup>+</sup> borate,	Fluorescence	91
47	≤0.04	<i>I</i> = 0.07 M	Fluorescence	98
49	0.2	D <sub>2</sub> O	<sup>1</sup> H NMR	112
57	0.01	17 °C	Surface tension	132
57	0.01	30 °C	Fluorescence	132
57	3.8		<sup>1</sup> H NMR	127
58 (I <sup>-</sup> )	8.7		<sup>1</sup> H NMR	127
58 (Cl <sup>-</sup> )	0.00879	22–23 °C	Surface tension	75
58 (Cl <sup>-</sup> )	9.8	22–23 °C; 30 °C	UV-vis, osmolality, surface tension	134

Table 4 (continued)

Compound	CAC (mM)	Condition <sup>a</sup>	Method <sup>b</sup>	Ref.
62	0.0052		Fluorescence	46
64	0.37		Fluorescence	72
64	0.067	20 mM Tris, pH 7.4	Fluorescence	72
64	0.081	20 mM Tris, pH 7.4, 150 mM NaCl	Fluorescence	72
64	4		UV-vis	73
64	0.12	0.05 mM NaCl	UV-vis	73
64	0.367	22–23 °C	Surface tension	75
64	0.39		Fluorescence	77
64	0.068	20 mM PB, pH 7.4	Fluorescence	77
64	0.064	20 mM PB, pH 7.4, 150 mM NaCl	Fluorescence	77
65	0.026		Fluorescence	77
65	0.0098	20 mM PB, pH 7.4	Fluorescence	77
65	0.0044	20 mM PB, pH 7.4, 150 mM NaCl	Fluorescence	77
66	0.048		Fluorescence	72
66	0.0062	20 mM Tris, pH 7.4	Fluorescence	72
66	0.003	20 mM Tris, pH 7.4, 150 mM NaCl	Fluorescence	72
66	0.019		Fluorescence	77
66	0.0044	20 mM PB, pH 7.4	Fluorescence	77
66	0.0027	20 mM PB, pH 7.4, 150 mM NaCl	Fluorescence	77
66	0.0478	22–23 °C	Surface tension	75
67	0.008		Fluorescence	101
69	0.00075		Fluorescence	77
69	0.001	20 mM PB, pH 7.4	Fluorescence	77
72	0.017		Fluorescence	77
72	0.0036	20 mM PB, pH 7.4	Fluorescence	77
72	0.0030	20 mM PB, pH 7.4, 150 mM NaCl	Fluorescence	77
72	0.014	20 mM acetate, pH 5	Fluorescence	77
73	1.4		<sup>1</sup> H NMR	127
74	0.01		Fluorescence	72
74	0.0029	20 mM Tris, pH 7.4	Fluorescence	72
74	0.0018	20 mM Tris, pH 7.4, 150 mM NaCl	Fluorescence	72
82	0.33		Fluorescence	48
91	0.11	50 mM NaCl, pH 3.0	Fluorescence	122
91	0.042	50 mM NaCl, pH 8.0	Fluorescence	122
91	0.11	pH 8.0 Tris-HCl, 50 mM NaCl	Fluorescence	123
91	0.11	pH 3.0, 50 mM NaCl	UV-vis	124
94	0.0040	50 mM NaCl, pH 3.0	Fluorescence	122
97	0.0029	50 mM NaCl, pH 3.0	Fluorescence	122
98	0.0045	MES pH 6.5	Fluorescence	136
98	0.0050	MES pH 6.5	Fluorescence	136
99	0.0028	MES pH 6.5	Fluorescence	136
99	0.0050	MES pH 6.5	Fluorescence	136
101	$(4.4 \pm 0.2) \times 10^{-3}$	50 mM NaCl, pH 3.0	Fluorescence	140
101	$(1.0 \pm 0.1) \times 10^{-3}$	50 mM NaCl, pH 8.3	Fluorescence	140
101	$(1.8 \pm 0.2) \times 10^{-3}$	pH 10, 50 mM NaCl	Fluorescence	140
101	0.0044	pH 3.2	—	63
101	0.0010	pH 7.5	—	63
101	0.0018	pH 10	—	63
105	0.0064	MES pH 6.5	Fluorescence	136
105	0.79	MES pH 6.5	Fluorescence	136
106	0.0048	MES pH 6.5	Fluorescence	136
106	0.16	MES pH 6.5	Fluorescence	136
108	$(1.8 \pm 0.2) \times 10^{-3}$	150 mM NaCl	Fluorescence	167
109	$(5.0 \pm 1.0) \times 10^{-4}$	150 mM NaCl	Fluorescence	167
124 (D)	0.13	pH 8.0 Tris-HCl, 50 mM NaCl	Fluorescence	123
124 (L)	0.10	pH 8.0 Tris-HCl, 50 mM NaCl	Fluorescence	123
125	0.00154	50 mM NaCl	Fluorescence	157
126	0.025		Fluorescence, surface tension	159
131	0.21	37 °C	Relaxivity	278
132	2.3		Relaxivity	175
133	0.12		Relaxivity	175
140	0.019		Fluorescence	142
141	0.015		Fluorescence	142
142	0.013		Fluorescence	146
142	0.013		Fluorescence	142
143	0.00014	50 mM NaCl	Fluorescence	150
144	0.00027	50 mM NaCl	Fluorescence	150
145	0.0045	50 mM NaCl	Fluorescence	150
158	0.0055		Fluorescence	46
160	1	30 °C	Conductivity	49

Table 4 (continued)

Compound	CAC (mM)	Condition <sup>a</sup>	Method <sup>b</sup>	Ref.
162	0.5	30 °C	Surface tension	5
162	0.67	30 °C	Conductivity	5
162	0.5	30 °C	Fluorescence	5
162	0.636	15 °C	ITC	53
162	0.751		ITC	53
162	0.850	35 °C	ITC	53
162	0.904	45 °C	ITC	53
162	0.957	55 °C	ITC	53
162	0.734		Conductivity	54
163 (micelle)	0.6		DLS	154
163 (domain)	$1 \times 10^{-4}$		DLS	154
163 (nanoassociate)	$1 \times 10^{-6}$		DLS	154
164	0.1		UV-vis	155
166	0.1	30 °C	Surface tension	49
166	0.16	30 °C	Conductivity	49
170	$(7.9 \pm 0.5) \times 10^{-3}$		Fluorescence	173
171	$(8.0 \pm 0.2) \times 10^{-3}$		Fluorescence	173
173	0.5	30 °C	Surface tension	49
173	0.7	30 °C	Conductivity	49
175	0.700	15 °C	ITC	53
175	0.750		ITC	53
175	0.810	35 °C	ITC	53
175	0.894	45 °C	ITC	53
175	0.994	55 °C	ITC	53
175	0.729		Conductivity	54
186	0.56	30 °C	Surface tension	49
186	0.55	30 °C	Conductivity	49
223	0.0005		UV-vis	257
230	0.4	10% DMF aqueous	Surface tension	200
231	CAC <sub>1</sub> : 0.95; CAC <sub>2</sub> : 5.0 <sup>c</sup>	10% DMF aqueous	Surface tension	200
232	CAC <sub>2</sub> : 2.2; CAC <sub>3</sub> : 80 <sup>c</sup>		Surface tension	200
232	2			205
233	2.2			208
234	2.1			208
236	2.1			208
237	0.1	10% DMF aqueous	Surface tension	200
238	CAC <sub>1</sub> : 0.6; CAC <sub>2</sub> : 3.8; CAC <sub>3</sub> : 75 <sup>c</sup>		Surface tension	200
238	6.5		Viscosity	200
238	CAC <sub>1</sub> : 0.95; CAC <sub>2</sub> : 6.0; CAC <sub>3</sub> : 60 <sup>c</sup>	10% DMF aqueous	Surface tension	200
238	27	10% DMF aqueous	Viscosity	200
239	2.1			204
239	2.7			227
240	CAC <sub>1</sub> : 0.2; CAC <sub>2</sub> : 2.0; CAC <sub>3</sub> : 16 <sup>c</sup>		Surface tension	200
240	78		Viscosity	200
240	CAC <sub>1</sub> : 0.95; CAC <sub>2</sub> : 7.6; CAC <sub>3</sub> : 60 <sup>c</sup>	10% DMF aqueous	Surface tension	200
240	CAC <sub>2</sub> : 36; CAC <sub>3</sub> : 65 <sup>c</sup>	10% DMF aqueous	Viscosity	200
241	CAC <sub>1</sub> : 0.18; CAC <sub>2</sub> : 4.5 <sup>c</sup>		Surface tension	200
241	5.5		Viscosity	200
242	CAC <sub>1</sub> : 0.13; CAC <sub>2</sub> : 0.9 <sup>c</sup>		Surface tension	200
242	2.5		Viscosity	200
261	0.51		Fluorescence	229
262	0.22		Fluorescence	229
294	0.64	D <sub>2</sub> O	DOSY	252
294	1.15	D <sub>2</sub> O	DOSY	254
296	0.0045		UV-vis	257
298	0.43	30 °C	Conductivity	49
299	0.61	30 °C	Surface tension	49
299	0.58	30 °C	Conductivity	49
300	0.21	30 °C	Surface tension	49
300	0.25	30 °C	Conductivity	49
305	0.00579		Fluorescence	259
322	0.15	30 °C	Surface tension	49
322	0.40	30 °C	Conductivity	49
325	0.00305		Fluorescence	259
407	CAC <sub>1</sub> : 0.19; CAC <sub>2</sub> : 6.9 <sup>c</sup>		Surface tension	22
416	0.016		Fluorescence	274
432	$(91 \pm 5) \times 10^{-3}$	pH 7.4 Tris, pyrene	Fluorescence	266
432	$(2.0 \pm 0.1) \times 10^{-3}$	pH 7.4 Tris, EY	Fluorescence	266
433	$(59 \pm 3) \times 10^{-3}$	pH 7.4 Tris, pyrene	Fluorescence	266



Table 4 (continued)

Compound	CAC (mM)	Condition <sup>a</sup>	Method <sup>b</sup>	Ref.
433	$(2.6 \pm 0.2) \times 10^{-3}$	pH 7.4 Tris, EY	Fluorescence	266
434	$(33 \pm 2) \times 10^{-3}$	pH 7.4 Tris, pyrene	Fluorescence	266
434	$(2.0 \pm 0.1) \times 10^{-3}$	pH 7.4 Tris, EY	Fluorescence	266
443	0.024		Fluorescence	267
444	0.025		Fluorescence	267
445	0.009		Fluorescence	267

<sup>a</sup> The condition is 25 °C in pure water if no label. *I* is the ionic strength. EY is Eosin Y. <sup>b</sup> ITC: isothermal titration microcalorimetry, DOSY: diffusion-ordered spectroscopy, AFM: atomic force microscopy, NMR: nuclear magnetic resonance. <sup>c</sup> The nomenclature and values of CAC<sub>1</sub>, CAC<sub>2</sub>, and CAC<sub>3</sub> were taken from the original literature without any change.

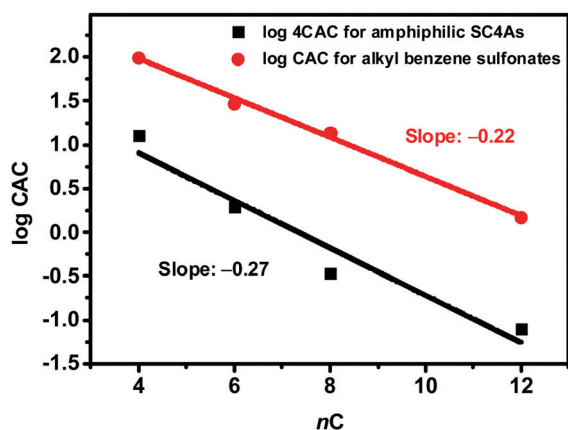


Fig. 1 Variation of the CAC with the number of carbons (*nC*) per alkyl chain for amphiphilic SC4As and alkyl benzene sulfonates.

(286) as hydrophilic groups. The 287 assembly has a significantly smaller radius (1.9 nm) than those of 284 (30.7 nm), 286 (7.3 nm), 289 (> 70.8 nm, Tris buffer) and 290 (> 37.7 nm, Tris buffer), owing to the small size of the ester. Similar results were reported by Shahgaldian and coworkers on diethylphosphate and phosphate modified calixarene, 192 (130 nm) and 226 (163 nm), respectively.<sup>190</sup> On the other hand, Li and coworkers reported cyclodextrin modified calixarene 279 and 278, which possess one and two  $\beta$ -cyclodextrins respectively.<sup>224</sup> In pure water, 279 forms small linear or dot like assemblies, whereas 278 shows large sheet like aggregations (Fig. 2). This phenomenon could be explained by hydrogen bonds between cyclodextrins. Besides, Klymchenko's group synthesized amphiphilic calixarenes modified by choline (66) and a *N*-(2-aminoethyl)-*N,N*-dimethylammonium group (72).<sup>76,77</sup> DLS results showed the micelles of 72 (3.04 nm) are little larger than those of 66 (2.82 nm), probably due to the larger hydration shell of amino groups as compared to hydroxyls. However, there are some examples showing that the morphology is not significantly influenced by different hydrophilic head groups. For example, Burilov and coworkers compared assembly behavior of amphiphilic thiocalix[4]arenes bearing carboxyl (427) and sulfonic (422) groups, respectively; these two compounds show similar shape and size.<sup>268</sup> Compounds 212, 196, and 193, reported by Martin and coworkers, which possess amine, aminodiacetate, and phosphate groups, respectively, present similar results.<sup>202,203</sup>

The morphologies of assemblies are largely related to experimental conditions<sup>283</sup> such as concentration. For example, Padnya and coworkers reported a series of quaternary ammonium based thiocalix[4]arenes 289 and 290, whose aggregate sizes increase with decreasing concentration (radii increase from 70.8 nm to 244.4 nm and from 37.7 nm to 226.9 nm, respectively, with concentration decrease from 1 mM to 1  $\mu$ M).<sup>247</sup> The authors assume that this phenomenon can be explained by the existence of two kinds of aggregates, spherical aggregates and elongated self-associates.

On the other hand, properties of solvents may modulate the morphology of amphiphilic calixarene assemblies, mainly by influencing the interactions of hydrophilic head groups. For instance, the polarity of solvent affects hydrogen bonds, resulting in a change in the packing mode of some amphiphiles. Liang and coworkers synthesized amphiphilic calix[6]biscrowns 450 and 451 possessing amide groups, interacting with each other *via* hydrogen bonds, at the hydrophilic part.<sup>273</sup> Their morphologies underwent a clear transition from spherical to tubular aggregates when the solvent polarity, *i.e.* content of water in water/ethanol solution, is increased (Fig. 2), whereas analogues 448 and 449, without any amide linkage, only showed a size decrease upon the same change in solvent polarity. Similarly, two cyclodextrin modified amphiphilic calix[4]arenes 278 and 279,<sup>224</sup> which we have already mentioned before, also present different assembly patterns in different solvents. With decreasing polarity, the morphology of 279 transferred from dots to linear aggregates and then to vesicles; meanwhile, 278 changed from sheet-like to bundle-like aggregations. All these examples show that lower solvent polarity enhances hydrogen bonds between head groups, resulting in larger aggregates.

pH of the solution is a common factor to modulate assembly morphology, by influencing electrostatic interactions and hydrophobicity. For groups whose  $pK_a$  values are in a regular range, such as amine, carboxyl acid, and pyridine, adjusting the pH could change the number of charges they possess. More like charges at the hydrophilic head cause stronger repulsion, resulting in a larger curvature. For example, Martin and coworkers reported a phosphate modified amphiphilic calix[4]arene 196, whose major assembly morphology is bilayer at pH 4.1 while small micelles at pH 12.<sup>203</sup> On the other hand, Houmadi and coworkers reported a sulfonatocalix[6]arene 164 with imidazolyl groups at the upper rim.<sup>155</sup> At pH 6.5, the average radius of its assembly is 25 nm, which is much smaller than those at pH 7.8 (25–125 nm) and

Table 5 Morphologies of amphiphilic calixarenes

Compound	Morphology <sup>a</sup>	Radius <sup>b</sup> (nm)	Condition <sup>c</sup>	Method <sup>d</sup>	Ref.
3	Ellipsoidal micelle	Minor: 1.15, major: 6.6 (prolate); 3.5 (oblate)	D <sub>2</sub> O	DOSY	54
4	Spherical micelle	$R_s$ : 2.13; $R_g$ : 1.64 ± 0.02	10 mM NaCl	SAXS	65
4	Spherical micelle	$R_s$ : 2.19; $R_g$ : 1.73 ± 0.03	15 mM NaCl	SAXS	65
6	Ellipsoidal micelle	Major: 4.6	D <sub>2</sub> O	DOSY	84
6	Ellipsoidal micelle	Minor: 1.40, major: 8.9 (prolate); 4.6 (oblate)	D <sub>2</sub> O	DOSY	54
6	Spherical micelle	$R_s$ : 2.40; $R_g$ : 1.97	10 mM NaCl	SAXS	64
7	Spherical micelle	$R_s$ : 2.65; $R_g$ : 2.15	10 mM NaCl	SAXS	64
8	Ellipsoidal micelle	Minor: 1.65, major: 7.8 (prolate); 4.3 (oblate)	D <sub>2</sub> O	DOSY	54
8	Spherical micelle	$R_s$ : 2.10	10 mM NaCl	SAXS	64
9	Micelle	6.9		DLS, AFM	109
11	Micelle	2.1–2.8	Various pH	DLS	114
12	SLN	85		DLS, AFM	126
12	SLN	78 ± 1	0.1 mM NaCl	DLS, AFM	126
12	SLN	81 ± 2	1 mM NaCl	DLS, AFM	126
12	SLN	81 ± 1	15 mM NaCl	DLS, AFM	126
12	SLN	80 ± 1	145 mM NaCl	DLS, AFM	126
12	SLN	66 ± 1	0.1 mM KCl	DLS, AFM	126
12	SLN	76 ± 3	1 mM KCl	DLS, AFM	126
12	SLN	86 ± 1	5 mM KCl	DLS, AFM	126
12	SLN	83 ± 2	140 mM KCl	DLS, AFM	126
12	SLN	85 ± 1	145 mM KCl	DLS, AFM	126
12	SLN	64 ± 1	0.1 mM CaCl <sub>2</sub>	DLS, AFM	126
12	SLN	60 ± 1	0.5 mM CaCl <sub>2</sub>	DLS, AFM	126
12	SLN	59 ± 1	1 mM CaCl <sub>2</sub>	DLS, AFM	126
12	SLN	105 ± 1	2 mM CaCl <sub>2</sub>	DLS, AFM	126
12	SLN	371 ± 13	2.5 mM CaCl <sub>2</sub>	DLS, AFM	126
12	SLN	1206 ± 1179	3 mM CaCl <sub>2</sub>	DLS, AFM	126
12	SLN	1429 ± 433	4 mM CaCl <sub>2</sub>	DLS, AFM	126
12	SLN	1560 ± 485	5 mM CaCl <sub>2</sub>	DLS, AFM	126
12	SLN	815 ± 1393	145 mM CaCl <sub>2</sub>	DLS, AFM	126
12	SLN	74 ± 2	0.1 mM MgCl <sub>2</sub>	DLS, AFM	126
12	SLN	64 ± 1	0.5 mM MgCl <sub>2</sub>	DLS, AFM	126
12	SLN	62 ± 1	1 mM MgCl <sub>2</sub>	DLS, AFM	126
12	SLN	104 ± 1	2 mM MgCl <sub>2</sub>	DLS, AFM	126
12	SLN	141 ± 6	2.5 mM MgCl <sub>2</sub>	DLS, AFM	126
12	SLN	507 ± 25	3 mM MgCl <sub>2</sub>	DLS, AFM	126
12	SLN	1048 ± 497	5 mM MgCl <sub>2</sub>	DLS, AFM	126
12	SLN	1247 ± 435	10 mM MgCl <sub>2</sub>	DLS, AFM	126
12	SLN	1141 ± 647	20 mM MgCl <sub>2</sub>	DLS, AFM	126
12	SLN	962 ± 1314	30 mM MgCl <sub>2</sub>	DLS, AFM	126
12	SLN	757 ± 493	145 mM MgCl <sub>2</sub>	DLS, AFM	126
13	SLN	69		DLS, AFM	126
13	SLN	69 ± 1	0.1 mM NaCl	DLS, AFM	126
13	SLN	69 ± 1	1 mM NaCl	DLS, AFM	126
13	SLN	68 ± 2	15 mM NaCl	DLS, AFM	126
13	SLN	66 ± 2	145 mM NaCl	DLS, AFM	126
13	SLN	70 ± 1	0.1 mM KCl	DLS, AFM	126
13	SLN	68 ± 1	1 mM KCl	DLS, AFM	126
13	SLN	65 ± 1	5 mM KCl	DLS, AFM	126
13	SLN	66 ± 1	140 mM KCl	DLS, AFM	126
13	SLN	66 ± 2	145 mM KCl	DLS, AFM	126
13	SLN	69 ± 3	0.1 mM CaCl <sub>2</sub>	DLS, AFM	126
13	SLN	58 ± 2	0.5 mM CaCl <sub>2</sub>	DLS, AFM	126
13	SLN	52 ± 1	1 mM CaCl <sub>2</sub>	DLS, AFM	126
13	SLN	191 ± 6	2 mM CaCl <sub>2</sub>	DLS, AFM	126
13	SLN	525 ± 22	2.5 mM CaCl <sub>2</sub>	DLS, AFM	126
13	SLN	1117 ± 467	3 mM CaCl <sub>2</sub>	DLS, AFM	126
13	SLN	1345 ± 860	4 mM CaCl <sub>2</sub>	DLS, AFM	126
13	SLN	1239 ± 1172	CaCl <sub>2</sub> 5 mM	DLS, AFM	126
13	SLN	1567 ± 3019	145 mM CaCl <sub>2</sub>	DLS, AFM	126
13	SLN	95 ± 65	0.1 mM MgCl <sub>2</sub>	DLS, AFM	126
13	SLN	64 ± 1	0.5 mM MgCl <sub>2</sub>	DLS, AFM	126
13	SLN	60 ± 2	1 mM MgCl <sub>2</sub>	DLS, AFM	126
13	SLN	136 ± 2	2 mM MgCl <sub>2</sub>	DLS, AFM	126
13	SLN	229 ± 20	2.5 mM MgCl <sub>2</sub>	DLS, AFM	126
13	SLN	837 ± 30	3 mM MgCl <sub>2</sub>	DLS, AFM	126
13	SLN	1365 ± 399	5 mM MgCl <sub>2</sub>	DLS, AFM	126

Table 5 (continued)

Compound	Morphology <sup>a</sup>	Radius <sup>b</sup> (nm)	Condition <sup>c</sup>	Method <sup>d</sup>	Ref.
13	SLN	650 ± 650	10 mM MgCl <sub>2</sub>	DLS, AFM	126
13	SLN	1425 ± 256	20 mM MgCl <sub>2</sub>	DLS, AFM	126
13	SLN	848 ± 1237	30 mM MgCl <sub>2</sub>	DLS, AFM	126
13	SLN	1242 ± 625	145 mM MgCl <sub>2</sub>	DLS, AFM	126
18	Vesicle	54 ± 3	10 mM PB 7.2, 154 mM NaCl	DLS	43
24	Mixture of large or small vesicles, distorted vesicles and rod-like micelles	R <sub>h</sub> : 43; R <sub>g</sub> : 58	0.1 M NH <sub>3</sub> aqueous	SLS, DLS, cryo-TEM	42
24	Liquid crystal	—	5 N NH <sub>3</sub> aqueous	OPM	42
24	Mixture of SLNs and lipid layers	100 (SLN)		PCS, AFM	67
25	Spherical aggregate	100–125	pH 3	FE-SEM, EF-TEM	23
25	Necklace-like aggregate	250	pH 7	FE-SEM, EF-TEM	23
26	Nanofiber	750	H <sub>2</sub> O–EtOH 9 : 1	DLS, FE-SEM, TEM	90
29	Multilamellar vesicle	84 ± 24		DLS, FE-SEM, TEM	111
34	Micelle	—	pH 6	—	41
34	Micelle	—	pH 8	—	41
35	Micelle	—	pH 6	—	41
35	Micelle	—	pH 8	—	41
36	Micelle	—	pH 6	—	41
36	Micelle	—	pH 8	—	41
37	Micelle	—	pH 6	—	41
37	Micelle	—	pH 8	—	41
38	Micelle	—	pH 6	—	41
38	Micelle	—	pH 8	—	41
39	Micelle	—	pH 6	—	41
39	Micelle	—	pH 8	—	41
40	Micelle	—	pH 6	—	41
40	Micelle	—	pH 8	—	41
41	Micelle	—	pH 6	—	41
41	Micelle	—	pH 8	—	41
42	Micelle	—	pH 6	—	41
42	Micelle	—	pH 8	—	41
43	Micelle	—	pH 6	—	41
43	Micelle	—	pH 8	—	41
44	Micelle	—	pH 6	—	41
44	Micelle	—	pH 8	—	41
46	Mixture of rod-like and spherical micelles	3.6 (rod-like); 4.2 (spherical)	Na <sup>+</sup> and K <sup>+</sup> PB, pH 7	Cryo-TEM	91
46	Spherical micelle	3.2	Na <sup>+</sup> borate, pH 9	Cryo-TEM	91
46	Membrane with a uniform pattern of pores	—	pH 4	Cryo-TEM	91
47	—	3	pH 7.2	PGSE NMR	97
47	Hollow spherical cage	3.8	27 mM Na <sup>+</sup> and K <sup>+</sup>	Cryo-TEM	97
47	Micelle	4.0–4.5	27 mM K <sup>+</sup> , pH 7.0	Cryo-TEM	99
47	Micelle	3.2–3.7	27 mM Na <sup>+</sup> and K <sup>+</sup> , pH 7.0	Cryo-TEM	99
49	—	3.27	D <sub>2</sub> O	DOSY	112
51	SLN	73 ± 3		DLS	117
57	Micellar aggregate	1–2	30 °C	DLS	132
58	Vesicle	40–650		DLS, TEM	134
60	Liquid crystal	—		OPM	42
61	Micelle	2.7 ± 0.3	10 mM PB, pH 7.2, 154 mM NaCl	DLS	43
62	Vesicle	75		DLS	46
63	Micelle	2.5	75 mM Na <sub>2</sub> SO <sub>4</sub>	DLS	60
64	Micelle	~2		DLS	71
64	—	~2		DLS, TEM	73
64	Micelle	1.47	20 mM Tris, pH 7.4	DLS	77
65	Micelle	2.74	20 mM Tris, pH 7.4	DLS	77
66	Micelle	3.2		DLS	72
66	Micelle	2.82	20 mM Tris, pH 7.4	DLS	77
67	Micelle	20		DLS	101
67	Micelle	3.69	20 mM Tris, pH 7.4	DLS	77
68	—	150–200	20 mM Tris, pH 7.4	DLS	77
69	Micelle	4.14	20 mM Tris, pH 7.4	DLS	77
72	Micelle	3.04	20 mM Tris, pH 7.4	DLS	77
72	Micelle	3.28	20 mM acetate, pH 5.0	DLS	77
74	Micelle	3.2		DLS	72
75	Spherical micelle	—	50 mM NaCl	SAXS	63
76	Spherical micelle	—	50 mM NaCl	SAXS	63

Table 5 (continued)

Compound	Morphology <sup>a</sup>	Radius <sup>b</sup> (nm)	Condition <sup>c</sup>	Method <sup>d</sup>	Ref.
77	Spherical micelle	—	50 mM NaCl	SAXS	63
77	Spherical micelle	—	100 mM NaCl	SAXS	63
77	Spherical micelle	—	200–300 mM NaCl	SAXS	63
77	Mixture of various micellar shapes	—	>400 mM NaCl	SAXS	63
78	Spherical micelle	—	50 mM NaCl	SAXS	63
79	Spherical micelle	—	50 mM NaCl	SAXS	63
82	Micelle	14	0.33 mM	DLS	48
82	Vesicle or aggregate of micelles	70	1 mM	DLS	48
86	SLN	95		PCS	93
91	Spherical micelle	—	pH < 6, 50 mM NaCl	AFM	122
91	Mixture of rod-like and spherical micelles	—	3 < pH < 8, 50 mM NaCl	AFM	122
91	Connected network	—	pH = 10, 50 mM NaCl	AFM	122
91	Cylindrical micelle	—	pH 8.0, 50 mM NaCl	AFM	122
91	Spherical micelle	2.05	pH 4.2, 50 mM NaCl	SAXS	122
91	Cylindrical micelle	1.68	pH 7.5, 50 mM NaCl	SAXS	122
91	Micelle	$R_g: 1.67$	—	SAXS	125
91	Spherical micelle	$R_h: 2.05; R_g: 1.47 \pm 0.11$	50 mM NaCl, pH 3.0	SAXS	124
92	Spherical micelle	$R_h: 2.10; R_g: 1.58 \pm 0.15$	50 mM NaCl, pH 3.0	SAXS	124
93	Spherical micelle	$R_h: 2.25; R_g: 1.94 \pm 0.17$	50 mM NaCl, pH 3.0	SAXS	124
94	Spherical micelle	—	pH < 6, 50 mM NaCl	AFM	122
94	Vesicular micelle	—	pH = 8, 50 mM NaCl	AFM	122
94	Mixture of rod-like and spherical micelles	—	pH = 6, 50 mM NaCl	AFM	122
94	Cylindrical micelle	—	pH 6.3, 50 mM NaCl	AFM	122
94	Spherical micelle	2.75	pH 4.3, 50 mM NaCl	SAXS	122
94	Cylindrical micelle	2.0	pH 6.3, 50 mM NaCl	SAXS	122
94	Plate micelle	1.91	pH 7.8, 50 mM NaCl	SAXS	122
94	Spherical micelle	$R_h: 2.75; R_g: 2.52 \pm 0.19$	50 mM NaCl, pH 3.0	SAXS	124
95	Cylindrical micelle	$R_h: 2.20; R_g: 1.70 \pm 0.10$	50 mM NaCl, pH 3.0	SAXS	124
96	Cylindrical micelle	$R_h: 2.35; R_g: 1.87 \pm 0.13$	50 mM NaCl, pH 3.0	SAXS	124
97	Rod-like micelle	—	pH < 6, 50 mM NaCl	AFM	122
97	Cylindrical micelle	2.40	pH 4.7, 50 mM NaCl	SAXS	122
98	—	$88 \pm 6$	50 mM MES, pH 6.5	DLS, SLS	136
99	—	$70 \pm 27$	50 mM MES, pH 6.5	DLS, SLS	136
100	Dot-like micelle	2.25	50 mM NaCl, pH 3.0	SAXS, AFM	139
101	Spherical micelle	2.15	50 mM NaCl, pH 3.0	SAXS	140
101	Spherical micelle	2.35	50 mM NaCl, pH 5.4	SAXS	140
101	Finite cylindrical micelle	1.90	50 mM NaCl, pH 6.2	SAXS	140
101	Infinite cylindrical micelle	1.80	50 mM NaCl, pH 7.4	SAXS	140
101	Infinite cylindrical micelle	1.80	50 mM NaCl, pH 8.3	SAXS	140
101	Finite cylindrical micelle	1.98	50 mM NaCl, pH 9.2	SAXS	140
101	Spherical micelle	2.38	50 mM NaCl, pH 10	SAXS	140
102	Spherical micelle	—	50 mM NaCl	SAXS	63
105	—	$97 \pm 2$	50 mM MES, pH 6.5	DLS, SLS	136
106	—	$77 \pm 9$	50 mM MES, pH 6.5	DLS, SLS	136
108	Micelle	$R_g: 1.76$	150 mM NaCl	DLS, SAXS, AFM	167
109	Micelle	$R_g: 2.46$	150 mM NaCl	DSL, SAXS, AFM	167
123	—	$10.1 \pm 0.8$	PBS	DLS	149
124	Vesicle	10–30	50 mM NaCl/Tris-HCl, pH 7–8	DLS, TEM	123
125	Cylindrical micelle	$R_h: 2.50$	50 mM NaCl, pH 7.0, 25 °C	SAXS	157
125	Spherical micelle	$R_h: 2.85; R_g: 2.81$	50 mM NaCl, pH 7.0, 40 °C	SAXS	157
125	Spherical micelle	$R_h: 2.72; R_g: 2.73$	50 mM NaCl, pH 12, 25 °C	SAXS	157
125	Spherical micelle	$R_h: 2.58; R_g: 1.80$	50 mM NaCl, pH 12, 40 °C	SAXS	157
126	Globular micelle	$R_h: 3; R_g: 2.43$		DLS, SAXS	159
127	SLN	65		DLS, AFM	163
127	Nanosphere	$65 \pm 1$		DLS, cryo-TEM	164
127	Nanocapsule	$60 \pm 1$		DLS, cryo-TEM	164
128	SLN	95		DLS, AFM	163
128	Nanosphere	$95 \pm 1$		DLS, cryo-TEM	164
128	Nanocapsule	$76 \pm 1$		DLS, cryo-TEM	164
129	Vesicle	25–50		DLS, TEM	169
130	Fiber	25 (radius), several micrometers long		DLS, TEM	169
131	Micelle	2.2		DLS	278
137	Vesicle	100		DLS, TEM, FE-SEM	185
138	Vesicle	18		DLS, TEM, FE-SEM	185
138	Micelle	3	pH 5	DLS, TEM	185

Table 5 (continued)

Compound	Morphology <sup>a</sup>	Radius <sup>b</sup> (nm)	Condition <sup>c</sup>	Method <sup>d</sup>	Ref.
139	Micelle	3		DLS, TEM	185
140	Micelle	2.9		DLS	142
140	Micelle	2.8		TEM	142
140	Irregular NP	7–16		TEM	142
141	Micelle	3.5		DLS	142
141	Micelle	3.6		TEM	142
141	Sole like NP	13–43		TEM	142
141	Solid micelle	3.6		TEM	143
142	Irregular NP	8–50		TEM	146
142	Mixture of micelles and NPs	3 (micelle); 40 (NP)		HR TEM	146
142	Mixture of micelles and NPs	3 (micelle); 25 (NP)		Cryo-TEM	146
142	Micelle	1.8		DLS	146
142	Micelle	1.8		DLS	142
142	Micelle	2.5		TEM, HR TEM, cryo-TEM	142
142	Irregular NP	8–50		TEM, HR TEM, cryo-TEM	142
142	Solid micelle	2.5		TEM	143
143	Micelle	$R_h$ : 2.90; $R_g$ : $2.26 \pm 0.14$	50 mM NaCl	SAXS	150
144	Micelle	$R_h$ : 3.60; $R_g$ : $2.63 \pm 0.12$	50 mM NaCl	SAXS	150
145	Micelle	$R_h$ : 4.10; $R_g$ : $3.75 \pm 0.34$	50 mM NaCl	SAXS	150
147	Spherical micelle	—	50 mM NaCl	SAXS	63
148	—	118		PCS	168
154	—	88	10 mM HEPES, pH 8.0	DLS	179
158	Vesicle	40		DLS	46
162	Ellipsoidal micelle	Minor: 2.10, major: 3.45		SAXS	147
162	Ellipsoidal micelle	Minor: 1.40, major: 6.6 (prolate); 3.7 (oblate)	D <sub>2</sub> O	DOSY	54
163	Micelle	Minor: 3.25, major: 10.675		SAXS	147
163	Micelle (>0.6 mM)	~123–190		DLS, NTA	154
163	Domain (100–0.1 μM)	~70–190		DLS, NTA	154
163	Nanoassociate (10–1 nM)	~160–195		DLS, NTA	154
164	Vesicle	25–125	pH 7.8	TEM, AFM, DLS	155
164	Vesicle	≤50	pH 7.8, sonicate 1 h	AFM	155
164	Vesicle	25	pH 6.5	TEM	155
164	Vesicle	225	pH 8.5	TEM, DLS	155
164	Micelle	1.3	1 mM AgClO <sub>4</sub>	TEM	155
168	—	30–100	0.1 mM	DLS, TEM	73
168	—	33–250	0.2 mM	DLS, TEM	73
168	—	40–150; 250–350	0.6 mM	DLS, TEM	73
168	—	50–350	0.8 mM	DLS, TEM	73
168	—	55–400	1.0 mM	DLS, TEM	73
168	—	35–55; 80–200	4.0 mM	DLS, TEM	73
168	—	65–350	6.0 mM	DLS, TEM	73
168	—	75–400	8.0 mM	DLS, TEM	73
168	—	35–60; 150–250	10.0 mM	DLS, TEM	73
170	Vesicle	60 ± 15	8 μM	Cryo-TEM, DLS	173
170	Vesicle	50, 230	20 μM	Cryo-TEM, DLS	173
171	Flattened bilayer	108	7.4 μM	Cryo-TEM, DLS	173
171	Flattened bilayer	150	15 μM	Cryo-TEM, DLS	173
175	Ellipsoidal micelle	Minor: 1.40, major: 7.3 (prolate); 4.0 (oblate)	D <sub>2</sub> O	DOSY	54
184	Vesicle	150 ± 50	pH 4.5–12	SLS, DLS	156
184	Micelle	5	pH 3	SLS, DLS	156
185	Vesicle	150 ± 50	pH 4.5–12	SLS, DLS	156
185	Micelle	5	pH 3	SLS, DLS	156
192	SLN	130	PBS	PCS	190
193	Mixture of micelles and large aggregates	12; 49; 133	Acetate pH 4.1	DLS, TEM	203
193	Mixture of micelles and large aggregates	8–10	Borate pH 8.6	DLS, TEM	203
196	Mixture of spherical micelles and large aggregates	9–10	HCl pH 1.2; phthalate pH 3; acetate pH 4.1	DLS, TEM	203
196	Mixture of spherical micelles and large aggregates	20–30	Borate pH 8.6	DLS, TEM	203
196	Mixture of spherical micelles, bilayers and cylindrical micelles	—	PB pH 12	DLS, TEM	203

Table 5 (continued)

Compound	Morphology <sup>a</sup>	Radius <sup>b</sup> (nm)	Condition <sup>c</sup>	Method <sup>d</sup>	Ref.
197	SLN	97		PCS	193
198	Mixture of tubular and ribbon-like aggregates	4–10 (radius), 8–100 (length)	1 mM	Cryo-TEM	92
198	Fiber	Liquid crystalline lamellar phase	30% THF aqueous	Cryo-TEM	92
199	—	—		AFM	198
200	—	—		AFM	198
205	Vesicle	100–250	EtOH	TEM, AFM	238
212	Vesicle	34, 125		DLS, TEM	202
212	Fiber	109	MeOH	DLS, TEM	202
216	SLN	170	PBS	PCS	190
217	SLN	177	PBS	PCS	190
218	SLN	175	PBS	PCS	190
219	SLN	74	Produced using THF	PCS, AFM	225 and 226
219	SLN	74	Produced using EtOH	PCS	226
219	SLN	98	Produced using acetone	PCS	226
219	SLN	107	Produced using MeOH	PCS	226
219	SLN	114	0.2 g L <sup>-1</sup>	PCS	226
219	SLN	132	0.3 g L <sup>-1</sup>	PCS	226
219	SLN	136	0.4 g L <sup>-1</sup>	PCS	226
219	SLN	130	0.5 g L <sup>-1</sup>	PCS	226
219	SLN	81	3% THF in production	PCS	226
219	SLN	86	4% THF in production	PCS	226
219	SLN	108	5% THF in production	PCS	226
219	SLN	103	6% THF in production	PCS	226
219	SLN	103	8% THF in production	PCS	226
219	SLN	110	10% THF in production	PCS	226
219	SLN	75	0.1 M NaCl	PCS	226
219	SLN	80	0.1 M NaI	PCS	226
219	SLN	83	0.1 M CH <sub>3</sub> CO <sub>2</sub> Na	PCS	226
219	SLN	75	0.1 M NaHCO <sub>3</sub>	PCS	226
219	SLN	73	0.1 M KNO <sub>3</sub>	PCS	226
219	SLN	93	0.1 M KH <sub>2</sub> PO <sub>4</sub>	PCS	226
219	SLN	65		PCS	215
219	SLN	175	PBS	PCS	190
219	SLN	75		PCS, AFM	193
219	SLN	69		PCS	225
219	SLN	70	Carbopol 980 aqueous	PCS	225
219	SLN	73	Carbopol 2020 aqueous	PCS	225
219	SLN	83	Hyaluronic acid aqueous	PCS	225
219	SLN	76	Xanthane aqueous	PCS	225
223	Vesicle	25–35, 100		TEM	233
223	Lamellar-like vesicle	25–500	MeOH	TEM	233
223	Fiber	—	CHCl <sub>3</sub>	TEM	233
223	Inverted micelle	13	Perfluorohexane	TEM	233
223	Circular assembly	50 (radius), 25–30 (height)		AFM	257
224	SLN	74	0.1 M NaH <sub>2</sub> PO <sub>4</sub>	PCS	226
224	SLN	73	0.1 M KCl	PCS	226
226	SLN	163	PBS	PCS	190
227	SLN	92		PCS	193
231	—	140–200	0.8–7 mM, 10% DMF aqueous	DLS	200
232	Micelle	R <sub>g</sub> : 25.6	0.1 mM	SAXS	205
232	Micelle	R <sub>g</sub> : 30.5	0.5 mM	SAXS	205
232	Micelle	R <sub>g</sub> : 35.2	1.0 mM	SAXS	205
232	Micelle	8–6	0.1–10 mM	DLS	205
237	—	62–130	0.09–3 mM, 10% DMF aqueous	DLS	200
238	—	14–8	0.25–16 mM	DLS	200
239	Mixture of micelle-like aggregates and layers	4		DLS	227
240	—	8–4	0.15–16 mM	DLS	200
241	—	9–5	0.15–16 mM	DLS	200
242	—	15–5	0.25–20 mM	DLS	200
247	Spherical particle	R <sub>h</sub> : 107.1; R <sub>g</sub> : 120.4		DLS, SLS, AFM	191
248	Spherical particle	R <sub>h</sub> : 108.0; R <sub>g</sub> : 120.3		DLS, SLS, AFM	191
249	Spherical particle	R <sub>h</sub> : 98.6; R <sub>g</sub> : 122.0		DLS, SLS, AFM	191
250	Spherical particle	R <sub>h</sub> : 121.7; R <sub>g</sub> : 135.0		DLS, SLS, AFM	191
251	Spherical particle	R <sub>h</sub> : 106.8; R <sub>g</sub> : 131.0		DLS, SLS, AFM	191
252	Spherical particle	R <sub>h</sub> : 77.7; R <sub>g</sub> : 91.0		DLS, SLS, AFM	191
255	—	14.3		DLS, TEM	213
256	—	5.5		DLS, TEM	213

Table 5 (continued)

Compound	Morphology <sup>a</sup>	Radius <sup>b</sup> (nm)	Condition <sup>c</sup>	Method <sup>d</sup>	Ref.
257	—	79.5		DLS, TEM	213
258	—	10.3		DLS, TEM	213
259	—	34.7		DLS, TEM	213
260	—	17.7		DLS, TEM	213
261	Mixture of grape-like superstructures and non-linear chains	60–85, 600–900 (length)		SEM, TEM	229
262	Mixture of micelles and large spherical aggregates	100–130; 350		DLS, SEM, TEM	229
278	Sheet-like monolayer	1.3		AFM, TEM	224
278	Bundles of sticks	1.4–16.6 (radius), 500–3500 (length)	DMSO–H <sub>2</sub> O 1 : 9	AFM, TEM	224
278	Vesicle	25	Acetone–H <sub>2</sub> O 1 : 9	AFM, TEM	224
279	Linear or dot-like aggregate	—		AFM, TEM	224
279	Vesicle	25	DMSO–H <sub>2</sub> O 1 : 9	AFM, TEM	224
282	—	241 ± 30	3 mM	DLS	232
282	—	240 ± 37	0.3 mM	DLS	232
282	—	84 ± 4	30 μM	DLS	232
282	—	131 ± 13	3 μM	DLS	232
283	—	87 ± 11	3 mM	DLS	232
283	—	227 ± 47	0.3 mM	DLS	232
283	—	203 ± 15	30 μM	DLS	232
283	—	415 ± 33	3 μM	DLS	232
284 (Br <sup>-</sup> )	Particle	90.5 ± 11.5		DLS	237
284 (NO <sub>3</sub> <sup>-</sup> )	Particle	30.7 ± 8.4		DLS	235
284 (NO <sub>3</sub> <sup>-</sup> )	Particle	24 ± 3		DLS	236
286	Particle	7.3 ± 1.3		DLS	235
286	Particle	8 ± 1		DLS	236
287	Particle	1.9 ± 0.4		DLS	235
289	Spherical particle	70.8	5 mM Tris–HCl, pH 7.5, 1 mM (CA)	DLS	247
289	Spherical particle	80.8	5 mM Tris–HCl, pH 7.5, 0.8 mM (CA)	DLS	247
289	Spherical particle	104.5	5 mM Tris–HCl, pH 7.5, 0.1 mM (CA)	DLS	247
289	Spherical particle	194.8	5 mM Tris–HCl, pH 7.5, 10 μM (CA)	DLS	247
289	Spherical particle	244.4	5 mM Tris–HCl, pH 7.5, 1 μM (CA)	DLS	247
290	Spherical particle	37.7	5 mM Tris–HCl, pH 7.5, 1 mM (CA)	DLS	247
290	Spherical particle	72.8	5 mM Tris–HCl, pH 7.5, 0.8 mM (CA)	DLS	247
290	Spherical particle	100.6	5 mM Tris–HCl, pH 7.5, 0.1 mM (CA)	DLS	247
290	Spherical particle	122.4	5 mM Tris–HCl, pH 7.5, 10 μM (CA)	DLS, TEM	247
290	Spherical particle	226.9	5 mM Tris–HCl, pH 7.5, 1 μM (CA)	DLS	247
292	—	211 ± 37	0.3 mM	DLS	250
292	—	168 ± 24	30 μM	DLS	250
292	—	159 ± 102	3 μM	DLS	250
292	—	99 ± 3	0.3 mM (CA), 0.3 mM Ag <sup>+</sup>	DLS	250
292	—	174 ± 61	30 μM (CA), 30 μM Ag <sup>+</sup>	DLS	250
292	—	218 ± 77	3 μM (CA), 3 μM Ag <sup>+</sup>	DLS	250
292	—	166 ± 12	0.3 mM (CA), 0.3 mM Ag <sup>+</sup>	DLS	250
292	—	265 ± 135	3 mM	DLS	232
292	—	211 ± 37	0.3 mM	DLS	232
292	—	168 ± 24	30 μM	DLS	232
292	—	159 ± 102	3 μM	DLS	232
293	—	378 ± 47	0.3 mM	DLS	250
293	—	265 ± 135	30 μM	DLS	250
293	—	118 ± 103	3 μM	DLS	250
293	—	195 ± 42	30 μM (CA), 30 μM Ag <sup>+</sup>	DLS	250
293	—	189 ± 31	3 μM (CA), 3 μM Ag <sup>+</sup>	DLS	250
294	Micelle	(17.0 ± 1.3)–(24.4 ± 1.4)	2–10 mM, D <sub>2</sub> O	DOSY, AFM	252
294	Mixture of premicelles and large aggregates	100; 300	0.5 mM	DOSY, DLS	254
294	Mixture of aggregate	50–100; 25		AFM	254
296	Homogeneous assembly	30–40 (radius), 3–5 (height)		AFM	257
305	Spherical particle	111.2 ± 17.4.	PBS pH 7.4	DLS, TEM	259
311	Vesicle	—	H <sub>2</sub> O–EtOH 1 : 3	TEM	242

Table 5 (continued)

Compound	Morphology <sup>a</sup>	Radius <sup>b</sup> (nm)	Condition <sup>c</sup>	Method <sup>d</sup>	Ref.
325	Spherical particle	89.8 ± 14.8	PBS pH 7.4	DLS, TEM	259
370	—	100–110	0.33–10 g L <sup>-1</sup>	DLS	258
371	—	R <sub>h</sub> : 100–300; R <sub>g</sub> : 70–140	0.8 mg L <sup>-1</sup> –1.2 g L <sup>-1</sup>	DLS	258
402	SLN	108		DLS	262
402	SLN	74	Produced using acetone	DLS	262
402	SLN	215	Produced using EtOH	DLS	262
402	SLN	106	0.2 g L <sup>-1</sup>	DLS	262
402	SLN	125	0.3 g L <sup>-1</sup>	DLS	262
402	SLN	123	0.4 g L <sup>-1</sup>	DLS	262
402	SLN	139	0.5 g L <sup>-1</sup>	DLS	262
402	SLN	117	5% glycerol	DLS	262
402	SLN	99	10% glycerol	DLS	262
402	SLN	114	15% glycerol	DLS	262
402	SLN	102	20% glycerol	DLS	262
402	SLN	104	25% glycerol	DLS	262
403	SLN	72		DLS	262
404	SLN	70		DLS	262
405	SLN	50		DLS	262
406	SLN	41		DLS	262
407	—	R <sub>h</sub> : 4.242; R <sub>g</sub> : 3.288 ± 0.044	0.5 mM	DLS, SAXS	22
407	—	R <sub>h</sub> : 3.296; R <sub>g</sub> : 2.555 ± 0.128	1 mM	DLS, SAXS	22
407	—	R <sub>h</sub> : 34.06; R <sub>g</sub> : 2.640 ± 0.014	5 mM	DLS, SAXS	22
407	—	R <sub>h</sub> : 4.074; R <sub>g</sub> : 3.158 ± 0.002	10 mM	DLS, SAXS	22
407	—	5; 100		DLS	22
415	Particle	3 ± 0.2; 10 ± 1		DLS	236
420	Tube	15 (radius), 70–300 (length)		SEM	265
421	Tube	10 <sup>6</sup> (radius), 10 <sup>8</sup> (length)		SEM, AFM	265
422	Vesicle	370 ± 28	10 mM Tris, pH 7.4	DLS	268
422	Vesicle	158 ± 3	10 mM Tris, pH 7.4, 65 °C	DLS	268
422	Vesicle	268 ± 13	10 mM Tris, pH 7.4, irradiated	DLS	268
422	Vesicle	133 ± 5	10 mM Tris, pH 7.4, 65 °C, irradiated	DLS	268
427	Vesicle	440 ± 40	10 mM Tris, pH 7.4	DLS	268
427	Vesicle	130 ± 10	10 mM Tris, pH 7.4, 65 °C	DLS	268
427	Vesicle	245 ± 40	10 mM Tris, pH 7.4, irradiated	DLS	268
427	Vesicle	120 ± 1	10 mM Tris, pH 7.4, 65 °C, irradiated	DLS	268
428	—	150 ± 13	3 mM	DLS	232
428	—	71 ± 16	0.3 mM	DLS	232
428	—	136 ± 38	30 μM	DLS	232
428	—	100 ± 19	3 μM	DLS	232
429	SLN	66		DLS, SEM	120
430	Spherical particle	49.9	5 mM Tris–HCl, pH 7.5, 1 mM (CA)	DLS	247
430	Spherical particle	52.2	5 mM Tris–HCl, pH 7.5, 0.8 mM (CA)	DLS	247
430	Spherical particle	103.7	5 mM Tris–HCl, pH 7.5, 0.1 mM (CA)	DLS	247
430	Spherical particle	119.8	5 mM Tris–HCl, pH 7.5, 10 μM (CA)	DLS	247
430	Spherical particle	448.0	5 mM Tris–HCl, pH 7.5, 1 μM (CA)	DLS	247
431	Spherical particle	46.4	5 mM Tris–HCl, pH 7.5, 1 mM (CA)	DLS	247
431	Spherical particle	69.9	5 mM Tris–HCl, pH 7.5, 0.8 mM (CA)	DLS	247
431	Spherical particle	212.9	5 mM Tris–HCl, pH 7.5, 0.1 mM (CA)	DLS	247
431	Spherical particle	412.3	5 mM Tris–HCl, pH 7.5, 10 μM (CA)	DLS	247
431	Spherical particle	502.0	5 mM Tris–HCl, pH 7.5, 1 μM (CA)	DLS	247
432	—	62 ± 9	50 mM Tris, pH 7.4	DLS	266
433	—	66 ± 2	50 mM Tris, pH 7.4	DLS	266
434	—	62 ± 1	50 mM Tris, pH 7.4	DLS	266
443	Vesicle	42 ± 2	0.025 mM	DLS	267
443	Vesicle	47 ± 1	0.05 mM	DLS	267
443	Vesicle	53 ± 1	0.1 mM	DLS	267
443	Vesicle	50 ± 2	0.25 mM	DLS	267
443	Vesicle	42 ± 1	0.5 mM	DLS	267
443	Vesicle	64 ± 2	0.75 mM	DLS	267
443	Vesicle	62 ± 2	1.0 mM	DLS	267



Table 5 (continued)

Compound	Morphology <sup>a</sup>	Radius <sup>b</sup> (nm)	Condition <sup>c</sup>	Method <sup>d</sup>	Ref.
444	Vesicle	31 ± 1	0.01 mM	DLS	267
444	Vesicle	24 ± 1	0.025 mM	DLS	267
444	Vesicle	26 ± 1	0.05 mM	DLS	267
444	Vesicle	25 ± 1	0.1 mM	DLS	267
444	Vesicle	24 ± 1	0.25 mM	DLS	267
444	Vesicle	25 ± 1	0.5 mM	DLS	267
444	Vesicle	31 ± 1	0.75 mM	DLS	267
444	Vesicle	31 ± 1	1.0 mM	DLS	267
448	Vesicle	40	H <sub>2</sub> O–EtOH 1 : 2	TEM, SEM, AFM, DLS	273
449	Vesicle	70	H <sub>2</sub> O–EtOH 1 : 1	TEM, SEM, AFM, DLS	273
449	Vesicle	46	H <sub>2</sub> O–EtOH 3 : 1	TEM, SEM, AFM, DLS	273
450	Spherical aggregate	60–90	H <sub>2</sub> O–EtOH 1 : 1	TEM, SEM, AFM, DLS	273
450	Tubular aggregate	28 (radius)	H <sub>2</sub> O–EtOH 3 : 1	TEM, SEM, AFM, DLS	273
451	Spherical aggregate	60–90	H <sub>2</sub> O–EtOH 1 : 1	TEM, SEM, AFM, DLS	273
451	Tubular aggregate	28 (radius)	H <sub>2</sub> O–EtOH 3 : 1	TEM, SEM, AFM, DLS	273
452	Vesicle	145	H <sub>2</sub> O–EtOH 1 : 3	TEM, AFM, DLS	242
452	Mixture of vesicles and fibers	—	H <sub>2</sub> O–EtOH 2 : 3	SEM, TEM	242
452	Fiber	50–100 (radius), 10 <sup>4</sup> (length)	H <sub>2</sub> O–EtOH 1 : 1	TEM, SEM, AFM	242
452	Nanotube	30–40	0.5 g L <sup>-1</sup> H <sub>2</sub> SO <sub>4</sub> , H <sub>2</sub> O–EtOH 2 : 1	TEM	275
452	Nanotube	—	0.5 g L <sup>-1</sup> AgNO <sub>3</sub> , H <sub>2</sub> O–EtOH 2 : 1	TEM	275
453	Tubular aggregate	—	H <sub>2</sub> O–EtOH 3 : 1	TEM, SEM, AFM, DLS	273

<sup>a</sup> NP: nanoparticle, SLN: solid lipid nanoparticle. <sup>b</sup> Radii are obtained from papers directly or calculated from diameters. Part of data which is not shown in papers clearly is read from figures which contain these data.  $R_s$  is the radius of the shell.  $R_g$  is the gyration radius.  $R_h$  is the hydrodynamic radius. <sup>c</sup> The condition is 25 °C in pure water if no label. CA is the corresponding amphiphilic calixarene. <sup>d</sup> SLS: static light scattering, cryo-TEM: cryogenic transmission electron microscopy, HR TEM: high resolution transmission electron microscopy, NTA: nanoparticle tracking analysis method, PGSE: pulse gradient spin echo, FE-SEM: field-emission scanning electron microscopy, EF-TEM: energy-filtered transmission electron microscopy, OPM: optical polarization microscopy, FFF-MALS: field flow fractionation combined with multi-angle light scattering.

pH 8.5 (225 nm). This phenomenon could be explained by protonation of imidazolyl group affecting the hydrophilic and hydrophobic balance.

Salt concentration influencing assembly is another interesting topic, and it is also related to further application in biological systems. Houel and coworkers did a systematic study on salt concentration affecting assembly using phosphonate-modified calix[4]arenes **12** and **13**.<sup>126</sup> In the presence of monovalent cations (Na<sup>+</sup>, K<sup>+</sup>), no apparent change in size was observed over a concentration range from 0.1 mM to 145 mM. In contrast, divalent cations could cause a significant size increase as the concentration is increased from 2 mM. The authors assumed that divalent cations have the ability to crosslink the assemblies.

**2.2.3 Uniform assembly.** Constructing precisely defined aggregates not only represents an enormous interest and challenge for fundamental research, but also has been widely used in fields such as pharmaceuticals, catalysts, sensors, film precursors, and information storage. As reported by Cui and coworkers, monodisperse nanoparticles with a size variation of less than 5% show unique properties and higher performances as compared with the corresponding polydisperse nanoparticles.<sup>284</sup> The major advantage of monodisperse particles may be attributed to the uniform properties of individual particles, which makes the property of whole particles strictly controllable.<sup>285</sup> However, most of the common surfactants self-assemble into polydisperse assemblies. Thus, lots of effort has been dedicated to developing reliable preparation methods such as freeze–thaw and extrusion; however, a tedious operating procedure is needed. An alternative is appropriate design of amphiphilic building blocks,

since the information determining their specific supra-molecular assembly architecture must be encoded in their molecular structure. Fortunately, amphiphilic calixarenes are promising candidates due to their unique assembly properties. Many aggregations based on calixarenes presented fantastic monodisperse<sup>92,93,111,142,191,202,226,252,259,262,277</sup> and unique aggregation numbers ( $N_{agg}$ s). The reported  $N_{agg}$ s are listed in Table 6.

In 2004, Kellermann and coworkers reported the first completely uniform and structurally precise micelle, whose structure was determined by cryo-TEM and 3D reconstruction techniques.<sup>97</sup> The micelle is formed spontaneously by exactly seven **47** molecules (Fig. 3), which is a T-shaped compound and with third generation dendritic heads. Later, they reported another uniform micelle formed by twelve **46** molecules, which is with second generation dendritic heads.<sup>91</sup> Compared with molecule **47**, the smaller space required by **46** allows denser packing, resulting in a larger  $N_{agg}$  value.

The Sakurai group systematically studied assembly behavior of a series of calixarene micelles, whose head groups, including sulfonate group,<sup>64,65</sup> primary amine group,<sup>63,122,124</sup> quaternary amine group,<sup>63</sup> cysteine,<sup>139</sup> glutamic acid,<sup>140</sup> polyamidoamine,<sup>63</sup> mono/disaccharides,<sup>63,157</sup> PEG,<sup>63,150</sup> and so on, were conjugated with calixarene at the upper rim by a click reaction. Using methods including SAXS, AUC, AF4-MALS and LS, the morphologies and  $N_{agg}$  values of these micelles were determined. They found that these  $N_{agg}$  values coincide with the vertex numbers of regular polyhedral structures when  $N_{agg}$  are less than 30, so they named these small micelles as platonic micelles since the regular polyhedral structures are called platonic solids. They proposed

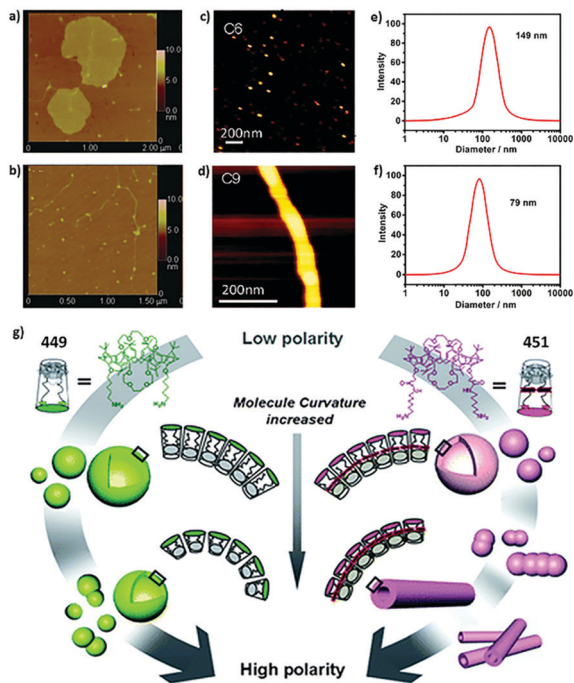


Fig. 2 AFM images of (a) **278** and (b) **279** in pure water. Reprinted with permission from ref. 224. Copyright 2012 from Science China Press and Springer-Verlag Berlin Heidelberg. AFM images of (c) **94** and (d) **97** in 50 mM NaCl, pH 3. Reprinted with permission from ref. 122. Copyright 2012 from American Chemical Society. DLS data of (e) **62** and (f) **158** in water. Reprinted with permission from ref. 46. Copyright 2016 Wiley-VCH Verlag GmbH & Co. KGaA, Weinheim. (g) Schematic representation for morphology transitions in self-assembly of **449** and **451** with changes in medium polarity. Reprinted with permission from ref. 273. Copyright 2011 from Royal Society of Chemistry.

that the formation of platonic micelles is a result of the maximal coverage ratio, which means the ratio of the total area of the caps to the surface area of the sphere (Fig. 4).

It is clear that the equilibrium interfacial area between the hydrophilic and hydrophobic domains ( $a_0$ ) has a significant effect on the  $N_{\text{agg}}$ , which was proved by studying a series of amphiphilic calixarenes bearing PEGs with different molecular weights as hydrophilic head groups.<sup>150</sup> Experiment results showed that amphiphile containing PEG of  $550 \text{ g mol}^{-1}$  forms a dodecamer while that of  $1000 \text{ g mol}^{-1}$  forms an octamer, since the former one has smaller  $a_0$ . Both of the micelles are monodispersed; meanwhile, high molecular weight PEG ( $2000 \text{ g mol}^{-1}$ ) leads to polydisperse micelles, because PEG 2000 exhibits a greater affinity for water and higher mobility than PEG 550 and 1000, resulting in a too large  $a_0$  to form stable monodisperse micelles.

The  $a_0$  value could be easily influenced by the solvent environment. As an example, high salt concentration decreases repulsion among head groups, resulting in smaller  $a_0$ , thus leading to larger  $N_{\text{agg}}$ .<sup>63,65</sup> Also, for head groups containing an amine or carboxyl group, pH variation may protonate or deprotonate them, resulting in a change in repulsion interaction among these head groups. Consequently, the  $a_0$  value increases with larger repulsion and *vice versa*, leading to different  $N_{\text{agg}}$ , or even a transition of morphology. For instance, amino-modified

compounds **87** and **88** form spheres at pH 3.0 while form cylinders at higher pH.<sup>122</sup>

A more complicated example is the glutamic acid containing **100**,<sup>140</sup> since it allows a continuous change in the state of its head groups from cationic to zwitterionic and then to anionic with increasing pH, resulting in a morphological transformation from spherical to cylindrical and again to spherical. Their  $N_{\text{agg}}$  at pH 3.0 and 10 were determined as 6 and 12 respectively. The molecular modeling results showed that the glutamic acid moieties exhibited folded-back structures with deprotonated carboxylic acid, resulting in a smaller hydrophilic volume than that with the protonated amino groups, causing increased  $N_{\text{agg}}$  from pH 3.0 to pH 10. It is also noteworthy that its  $l_c$  could also change during pH variation, because anions at pH 10 are more far away from the center of the molecule than cations at pH 3.0.

The ionized state change induced by pH change could also influence the hydrogen bond formation. Disaccharides containing **120** provides an interesting example.<sup>157</sup> The micellar morphologies are cylindrical at pH 7.0 and micelles with  $N_{\text{agg}}$  of 20 at pH 12 (25 °C), due to the cleavage of the hydrogen bonds by deprotonation of the hydroxyl groups in the sugar molecules. Similarly, temperature also affects hydrogen bonds. As a result, compound **120** forms micelles with  $N_{\text{agg}}$  of 24 at 40 °C (pH 7), and forms micelles with  $N_{\text{agg}}$  of 12 at 40 °C (pH 12).

As we mentioned before,  $l_c$  is also important to the  $N_{\text{agg}}$  of aggregates. According to packing parameter theory,  $N_{\text{agg}}$  is proportional to  $l_c^2$ , whose trend is consistent with experimental results of a series of quaternary amine group bearing calixarenes.<sup>63</sup> As the number of carbons in the alkyl chain increases from 3 to 7,  $N_{\text{agg}}$  increases discretely from 8 to 12, and then to 20. However, a series of amine group bearing calixarenes show a different behavior.<sup>124</sup> Their platonic micelles bearing butyl, heptyl, and hexyl chains remain at 12-mer. This phenomenon and discrete  $N_{\text{agg}}$  may indicate that the coverage ratio defined by the Tammes problem is more suitable than packing parameter theory in the case of investigating small micelles.

To test the universality of the platonic micelles, Sakurai's group also studied assembly behavior of a series of amphiphilic SC4As **4**, **6**–**8**.<sup>64,65</sup>  $N_{\text{agg}}$ s of these micelles increase from 4 to 17 to 24 and then to cylindrical structures with increasing alkyl chain length from pentyl to hexyl to heptyl and then to octyl, respectively. Although the values of 17 and 24 do not agree with the vertex numbers of regular polyhedra, but they match the local maxima in the Thomson problem considering the Coulomb potential for the calculation of the best packing on a sphere with multiple identical spherical caps.

**2.2.4 Compact packing.** Compactness of assemblies is another crucial factor for the performances of various applications, for example, construction of a reliable drug delivery system<sup>180</sup> or an efficient light harvesting material.<sup>46</sup> However, compared with CAC and morphology, such a significant assembly property did not attract much attention, and there is no unified definition of compactness up to now. In general, the microviscosity of assemblies presents their compactness, which could be measured by fluorescence polarization ( $P$ ). The shape of the IR or NMR peak reflects the environment surrounding a bond or nucleus, and is also used as a measure of compactness.

Table 6  $N_{agg}$ s of amphiphilic calixarene assemblies

Compound	$N_{agg}$	Condition <sup>a</sup>	Method <sup>b</sup>	Ref.
4	4	10 mM NaCl	SAXS, AF4-MALS, AUC	64 and 65
4	6	15 mM NaCl	SAXS, AF4-MALS, AUC	65
6	17	10 mM NaCl	SAXS, AF4-MALS, AUC	64
7	24	10 mM NaCl	SAXS, AF4-MALS, AUC	64
46	12	pH 7	Cryo-TEM	91
47	7	27 mM Na <sup>+</sup> and K <sup>+</sup>	Cryo-TEM	97
75	8	50 mM NaCl	SAXS, AF4-MALS, AUC	63
76	8	50 mM NaCl	SAXS, AF4-MALS, AUC	63
77	12	50 mM NaCl	SAXS, AF4-MALS, AUC	63
77	12	100 mM NaCl	SAXS	63
77	20	200–300 mM NaCl	SAXS	63
78	12	50 mM NaCl	SAXS, AF4-MALS, AUC	63
79	20	50 mM NaCl	SAXS, AF4-MALS, AUC	63
91	6	50 mM NaCl, pH 3.0	SAXS, AF4-MALS, AUC	122 and 124
92	12	50 mM NaCl, pH 3.0	SAXS, AF4-MALS, AUC	124
93	12	50 mM NaCl, pH 3.0	SAXS, AF4-MALS, AUC	124
94	12	50 mM NaCl, pH 3.0	SAXS, AF4-MALS, AUC	122 and 124
100	12	50 mM NaCl, pH 3.0	SAXS, AF4-MALS, AUC	122 and 124
100	12	50 mM NaCl, pH 3.0	SAXS, AFM, DLS	139
101	6	pH 3.2	SAXS, AF4-MALS	63
101	12	pH 10	SAXS, AF4-MALS	63
101	6	50 mM NaCl, pH 3.0	SAXS, FFF-MALS	140
101	12	50 mM NaCl, pH 10	SAXS, FFF-MALS	140
102	8	50 mM NaCl	SAXS, AF4-MALS	63
125	24	50 mM NaCl, pH 7.0, 40 °C	SAXS, AF4-MALS, AUC	157
125	20	50 mM NaCl, pH 12	SAXS, AF4-MALS, AUC	157
125	21	50 mM NaCl, pH 12, 40 °C	SAXS, AF4-MALS, AUC	157
143	20	50 mM NaCl	SAXS, AF4-MALS	63
143	12	50 mM NaCl	SAXS, FFF-MALS	150
144	8	50 mM NaCl	SAXS, FFF-MALS	150
145	3–4	50 mM NaCl	SAXS, FFF-MALS	150
146	12	50 mM NaCl	SAXS, AF4-MALS	63
147	3.6	50 mM NaCl	AF4-MALS	63

<sup>a</sup> The condition is 25 °C in pure water if no label. <sup>b</sup> AUC: analytical ultracentrifugation. AF4-MALS: multiangle light scattering coupled with asymmetric field flow fractionation.

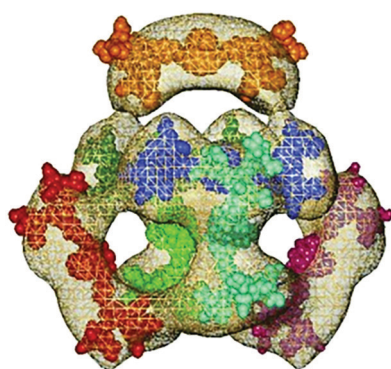


Fig. 3 A structurally precise micelle formed by exactly seven **47** molecules is determined by 3D reconstruction techniques. Reprinted with permission from ref. 97. Copyright 2004 Wiley-VCH Verlag GmbH & Co. KGaA, Weinheim.

Due to their preorganized structures, amphiphilic calixarene assemblies show different compactness from that of the corresponding monomers. Shinkai and co-workers investigated the microviscosity of a series of amphiphilic calixarenes above their CACs by measuring  $P$ .<sup>49</sup>  $P$  values of a series of sulfonic group modified amphiphilic calixarenes **162**, **299**, **300**, and **322** (0.033–0.106) are higher than those of SDS (0.020) and hexadecyltrimethylammonium chloride (0.016), which means

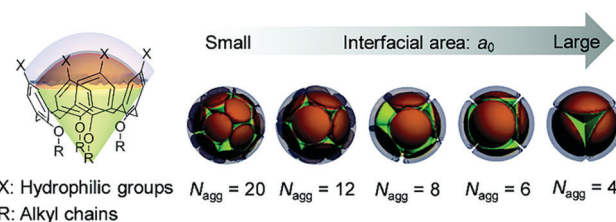


Fig. 4 Chemical structure of a calix[4]arene-based amphiphile and the schematic illustration of the effect of the size of interfacial area on the  $N_{agg}$  of the micelles composed of the amphiphiles. Reprinted with permission from ref. 65. Copyright 2018 from Royal Society of Chemistry.

more compact packing of calixarene micelles than conventional surfactant micelles.

Cho and co-workers reported that alanine-modified calix[4]arene **25** self-assembles into a hollow necklace-like structure at neutral pH.<sup>23</sup> IR spectra showed strong hydrogen bonding between the carbonyl groups and the highly organized, closely packed hydrocarbon chains exhibiting sharp IR bands.

As an assembly property, compactness is also influenced by pH and salt concentration, which modulate head group interactions. For example, Becherer and co-workers reported that carboxylic group modified calix[4]arene **46** micelles are clearly smaller at pH 9 than those at neutral pH, which can be concluded that denser packing of the micelles occurs under

basic conditions in comparison with the aggregates obtained at neutral pH.<sup>91</sup> The required smaller space of head groups allows denser packing.

Xu and co-workers demonstrated choline-modified calixarene (62 and 158) based molecular light-harvesting platforms, whose spectrum tunability is affected by assembly compactness.<sup>46</sup> When they increased the ionic strength of solvent, the ionic heads packed closer resulted in more compact aggregation, which led to higher energy-transfer efficiency and acceptor emission.

Although there have been only limited examples related to the compactness until now, we believe more and more systematic investigations will come up soon, since it is necessary for developing materials with better performance and reliability.

**2.2.5 Slow kinetics.** All four properties we mentioned above are related to thermodynamics, while kinetics, which is an interesting fundamental research topic as well as important basis of material preparation, is also essential. Due to the development of instruments and characterization methods, such as 2D exchange spectroscopy (2D EXSY), stop-flow, and time-resolved spectroscopy, kinetics of amphiphilic aggregation was investigated in detail. Originating from their multivalent feature, some amphiphilic calixarenes meet the higher energy barrier of assembly–bulky water exchange compared to conventional amphiphiles, resulting in slower kinetics.

As Basilio and co-workers reported, in contrast to conventional surfactants, the exchange rate of amphiphilic SC4A 6 between solution and micelle is slow on the NMR time scale.<sup>84</sup> The rate constants were determined by 2D EXSY experiments and these constants were found to be several orders of magnitude lower than those of conventional surfactants and comparable to those of other amphiphilic calixarenes and gemini surfactants. The explanation for this result presumably lies in the fact that the sole barrier felt by the amphiphile entering the micelle arises from long-range electrostatic repulsions due to the micellar charge. As 6 is a preorganized surfactant with four negative charges at the upper rim, this could increase the activation barrier and consequently slow down the rate constant for the association.

Takahashi and co-workers observed that quaternary ammonium modified 77 micelles transit from a dodecamer to an icosamer induced by a rapid increase in the NaCl concentration ( $c_{\text{NaCl}}$ ), using a stopped-flow device and time-resolved SAXS.<sup>133</sup> The  $N_{\text{agg}}$  remained at 12 during the first 60 s after the increase in  $c_{\text{NaCl}}$ , and then abruptly increased to 20 (Fig. 5). They speculated that the following kinetic process might take place: (1) the micelles with  $N_{\text{agg}} = 12$  become metastable after the  $c_{\text{NaCl}}$  increases to 290 mM. (2) Within the micelles, fluctuation of 77 takes place, providing sufficient space for the insertion of other 77 molecules in a process that might be very slow. (3) Once one 77 has been inserted into the metastable micelle,  $N_{\text{agg}}$  rapidly increases to 20.

Similar examples of amphiphilic calixarenes forming metastable “kinetic trap” states were reported, with more diverse morphologies.<sup>286</sup> For example, Strobel and co-workers reported that carboxylatocalix[4]arene 24 self-assembles into vesicles and long thin features that could possibly be rod-like micelles in dilute solution according to light scattering and cryo-TEM

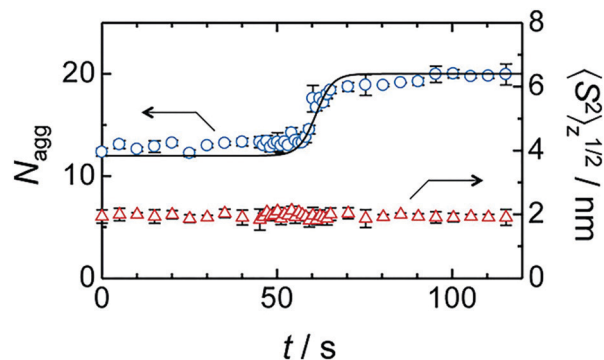


Fig. 5 Time evolution of  $N_{\text{agg}}$  (blue circles) and the radius of gyration  $\langle S^2 \rangle_z^{1/2}$  (red triangles). The solid curve for  $N_{\text{agg}}$  represents the fitted model curve. Reprinted with permission from ref. 133. Copyright 2017 from Wiley-VCH Verlag GmbH & Co. KGaA, Weinheim.

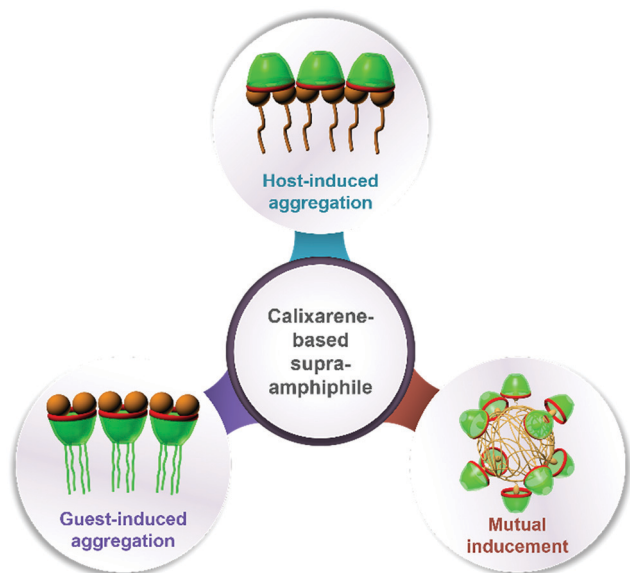
experiments.<sup>42</sup> Houmadi and co-workers reported that 164 self-assembles into vesicles in freshly prepared solution.<sup>155</sup> Vesicles of similar size and shape but with larger membrane shells were observed by TEM in 1 day old solutions, whereas giant vesicles appear after 1 week.

Despite scant examples, we have enough reason to predict a prosperous development of amphiphilic calixarene assembly kinetics. In general, highly kinetic systems at or close to equilibrium show uniform aggregate shapes and sizes, whereas systems with slow kinetics exhibit rather broad shape and size distributions.<sup>42</sup> Consequently, kinetics is critical for preparation procedures of amphiphilic calixarene assemblies. The tailored preparation process is needed for fabricating well-designed assemblies according to their kinetics features. Moreover, the slow assembling kinetics of amphiphilic calixarenes can be applied in extensive fields, such as controlled release in drug delivery systems and dissipative self-assembly systems.

### 3. Calixarene-based supra-amphiphiles

Amphiphilic macrocycles possess cavities, which endow them with binding affinity to various guests. Taking this advantage, guests could modulate the aggregation behavior of amphiphilic macrocycles. By host–guest interactions as well, non-amphiphilic macrocycles own the ability to influence the aggregate properties of some surfactants. The concept of “supra-amphiphiles” proposed by Zhang and co-workers covers those behaviors, describing amphiphiles constructed on the basis of non-covalent interactions or dynamic covalent bonds.<sup>10,287–292</sup>

Specific to water soluble calixarenes, they interact with guests including dyes, drugs, and biomacromolecules by hydrophobic interactions,  $\pi$ – $\pi$  interactions, electrostatic interactions and so on. Furthermore, their unique skeletons provide multivalent interaction sites. As a result, these guests efficiently affect the aggregation of amphiphilic calixarenes, and the aggregation behavior of these guests could be modulated by calixarenes conveniently. Based on the amphiphilicity of the host and guest



Scheme 5 Schematic illustration of various types of calixarene-based supra-amphiphiles.

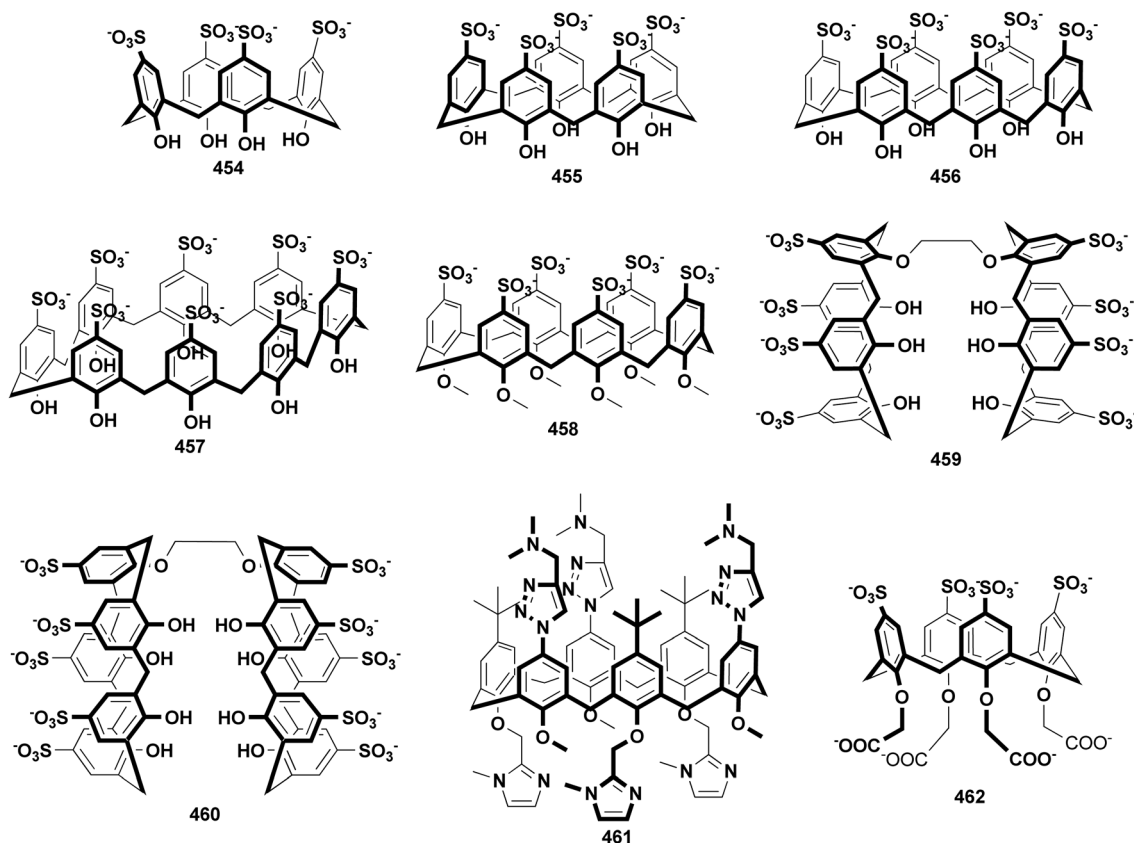
molecules, the assembling features of calixarene-based supra-amphiphiles can be divided into guest-induced aggregation of host, host-induced aggregation of guest and mutual induction (Scheme 5).

Chemical structures of host and guest molecules which have been used to construct supra-amphiphiles are summarized in Schemes 6, 7 and Tables 7, 8.

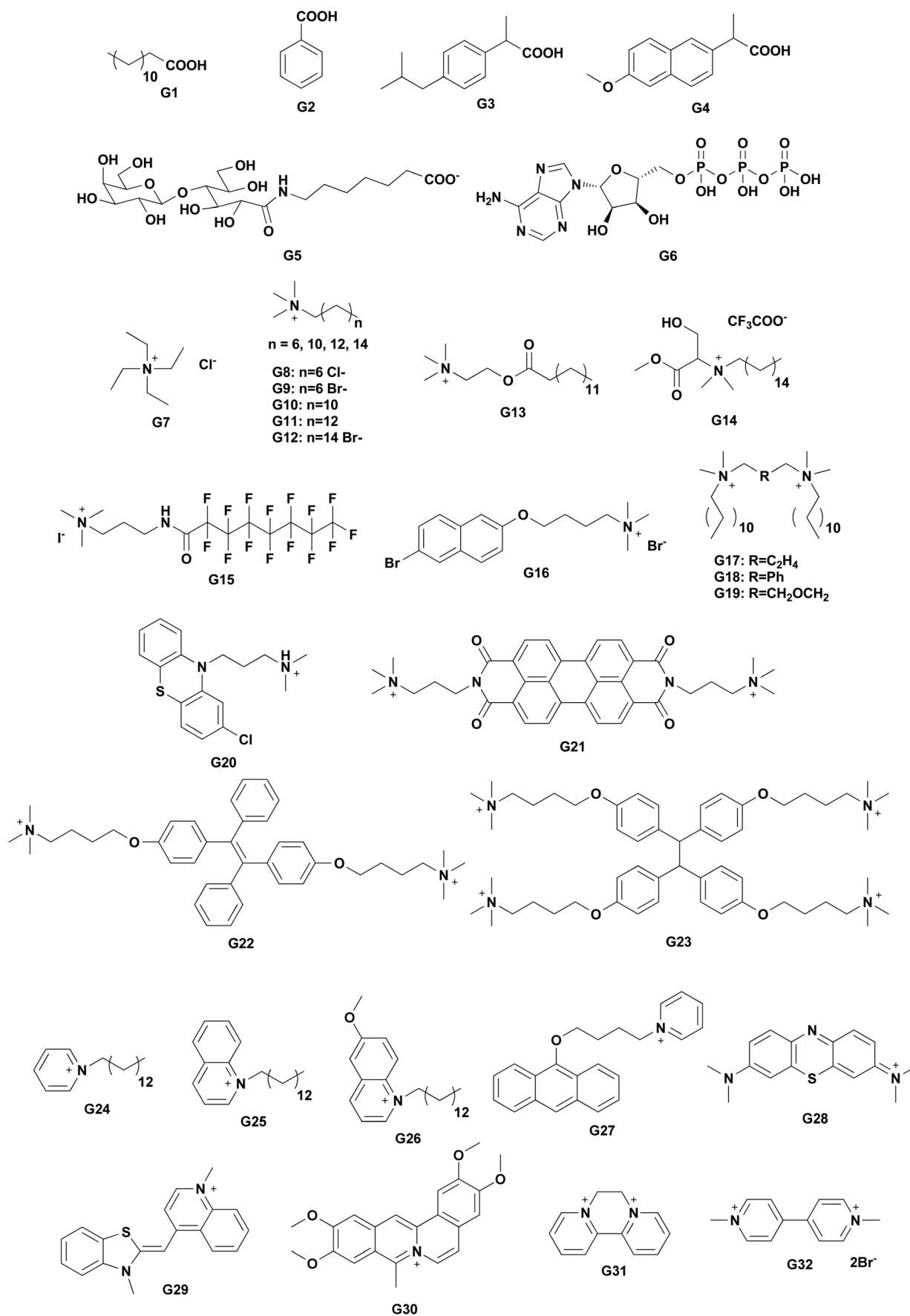
### 3.1 Guest-induced aggregation of host

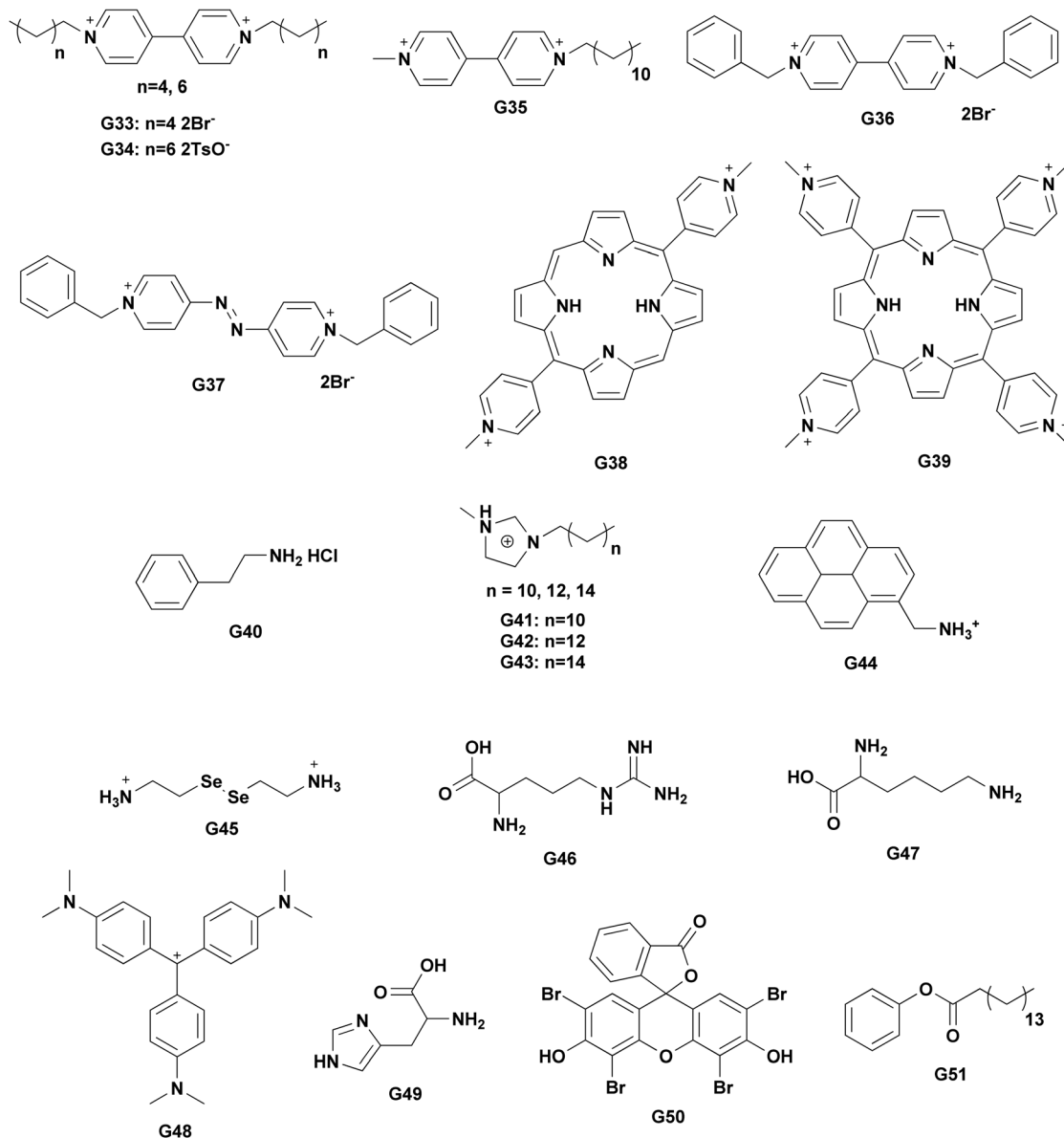
**3.1.1 Guest-decreased CAC.** A series of typical host molecules whose aggregation could be induced by guests is amphiphilic SC $n$ As owing to their good water solubility and binding affinity (Table 9). The interaction with cationic guests reduces electrostatic repulsion between their sulfonic groups, resulting in a smaller CAC. For instance, Hu and coworkers reported the aggregation of amphiphilic calix[4]arene **3** induced by diquat (**G31**).<sup>55</sup> In the absence of **G31**, the CAC value of **3** is 3.18 mM, while it decreases about 12 times (0.25 mM) in the presence of **G31**. Later, Fernandez-Abad and coworkers reported that DSMI (**G7**) could also decrease the CAC of **3** to 1.4 mM.<sup>57</sup> Moreover, it is also reported that the CAC of analogue **6** decreases in the presence of **G45**.<sup>88</sup>

Aggregation of calixarenes bearing sulfonic groups at the lower rim could also be induced by cationic guests. Gattuso and coworkers synthesized an amphiphilic calix[5]arene **294**, and DOSY results showed that its CAC was 0.64 mM.<sup>252</sup> In the presence of **G40**, its CAC decreases to 0.35 mM.<sup>251,252</sup> The inclusion of guests into the cavity of **294** is clearly proved by DOSY results, while some guests involved in the assembly are located outside the cavity. It is noteworthy that the CAC values of guests also decrease upon addition of **294**.



Scheme 6 Structures of hydrophilic host molecules which have been used to construct supra-amphiphiles.





Scheme 7 Structures of guest molecules which have been used to construct supra-amphiphiles.

Table 7 References of host molecules which have been used to construct supra-amphiphiles in Scheme 6

Compound	Ref.	Compound	Ref.	Compound	Ref.
454	293–308	457	293, 296 and 307	460	309
455	298, 309 and 310	458	311–315	461	316
456	293, 296 and 317–319	459	303 and 320	462	321

Following the same principle, anionic guest induced cationic calixarene aggregation was also reported by Wang and coworkers.<sup>138</sup> The CAC value of a quaternary ammonium-modified calix[4]arene **59** decreases by 45 times in the presence of ATP (**G6**). Similarly, Burilov and coworkers synthesized several ammonium modified amphiphilic thiocalix[4]arenes (**432–434**) and studied their

aggregation behavior in the absence and presence of Eosin Y (**G50**).<sup>266</sup> CAC values of all these thiocalix[4]arenes, no matter the length of the hydrophobic chain, showed a significant decrease (at least 15 folds) with addition of **G50**.

**3.1.2 Guest-regulated morphology.** Besides decreasing CAC, guest promoted amphiphilic calixarene assembly also presents a transfer of morphology. Since the electrostatic repulsion is reduced by guests, the amphiphilic calixarenes tend to form larger aggregates.

For example, **6** forms small micelles in the absence of a guest, while forms aggregates with 81 nm average radius in the presence of **G45**, which was proved by DLS, TEM, and significant Tyndall effect.<sup>88</sup> Similar results were reported in the study of **59** in the presence of **G6** (Fig. 6).<sup>138</sup>

Moreover, guest induced larger aggregates could further form hydrogels. Liu's group reported several hydrogels constructed by

**Table 8** References of guest molecules which have been used to construct supra-amphiphiles in Scheme 7

Compound	Ref.	Compound	Ref.	Compound	Ref.	Compound	Ref.
G1	322	G14	305	G27	306	G40	252
G2	322	G15	302	G28	293	G41	317
G3	322	G16	320	G29	295	G42	307 and 317–319
G4	322	G17	300	G30	296	G43	317
G5	316	G18	300	G31	55	G44	310
G6	138	G19	300	G32	162	G45	88
G7	57	G20	304	G33	162	G46	161
G8	311	G21	298	G34	173	G47	161
G9	312	G22	303	G35	297	G48	301
G10	311–315	G23	308	G36	162	G49	161
G11	294 and 319	G24	319	G37	162	G50	266
G12	311	G25	319	G38	309	G51	211
G13	299	G26	319	G39	309	—	—

proline modified calix[4]arene **107**, in the presence of different guests.<sup>161,162</sup> **107** itself forms spherical aggregates with a wide size dispersion. However, upon mixing with **G32**, **G33**, **G36**, **G37**, **G46**, **G47**, and **G49**, the morphology of **107** changed to fibers, resulting in a binary hydrogel. AFM, SEM, and TEM results showed that the fiber shapes differed with guests. For example, the fibers of the **107**–**G46** are composed of long and branched fibers, while **107**–**G49** are shorter and twisted. And a denser network with stacks of rod-like nanofibers was observed in **107**–**G47** (Fig. 6).

### 3.2 Host-induced aggregation of guests

As we mentioned before, when a cationic surfactant **G45** is used to promote aggregation of an anionic amphiphilic calixarene **6**, the CAC value of **G45** decreases as well. This mutually inducing phenomenon further provides us the idea that hydrophilic calixarenes should also have the ability to enhance aggregation of amphiphiles. In fact, calixarene-induced aggregation (CIA) was first reported in 2001,<sup>321</sup> and has become more popular since 2009. The most typical hosts are SCnAs, which are capable of binding hundreds of guests with impressive affinity and promoting self-assembly of about 30 molecules in aqueous media. The concept of CIA was proposed in 2012, which means an appropriate concentration of SCnAs could lower some amphiphilic molecules' CAC, enhance aggregate stability and compactness, and regulate the degree of order in the aggregates. This strategy could be applied to aromatic fluorescent dyes, surfactants, drugs, and biomacromolecules. Some of them have been summarized in previous reviews by García-Río<sup>16</sup> and our group.<sup>3,323</sup> Herein, instead of listing all the results in this field, we focus on the properties of CIA assembly with assistance of some typical works.

From the viewpoint of intermolecular interactions, the hydrophobic interaction is the main driving force of conventional surfactant micelle formation, while electrostatic repulsion of its head group is unfavorable for assembly. SCnAs possessing multivalent negative charges could lower the potential energy

of electrostatic repulsion efficiently. As a result, in the presence of SCnAs, surfactants tend to show lower CAC, more regular arrangement, and more compact packing (Table 10).

**3.2.1 Host-decreased CAC.** A representative example of CIA is SC4A (**454**) inducing myristoylcholine (**G13**) aggregation. In this work, the CAC value of **G13** decreased significantly by a factor of *ca.* 100 with addition of an appropriate amount of **454**. Similar results were reported on various guests such as gemini surfactants **G17**–**G19**,<sup>300</sup> 1-pyrenemethylammonium (**G44**),<sup>310</sup> 1-methyl-3-tetradecylimidazolium (**G41**),<sup>317</sup> cationic serine-based surfactant **G14**<sup>305</sup> and so on. In general, the CAC value depends on the ratio of guest and SCnA, and the appropriate ratio was often determined by transmittance measurements. If the SCnA concentration is much less than that of the surfactant, there is no enough opposite charges to reduce electrostatic repulsion efficiently. On the other hand, too much SCnA concentration provides excess cavities to include surfactants, resulting in disassembling. However, García-Río and coworkers reported that sulfonatocalix[6]arene hexamethyl ether (**458**) concentration hardly effected the CAC value of the mixed system, while micelle concentration was highly dependent on **458** concentration. This phenomenon may be explained as the weak binding affinity of **458**, which has a flexible conformation without hydrogen bonds at the lower rim since methylation of lower-rim hydroxyls results in loss of hydrogen bonds, leading to a flexible conformation of **458**.

**3.2.2 Host-regulated morphology.** Following the same principle as guest induced amphiphilic calixarene aggregation, SCnAs reduced electrostatic repulsion of surfactants also leads to a larger size aggregation with a smaller curvature. Many examples of arrangement transfer from small micelles to vesicles were reported, with a significant Tyndall effect. For instance, the aggregation of **454** and an asymmetric viologen **G35** was studied by DLS, TEM, and SEM.<sup>297</sup> The DLS result showed that the average diameter of the aggregates was 362 nm, with a narrow size distribution. TEM and SEM images showed the hollow spherical morphology, indicating convincingly the vesicular structure. Moreover, the thickness of the bilayer membrane obtained was about 7 nm, which was almost equal to the total height of lengths of two **G35** and two **454**.

Harangozo and coworkers reported a nanoparticle consisting of **G42** and SC6A (**456**).<sup>307</sup> Small angle neutron scattering (SANS) and cryo-TEM results indicated that the diameter of the multilayered nanoparticles was around 160 nm. Interestingly, they found that the nanoparticles have a tendency to transform into supramolecular micelles (around 6 nm diameter) in the presence of NaCl (Fig. 7c), which may be due to additional ions interfering the hydrate structure around the hydrophobic chains and the cross-sectional area of this supra-amphiphile.

Besides the size of assemblies, SCnA could also modulate their shape. Guo and coworkers studied the morphology of the SC5A **455** and **G21** aggregates.<sup>298</sup> The TEM image of free **G21** showed some irregular arrangement without a specific topological structure, while nano-rod structures with an average length of 220 nm appeared in the presence of **455**. These rods are considered to be composed of bundles of fibers, resulting from the hierarchical assembly of calixarenes (Fig. 7).



Table 9 Morphologies of guest-induced host assemblies and CACs of corresponding hosts

Host	Guest	Morphology	Radius (nm)	CAC	Quantity (host : guest)	Condition <sup>a</sup>	Method	Ref.
3	—	—	—	3.18 mM	—	—	—	55
3	G31	—	—	0.25 mM	1 : 1	—	Fluorescence	55
3	G7	—	—	1.4 mM	3 mM (guest)	—	Conductivity	57
6	—	Micelle	—	330 μM	—	—	Fluorescence	88
6	G45	Multi-lamellar sphere	81	35 μM	50 μM (guest)	—	DLS, TEM	88
62	—	Micelle	2.7	0.9 mM	—	—	ITC, DLS	138
62	G6	Vesicle	247	0.02 mM	1 : 1	—	UV-vis, DLS, SEM, TEM, AFM	138
111	—	Micelle	20–100	1.2 mM	—	pH 3.0	CD, DLS, AFM, TEM, SEM	161
111	G46	Branched fiber	10 <sup>3</sup> –10 <sup>4</sup> (length)	—	1 : 4	pH 3.0	AFM, TEM, SEM	161
111	G49	Twisted fiber	10 <sup>3</sup> –3 × 10 <sup>3</sup> (length)	—	1 : 4	pH 3.0	AFM, TEM, SEM	161
111	G47	Network	—	—	1 : 4	pH 3.0	AFM, TEM, SEM	161
111	G32	Rod-like fiber	—	—	1 : 1	pH 3.0	AFM, SEM	162
111	G33	Rod-like fiber	—	—	1 : 1	pH 3.0	AFM, SEM	162
111	G36	Network	2 × 10 <sup>3</sup> –5 × 10 <sup>3</sup> (length)	—	1 : 1	pH 3.0	AFM, SEM	162
111	G37	Network	—	—	1 : 1	pH 3.0	AFM, SEM	162
142	—	Mixture of micelles and NPs	2.5; 40	13 μM	—	—	DLS, HR TEM	322
142	G4	Mixture of hollow micelles and hollow rod-like micelles	6	—	1 : 1	—	DLS, HR TEM, cryo-TEM	322
142	G3	Mixture of micelles and NPs	5	—	1 : 1	—	DLS, HR TEM, cryo-TEM	322
143	G1	Hollow micelle	5–10	—	1 : 1	—	DLS, HR TEM, cryo-TEM	322
143	G2	Linear micelle	3.8 (radius), 50–400 (length)	—	1 : 1	—	DLS, HR TEM, cryo-TEM	322
170	—	Vesicle	60 ± 15	7.9 ± 0.5 μM	—	—	Fluorescence, DLS	173
170	G34	Mixture of micelles, vesicles and super-aggregates	<10; >25; 50–100	7.2 ± 0.3 μM	1 : 1	—	Fluorescence, DLS, cryo-TEM, TEM	173
254	G51	Vesicle	40–155	—	10 : 1	Dioxane : water 5 : 1	TEM, DLS	211
254	G51	Vesicle	85	—	5 : 1	Dioxane : water 5 : 1	TEM, DLS	211
254	G51	Spherical micelle	65	—	1 : 1	Dioxane : water 5 : 1	TEM, DLS	211
254	G51	Micelle	~150	—	1 : 5	Dioxane : water 5 : 1	TEM, DLS	211
254	G51	Mixture of network aggregates and spherical micelles	~200	—	1 : 10	Dioxane : water 5 : 1	TEM, DLS	211
432	—	—	62 ± 9	91 ± 5 μM	—	50 mM Tris pH 7.4	Fluorescence	266
432	G50	—	45 ± 3	2.0 ± 0.1 μM	10 : 1	50 mM Tris pH 7.4	Fluorescence, DLS	266
433	—	—	66 ± 2	59 ± 3 μM	—	50 mM Tris pH 7.4	Fluorescence	266
433	G50	—	53 ± 2	2.6 ± 0.2 μM	10 : 1	50 mM Tris pH 7.4	Fluorescence, DLS	266
434	G50	—	58 ± 4	2.0 ± 0.1 μM	10 : 1	50 mM Tris pH 7.4	Fluorescence, DLS	266
434	—	—	62 ± 1	33 ± 2 μM	—	50 mM Tris pH 7.4	Fluorescence	266
294	—	Micelle	2.44	0.64 mM	—	D <sub>2</sub> O	DOSY, AFM	252
294	G40	Micelle	—	0.35 mM	1 : 1	D <sub>2</sub> O	DOSY	252

<sup>a</sup> The condition is 25 °C in pure water if no label.

**3.2.3 Host-enhanced packing compactness.** Direct evidence of enhancing the packing compactness is the XRD results of **G21**. As reported by Guo and coworkers, free **G21** shows a  $\pi$ - $\pi$  stacking distance of 3.54 Å, while the results are 3.42 and 3.39 Å in the presence of **454** and **455**, respectively (Fig. 7a).<sup>298</sup>

However, measuring XRD is not suitable for every assembly. So the García-Río group and the Biczok group took hydrophobicity of assembly as a parameter for compactness comparison. They assumed that a more hydrophobic assembly means more compactness.

Basilio and coworkers measured the hydrophobicity of dodecyltrimethylammonium bromide (**G10**) assembly by measuring the hydrolysis rate of two kinetic probes.<sup>314</sup> Hydrolysis rates at different surfactant concentrations were plotted and fitted, from which the binding constant of the kinetic probe between the micelles and the bulk water ( $K_m^S$ ) was obtained. The  $K_m^S$  value of **G10** in the absence of **458** is smaller than that in the presence of **458**, which means the addition of **458** leads to stronger hydrophobicity of aggregates.

Biczok and coworkers investigated the polarity of interfacial layers by using a fluorescent probe, from whose maximum fluorescence emission wavelength, the local polarity around the probe can be determined.<sup>307</sup> The polarity results were in the order **456**–**G42** supramolecular micelle < **457**–**G42** supramolecular micelle < **G42** micelle, which indicated more compact stacking of micelles.

### 3.3 Mutual inducement

In addition to the aforementioned two complexation-induced aggregation strategies, mutual inducement involves a larger range of host and guest molecules to fabricate supra-amphiphiles. For example, amphiphilic hosts and amphiphilic guests generate new supra-amphiphiles with different CACs and morphologies.<sup>251,304,324</sup> Hydrophilic hosts and hydrophobic drugs form supra-amphiphiles which can be applied in medical diagnosis and treatment.<sup>325,326</sup> Hydrophilic hosts and polymers, especially biomacromolecules like protein, DNA, and chitosan, are able to mutually induce aggregation.<sup>77,205,227,304,327–330</sup> Supra-amphiphiles consisting of

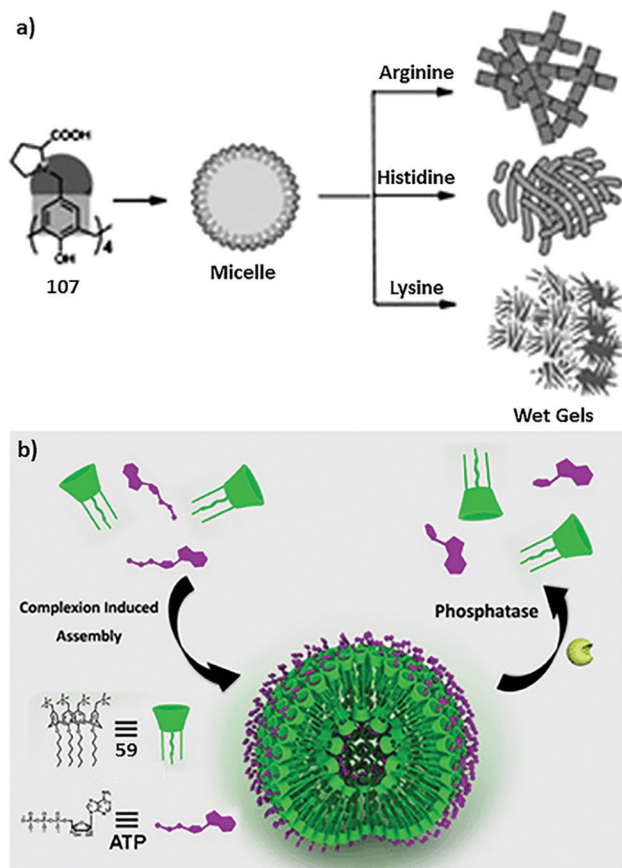


**Fig. 6** (a) Schematic illustration of gel generation from gelator **107** induced by basic amino acids. Reprinted with permission from ref. 161. Copyright 2011 from Royal Society of Chemistry. (b) Schematic illustration of the self-assembly of **59** with ATP (**G6**) and its phosphatase-response. Reprinted with permission from ref. 138. Copyright 2013 from Royal Society of Chemistry.

various kinds of host and guest molecules not only enrich the supra-amphiphile concept but also promise potential applications such as drug delivery and gene transfection.

## 4. Conclusion and outlook

In this review, we systematically summarized the assembling features of calixarene-based amphiphiles and supra-amphiphiles. Hundreds of amphiphilic calixarenes were fabricated by facile covalent modification, including upper-rim hydrophilic amphiphiles, lower-rim hydrophilic amphiphiles and bola-type amphiphiles. Compared with conventional amphiphiles, amphiphilic calixarenes usually show lower CACs and more diverse morphologies. Moreover, amphiphilic calixarenes are able to form uniform assemblies with precise  $N_{agg}$ s. The assemblies of amphiphilic calixarenes pack more compactly than those of common surfactants and their assembling kinetics is much slower. The preorganized framework of calixarenes is the most important factor to influence these unique assembly properties. In general, a larger number of repeat units lead to higher assembling tendency when the conformation is fixed, and the cone conformation is more beneficial to aggregation than the alternative conformation.

On the other hand, benefiting from their cavities, aggregation of amphiphilic calixarenes could be induced by various guests. Similarly, hydrophilic calixarenes possess the ability to enhance the assembly of amphiphilic guests. These induced aggregation phenomena are due to additional attractive interactions decreasing the repulsion of head groups of amphiphiles. Construction of such supra-amphiphiles avoids tedious synthesis, and the obtained assemblies also bear the properties of low CAC, regular morphology, and compact packing.

With prosperous development, there are still some promising objectives and challenges for the development of this area. First, the fundamental studies of assembly behaviors, such as the relationship between molecular structures and assembly properties, compactness and kinetics, need to be systematical investigated urgently. Up to now, hundreds of amphiphilic calixarenes as well as their CACs and morphologies have been reported, but there is no appropriate rule to describe how these properties depend on structures, which is extremely important to rational design of amphiphilic calixarenes with superior performance. On the other hand, compactness and kinetics behavior are featured properties of amphiphilic calixarenes, but only demonstrated in limited works. More attention is needed in the future because they are not only the important fundamental topics, but also related to further applications. For example, compact vesicles provide reliable platforms for capsuling cargo and constructing fluorescence materials with high efficiency,<sup>46,180</sup> while the kinetics feature is critical for preparation procedures of these materials.

Second, crosslinking represents a convenient avenue to obtain assemblies with better stability. For instance, Shulov and coworkers proposed a new platform for bioimaging by cyanine 3 and cyanine 5 corona crosslinked calixarene micelles.<sup>60</sup> The obtained protein-sized nanoparticles present excellent stability in various environments, showing a high fluorescence signal to noise ratio without dye leakage. Crosslinking can also be employed on the basis of supra-amphiphiles. Peng and coworkers constructed a novel supramolecular crosslinked vesicle by post-modification of a dynamic SC4A-(dodecyloxybenzyl)tripropargylammonium vesicle with the “click” reaction.<sup>331</sup> The obtained vesicle is stable enough in diverse and complex surroundings and can be disrupted with specific chemical stimuli to realize controlled release. These pioneering works demonstrate the advantages of the crosslinking strategy, which may inspire more fascinating applications in the future.

Third, by combining amphiphilic calixarenes with various kinds of other amphiphiles, such as conventional surfactants, phospholipids or macrocyclic amphiphiles, the obtained co-assemblies exhibit different assembly behaviors. Co-assembled amphiphiles may introduce attractive interactions between hydrophilic head groups of amphiphilic calixarenes, leading to lower CACs and various morphologies.<sup>66</sup> Moreover, calixarene conformations may be regulated by co-assembling, resulting in better binding affinity.<sup>86</sup> Besides, co-assembly of different amphiphilic macrocycles enables heteromultivalent recognition.<sup>179</sup>

Last but not least, although the cavities of calixarenes are well utilized in supra-amphiphiles, they have not attracted much attention in calixarene amphiphilic assemblies up to now.

Table 10 Morphologies of host-induced guest assemblies and CACs of corresponding guests

Host	Guest	Morphology	Radius (nm)	CAC	Quantity (host:guest)	Condition <sup>a</sup>	Method	Ref.
461	G5	Vesicle	150–300	74 $\mu\text{M}$	1:3	pH 6.8	Surface tension, DLS, TEM	316
461	G5	Vesicle	220–310	—	1:3	pH 4–11	DLS	316
—	G8	Micelle	—	340 $\mu\text{M}$	—	—	Surface tension	311
458	G8	Micelle	—	23 $\mu\text{M}$	1 mM (host)	—	Surface tension	311
—	G9	Micelle	—	310 mM	—	—	Surface tension	311
458	G9	Micelle	—	25 mM	1 mM (host)	—	Surface tension	311
—	G10	Micelle	0.9	14 mM	—	—	Surface tension, fluorescence, DLS	311
458	G10	Micelle	3.0	0.20 mM	5:1	—	Surface tension, fluorescence, DLS	311
458	G10	Micelle	3.3	0.20 mM	5:2	—	Surface tension, fluorescence, DLS	311
458	G10	Micelle	3.5	0.20 mM	1:1	—	Surface tension, fluorescence, DLS	311
458	G10	Micelle	6.1	0.20 mM	1:10	—	Surface tension, fluorescence, DLS	311
458	G10	Micelle	3.0	0.20 mM	1:20	—	Surface tension, fluorescence, DLS	311
458	G10	Micelle	1.6	0.20 mM	1:40	—	Surface tension, fluorescence, DLS	311
458	G10	Micelle	1.1	0.20 mM	1:80	—	Surface tension, fluorescence, DLS	311
454	G11	Vesicle, small NP	250–2500	—	50 mM, 1:2.5	—	Nomarski light microscopy	294
454	G11	Vesicle	57.2 $\pm$ 0.4	—	2 mM, 1:2.5	—	DLS, TEM	294
456	G11	Spherical and ellipsoid NP	46	—	1:6–7	—	DLS	319
456	G11	Supramolecular micelle	3.4 $\pm$ 0.3	—	1:4	15 mM NaCl, 10 $^{\circ}\text{C}$	DLS	319
456	G11	Supramolecular micelle	—	20 $\mu\text{M}$	1:2, 3	50 mM NaCl	DLS	319
—	G12	—	—	14 mM	—	—	Fluorescence	319
458	G12	Micelle	—	0.16 mM	0.1 mM (host)	—	Surface tension, conductivity	313
458	G12	Micelle	—	0.16 mM	0.5 mM (host)	—	Surface tension, conductivity	313
458	G12	—	—	0.3 mM	0.5 $\mu\text{M}$ (host)	—	Surface tension, conductivity	313
458	G12	—	—	0.4 mM	1 $\mu\text{M}$ (host)	—	Surface tension	315
458	G12	—	—	20 mM	0.2 $\mu\text{M}$ (host)	—	Surface tension	315
458	G12	—	—	0.3 mM	2 $\mu\text{M}$ (host)	—	Fluorescence	315
458	G12	—	—	0.2 mM	0.5 mM (host)	—	Fluorescence	315
—	G13	Micelle	—	2.5 mM	—	—	—	299
454	G13	—	—	16 $\mu\text{M}$	0.02 mM (host)	—	UV-vis	299
454	G13	—	—	31 $\mu\text{M}$	0.05 mM (host)	—	UV-vis	299
454	G13	—	—	31 $\mu\text{M}$	0.08 mM (host)	—	UV-vis	299
454	G13	Vesicle	97	—	1:10	—	UV-vis, DLS, TEM, SEM, cryo-TEM, HR TEM	299
—	G14	Micelle	4.3 $\pm$ 0.7	(162 $\pm$ 8) $\mu\text{M}$	—	35 $^{\circ}\text{C}$	Surface tension, NMR, light microscopy, cryo-TEM	305
454	G14	Micelle	30 $\pm$ 2	(93 $\pm$ 2) mM	1:250	35 $^{\circ}\text{C}$	Surface tension, NMR, light microscopy, cryo-TEM	305
454	G14	Micelle	—	(13 $\pm$ 1) mM	1:100	35 $^{\circ}\text{C}$	Surface tension, NMR, light microscopy, cryo-TEM	305
454	G14	Micelle	29 $\pm$ 3	(6.5 $\pm$ 0.8) mM	1:70	35 $^{\circ}\text{C}$	Surface tension, NMR, light microscopy, cryo-TEM	305
454	G14	Mixture of bilayer-based tubules and vesicles	12 $\pm$ 1	—	1:25	35 $^{\circ}\text{C}$	Surface tension, NMR, light microscopy, cryo-TEM	305
454	G14	Mixture of bilayer-based tubules and vesicles	6.0 $\pm$ 0.2	—	1:15	35 $^{\circ}\text{C}$	Surface tension, NMR, light microscopy, cryo-TEM	305
—	G15	—	—	6.0 mM	—	—	Fluorescence, surface tension	302
454	G15	—	—	70 $\mu\text{M}$	20 $\mu\text{M}$ (host)	—	Fluorescence, surface tension	302
454	G15	—	—	80 $\mu\text{M}$	50 $\mu\text{M}$ (host)	—	Fluorescence, surface tension	302
454	G15	—	—	100 $\mu\text{M}$	80 $\mu\text{M}$ (host)	—	Fluorescence, surface tension	302
454	G15	Spherical aggregate	196	—	4:15	—	DLS, TEM, SEM	302
459	G16	Platelet-like micelle	300 (length); 100 (width); 20 (height)	—	1.2:2	25 $^{\circ}\text{C}$	TEM, AFM	320

Table 10 (continued)

Host	Guest	Morphology	Radius (nm)	CAC	Quantity (host:guest)	Condition <sup>a</sup>	Method	Ref.
459	G16	Cross-linked NP	—	—	1.2:2	37 °C	DLS, TEM	320
—	G17	—	—	1 mM	—	—	—	300
454	G17	—	—	2.5 μM	0.02 mM (host)	—	UV-vis	300
454	G17	—	—	5.3 μM	0.04 mM (host)	—	UV-vis	300
454	G17	—	—	7.3 μM	0.06 mM (host)	—	UV-vis	300
454	G17	Vesicle	66.2	—	2:5	—	DLS, TEM, SEM, AFM	300
—	G18	—	—	1 mM	—	—	—	300
454	G18	—	—	3.1 μM	0.02 mM (host)	—	UV-vis	300
454	G18	—	—	3.2 μM	0.04 mM (host)	—	UV-vis	300
454	G18	—	—	3.7 μM	0.06 mM (host)	—	UV-vis	300
454	G18	Vesicle	62.3	—	2:5	—	DLS, TEM, SEM, AFM	300
—	G19	—	—	1 mM	—	—	—	300
454	G19	—	—	3.7 μM	0.02 mM (host)	—	UV-vis	300
454	G19	—	—	5.0 μM	0.04 mM (host)	—	UV-vis	300
454	G19	—	—	6.6 μM	0.06 mM (host)	—	UV-vis	300
454	G19	Vesicle	49.0	—	2:5	—	DLS, TEM, SEM, AFM	300
—	G20	—	—	0.14 mM	—	—	Conductivity	304
454	G20	—	—	0.125 mM	50 μM (host)	—	UV-vis	304
454	G20	Multilamellar sphere	$R_h: 141, R_g: 108$	—	1:4	—	DLS, SLS, TEM	304
454	G21	Mixtures of fibers and something larger	96	—	—	—	DLS	298
454	G21	Mixture of fibers and columnar stacks	100	—	—	—	DLS, TEM, SEM, AFM	298
—	G22	Spherical aggregate	55	—	—	—	Surface tension, DLS, TEM, AFM	303
454	G22	—	—	0.14 mM	1:2	—	Surface tension	303
454	G22	Multilamellar spherical aggregate	30	—	1:2	—	DLS, TEM, AFM	303
459	G22	Spherical and linear aggregate	60	—	1:4	—	DLS, TEM, AFM	303
—	G23	—	240	90 μM	—	—	DLS	308
454	G23	—	72	0.8 μM	1:1	—	DLS	308
456	G24	Spherical and oblate lamellar NP	15–48	—	1:2–7	—	DLS	319
456	G24	Supramolecular micelle	$2.4 \pm 0.2$	—	1:3	50 mM NaCl, 15 °C	DLS	319
456	G24	Supramolecular micelle	—	—	1:2	50 mM NaCl	DLS	319
456	G25	Spherical lamellar NP	20–39	16 μM	1:2	—	Fluorescence	319
456	G26	Spherical NP	25–41	—	1:2–6	—	DLS	319
454	G27	—	—	0.078 mM	1:2–6	—	DLS	319
454	G27	—	—	0.062 mM	0.05 mM	—	UV-vis	306
454	G27	—	—	0.103 mM	0.02 mM	—	UV-vis	306
454	G27	Spherical NP	133.36	—	0.08 mM	—	UV-vis	306
—	G35	—	—	20 mM	2:5	—	DLS, TEM	306
454	G35	—	—	0.02 mM	—	—	UV-vis	297
454	G35	—	—	0.04 mM	0.02 mM (host)	—	UV-vis	297
454	G35	—	—	0.07 mM	0.08 mM (host)	—	UV-vis	297
454	G35	Vesicle	181	—	1:2	—	DLS, TEM, SEM	297
460	G38	Fiber-like	$10^4$ (length)	—	1:5	0.1 M PB, pH 7.2	AFM, SEM	309
460	G39	Flake-like	$1.5-1.7$ (height)	—	1:2	0.1 M PB, pH 7.2	AFM, SEM	309
455	G39	NP	0.8–0.9	—	1:1	0.1 M PB, pH 7.2	AFM	309
456	G41	NP	$65 \pm 10$	—	1:2	—	DLS	317
456	G41	NP	$88 \pm 28$	—	1:5	—	DLS	317
456	G41	NP	80–190	—	1:3–120	—	DLS	317
456	G42	NP	$80 \pm 30$	—	1:1	—	DLS	317
456	G42	NP	75–150	—	1:1–200	—	DLS	317
456	G42	Lamellar spherical aggregate	65–100	—	1:2	—	DLS, cryo-TEM, SANS	317
456	G42	Multilayered spherical aggregate	35–75	—	1:20	—	DLS, cryo-TEM, SANS	317

Table 10 (continued)

Host	Guest	Morphology	Radius (nm)	CAC	Quantity (host : guest)	Condition <sup>a</sup>	Method	Ref.
—	G42	Micelle	2.3 ± 0.2	—	—	20 mM NaCl	DLS	318
456	G42	NP	33–100	—	1:6	0–110 mM NaCl	DLS	318
456	G42	NP	33–119	—	1:5	0–110 mM NaCl	DLS	318
456	G42	NP	25–87	—	1:4	0–40 mM NaCl	DLS	318
456	G42	Supramolecular micelle	3.0 ± 0.2	—	1:4	40–53 mM NaCl	DLS	318
456	G42	NP	28–69	—	1:3	0–25 mM NaCl	DLS	318
456	G42	Supramolecular micelle	3.0 ± 0.2	—	1:3	25–33 mM NaCl	DLS	318
456	G42	NP	33–94	—	1:2	0–15 mM NaCl	DLS	318
456	G42	Supramolecular micelle	3.0 ± 0.2	—	1:2	15–17 mM NaCl	DLS	318
456	G42	Supramolecular micelle – NP	3–250	—	1:2	15 mM NaCl, 27–33 °C	DLS	318
456	G42	Supramolecular micelle – NP	3–250	—	1:2	50 mM NaCl, 33–38 °C	DLS	318
456	G42	NP	80	—	1:3	15 mM NaCl, 20 °C	DLS	318
456	G42	Supramolecular micelle	3	—	1:3	15 mM NaCl, 25 °C	DLS	318
456	G42	NP	185	—	1:3	15 mM NaCl, 30 °C	DLS	318
456	G42	NP	36 ± 10	—	1:4	—	DLS	318
456	G42	Supramolecular micelle	<8	—	1:4	53 mM NaCl	Cryo-TEM	318
456	G42	Micelle	—	720 μM	—	50 mM NaCl	Cryo-TEM	318
456	G42	—	—	15 μM	1:2	50 mM NaCl	Fluorescence	318
456	G42	—	—	15 μM	1:1	50 mM NaCl	Fluorescence	318
456	G42	—	—	15 μM	1:3	50 mM NaCl	Fluorescence	318
456	G42	—	—	15 μM	1:3.6	50 mM NaCl	Fluorescence	318
454	G42	NP	100	—	1:2	0–0.08 mM NaCl	DLS, cryo-TEM	307
454	G42	NP	100	—	1:4	0–0.07 mM NaCl	DLS, cryo-TEM	307
457	G42	NP	23–45	—	1:2–9	—	DLS	307
457	G42	NP	45	—	1:6.8–8.8	0–50 mM NaCl	DLS	307
457	G42	Supramolecular micelle – NP	2.5–350	—	1:4.9	30 mM NaCl, 45–55 °C	DLS	307
457	G42	Supramolecular micelle – NP	2.5–320	—	1:4.9	50 mM NaCl, 50–55 °C	DLS	307
457	G42	NP – supramolecular micelle	45–2.5	—	1:5.8	0–50 mM NaCl	DLS	307
457	G42	NP – supramolecular micelle	38–2.5	—	1:3.9	0–50 mM NaCl	DLS	307
457	G42	—	—	15 μM	1:2.0	50 mM NaCl	Fluorescence	307
457	G42	—	—	12 μM	1:5.9	50 mM NaCl	Fluorescence	307
456	G43	NP	55 ± 13	—	1:1	—	DLS	317
456	G43	NP	60–90	—	1:1–200	—	DLS	317
—	G44	—	—	0.27 mM	—	—	DLS	310
455	G44	—	—	0.07 mM	0.02 mM (host)	—	Fluorescence	310
455	G44	—	—	0.09 mM	0.05 mM (host)	—	Fluorescence	310
455	G44	—	—	0.08 mM	0.08 mM (host)	—	Fluorescence	310
455	G44	Vesicle	49.4	—	1:4	—	DLS, TEM, SEM	310

<sup>a</sup> The condition is 25 °C in pure water if no label.

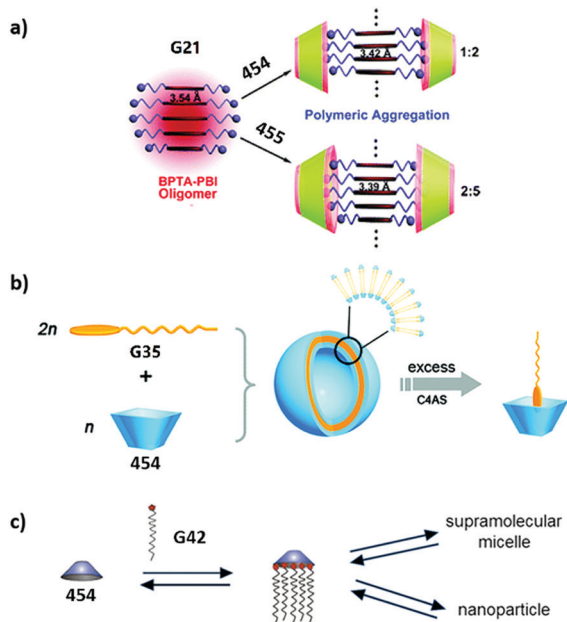


Fig. 7 (a) Schematic illustration of the complex-induced aggregation of BPTA-PBI (G21) by 454 and 455. Reprinted with permission from ref. 298. Copyright 2012 from Royal Society of Chemistry. (b) Schematic representation of the construction of a supramolecular binary vesicle based on the host-guest complexation of 454 with G35. Reprinted with permission from ref. 297. Copyright 2011 from American Chemical Society. (c) Illustration of 454 induced G42 formation of nanoparticles and supramolecular micelles. Reprinted with permission from ref. 307. Copyright 2016 from American Chemical Society.

Actually, binding and assembling abilities complement each other and influence each other. As we mentioned above, aggregation enhances the binding ability by regulating the calixarene conformation.<sup>86</sup> Furthermore, by utilizing the host-guest recognition cavity of calixarenes on the assembly surface, the morphology of the assembly can be controlled by guests, non-covalent modification of specific functional groups can be performed, and multidimensional and hierarchical self-assemblies can be achieved.

In summary, aiming on these objectives and challenges will lead to a deep understanding of the assembling features of amphiphiles and supra-amphiphiles based on calixarenes, and also enrich their construction motifs and strategies, which are essential to develop functional materials based on calixarenes. Moreover, although this review focused on calixarenes, the conclusions are also transferable to other macrocyclic amphiphiles and supra-amphiphiles.

## Conflicts of interest

There are no conflicts to declare.

## Acknowledgements

This work was supported by the NSFC (51873090 and 21672112), the Fundamental Research Funds for the Central Universities

and the Innovation Project of Hebei Province (19241303D), which are gratefully acknowledged.

## Notes and references

- 1 Y. Chang, Y. Jiao, H. E. Symons, J. F. Xu, C. F. J. Faul and X. Zhang, *Chem. Soc. Rev.*, 2019, **48**, 989–1003.
- 2 A. Sorrenti, O. Illa and R. M. Ortuno, *Chem. Soc. Rev.*, 2013, **42**, 8200–8219.
- 3 Y.-C. Liu, H.-W. Sun and D.-S. Guo, *Curr. Org. Chem.*, 2018, **22**, 2127–2149.
- 4 Y. Yao, R.-B. Zhao, Y.-J. Shi, Y. Cai, J. Chen, S.-Y. Sun, W. Zhang and R.-K. Tang, *Chem. Commun.*, 2018, **54**, 8068–8071.
- 5 S. Shinkai, S. Mori, H. Koreishi, T. Tsubaki and O. Manabe, *J. Am. Chem. Soc.*, 1986, **108**, 2409–2416.
- 6 G. Varan, C. Varan, N. Erdogor, A. A. Hincal and E. Bilensoy, *Int. J. Pharm.*, 2017, **531**, 457–469.
- 7 J. Gao and D.-S. Guo, *Sci. Sin.: Chim.*, 2019, **49**, 811–820.
- 8 H. Zhang, Z. Liu and Y. Zhao, *Chem. Soc. Rev.*, 2018, **47**, 5491–5528.
- 9 S.-Y. Sun, M. Geng, L. Huang, Y.-M. Chen, M.-P. Cen, D. Lu, A.-W. Wang, Y. Wang, Y.-J. Shi and Y. Yao, *Chem. Commun.*, 2018, **54**, 13006–13009.
- 10 X. Zhang and C. Wang, *Chem. Soc. Rev.*, 2011, **40**, 94–101.
- 11 G.-C. Yu, K.-C. Jie and F.-H. Huang, *Chem. Rev.*, 2015, **115**, 7240–7303.
- 12 D.-Y. Xia, Y. Li, K.-C. Jie, B.-B. Shi and Y. Yao, *Org. Lett.*, 2016, **18**, 2910–2913.
- 13 C. D. Gutsche, *Acc. Chem. Res.*, 1983, **16**, 161–170.
- 14 V. Bohmer, *Angew. Chem., Int. Ed. Engl.*, 1995, **34**, 713–745.
- 15 K. Helttunen and P. Shahgaldian, *New J. Chem.*, 2010, **34**, 2704–2714.
- 16 N. Basilio, V. Francisco and L. Garcia-Rio, *Int. J. Mol. Sci.*, 2013, **14**, 3140–3157.
- 17 R. V. Rodik, A. S. Klymchenko, Y. Mely and V. I. Kalchenko, *J. Inclusion Phenom. Macrocyclic Chem.*, 2014, **80**, 189–200.
- 18 J. Wang, X. Ding and X. Guo, *Adv. Colloid Interface Sci.*, 2019, **269**, 187–202.
- 19 S. Kolusheva, O. Molt, M. Herm, T. Schrader and R. Jelinek, *J. Am. Chem. Soc.*, 2005, **127**, 10000–10001.
- 20 T. Sun, L.-R. Qi, W.-W. Li, Y. Li, X.-M. Shuai, Z.-Q. Cai, H.-P. Chen, X.-G. Qiao and L.-F. Ma, *J. Chromatogr. A*, 2019, **1601**, 310–318.
- 21 V. I. Kalchenko, *Theor. Exp. Chem.*, 2018, **54**, 74–84.
- 22 A. B. Mirgorodskaya, E. I. Yackevich, Y. R. Kudryashova, R. R. Kashapov, S. E. Solovieva, A. T. Gubaidullin, I. S. Antipin, L. Y. Zakharova and A. I. Konovalov, *Colloids Surf., B*, 2014, **117**, 497–504.
- 23 E. J. Cho, J. K. Kang, W. S. Han and J. H. Jung, *Langmuir*, 2008, **24**, 5229–5232.
- 24 J. Luo and Y.-S. Zheng, *Prog. Chem.*, 2018, **30**, 601–615.
- 25 Z. Xu, D. Gonzalez-Abradelo, J. Li, C. A. Strassert, B. J. Ravoo and D.-S. Guo, *Mater. Chem. Front.*, 2017, **1**, 1847–1852.
- 26 Z. Zheng, W.-C. Geng, Z. Xu and D.-S. Guo, *Isr. J. Chem.*, 2019, **59**, 1–16.

- 27 W.-C. Geng, Q. Huang, Z. Xu, R. Wang and D.-S. Guo, *Theranostics*, 2019, **9**, 3094–3106.
- 28 E. S. Espanol and M. M. Villamil, *Biomolecules*, 2019, **9**, DOI: 10.3390/biom9030090.
- 29 J. Gao and D.-S. Guo, *Sci. Sin.: Chim.*, 2018, **48**, 949–956.
- 30 J. L. J. Blanco, J. M. Benito, C. O. Mellet and J. M. G. Fernandez, *J. Drug Delivery Sci. Technol.*, 2017, **42**, 18–37.
- 31 S. Karakurt, T. F. Kellici, T. Mavromoustakos, A. G. Tzakos and M. Yilmaz, *Curr. Org. Chem.*, 2016, **20**, 1043–1057.
- 32 Y. Zhou, H. Li and Y.-W. Yang, *Chin. Chem. Lett.*, 2015, **26**, 825–828.
- 33 X. Ma and Y. Zhao, *Chem. Rev.*, 2015, **115**, 7794–7839.
- 34 M. Giuliani, I. Morbioli, F. Sansone and A. Casnati, *Chem. Commun.*, 2015, **51**, 14140–14159.
- 35 M.-F. Ma, P.-Y. Xing, S.-Y. Li, X.-X. Chu, B. Wang and A.-Y. Hao, *Prog. Chem.*, 2014, **26**, 1317–1328.
- 36 K.-C. Jie, Y.-J. Zhou, Y. Yao and F.-H. Huang, *Chem. Soc. Rev.*, 2015, **44**, 3568–3587.
- 37 S. Sayin and M. Yilmaz, *Tetrahedron*, 2016, **72**, 6528–6535.
- 38 J. J. Michels, J. Huskens, J. F. J. Engbersen and D. N. Reinhoudt, *Langmuir*, 2000, **16**, 4864–4870.
- 39 M. Moradi, L. G. Tulli, J. Nowakowski, M. Baljovic, T. A. Jung and P. Shahgaldian, *Angew. Chem., Int. Ed.*, 2017, **56**, 14395–14399.
- 40 Z.-F. Xiao, W.-P. Yang, F.-Y. Yan, L.-B. Ji, W. Li and W. Wang, *CrystEngComm*, 2019, **21**, 439–448.
- 41 K. Suwinska, O. Shkurenko, C. Mbemba, A. Leydier, S. Jebors, A. W. Coleman, R. Matar and P. Falson, *New J. Chem.*, 2008, **32**, 1988–1998.
- 42 M. Strobel, K. Kita-Tokarczyk, A. Taubert, C. Vebert, P. A. Heiney, M. Chami and W. Meier, *Adv. Funct. Mater.*, 2006, **16**, 252–259.
- 43 P. K. Eggers, T. Becker, M. K. Melvin, R. A. Boulos, E. James, N. Morellini, A. R. Harvey, S. A. Dunlop, M. Fitzgerald, K. A. Stubbs and C. L. Raston, *RSC Adv.*, 2012, **2**, 6250–6257.
- 44 Q. Zhao, Y. Chen, S. H. Li and Y. Liu, *Chem. Commun.*, 2018, **54**, 200–203.
- 45 S. E. Sestito, F. A. Facchini, I. Morbioli, J. M. Billod, S. Martin-Santamaria, A. Casnati, F. Sansone and F. Peri, *J. Med. Chem.*, 2017, **60**, 4882–4892.
- 46 Z. Xu, S. Peng, Y.-Y. Wang, J.-K. Zhang, A. I. Lazar and D.-S. Guo, *Adv. Mater.*, 2016, **28**, 7666–7671.
- 47 K. I. Assaf, A. Hennig, S. Peng, D.-S. Guo, D. Gabel and W. M. Nau, *Chem. Commun.*, 2017, **53**, 4616–4619.
- 48 V. A. Burilov, G. A. Fatikhova, D. A. Mironova, S. E. Solovieva and I. S. Antipin, *Macroheterocycles*, 2015, **8**, 409–414.
- 49 S. Shinkai, T. Arimura, K. Araki and H. Kawabata, *J. Chem. Soc., Perkin Trans. 1*, 1989, 2039–2045.
- 50 J. Cui, V. D. Uzunova, D.-S. Guo, K. Wang, W. M. Nau and Y. Liu, *Eur. J. Org. Chem.*, 2010, 1704–1710.
- 51 X.-P. Ding, D.-B. Tang, T. Li, S.-F. Wang and Y.-Y. Zhou, *Spectrochim. Acta, Part A*, 2011, **81**, 44–47.
- 52 N. Basilio, V. Francisco and L. Garcia-Rio, *J. Org. Chem.*, 2012, **77**, 10764–10772.
- 53 N. Basilio and L. Garcia-Rio, *ChemPhysChem*, 2012, **13**, 2368–2376.
- 54 N. Basilio, L. Garcia-Rio and M. Martin-Pastor, *Langmuir*, 2012, **28**, 2404–2414.
- 55 X.-Y. Hu, S. Peng, D.-S. Guo, F. Ding and Y. Liu, *Supramol. Chem.*, 2015, **27**, 336–345.
- 56 Y.-C. Pan, H.-W. Tian, S. Peng, X.-Y. Hu and D.-S. Guo, *Chin. Chem. Lett.*, 2017, **28**, 787–792.
- 57 S. Fernandez-Abad, M. Pessego, N. Basilio and L. Garcia-Rio, *Chem. – Eur. J.*, 2016, **22**, 6466–6470.
- 58 Y.-X. Wang, Y.-M. Zhang, Y.-L. Wang and Y. Liu, *Chem. Mater.*, 2015, **27**, 2848–2854.
- 59 M. Esmailzade Rostami, B. Gorji and R. Zadmand, *Tetrahedron Lett.*, 2018, **59**, 2393–2398.
- 60 I. Shulov, R. V. Rodik, Y. Arntz, A. Reisch, V. I. Kalchenko and A. S. Klymchenko, *Angew. Chem., Int. Ed.*, 2016, **55**, 15884–15888.
- 61 S. Kulusheva, R. Zadmand, T. Schrader and R. Jelinek, *J. Am. Chem. Soc.*, 2006, **128**, 13592–13598.
- 62 S. Peng, A. Barba-Bon, Y.-C. Pan, W. M. Nau, D.-S. Guo and A. Hennig, *Angew. Chem., Int. Ed.*, 2017, **56**, 1–5.
- 63 S. Fujii, S. Yamada, S. Matsumoto, G. Kubo, K. Yoshida, E. Tabata, R. Miyake, Y. Sanada, I. Akiba, T. Okobira, N. Yagi, E. Mylonas, N. Ohta, H. Sekiguchi and K. Sakurai, *Sci. Rep.*, 2017, **7**, 44494.
- 64 S. Fujii, J. H. Lee, R. Takahashi and K. Sakurai, *Langmuir*, 2018, **34**, 5072–5078.
- 65 S. Fujii, R. Takahashi, J. H. Lee and K. Sakurai, *Soft Matter*, 2018, **14**, 875–878.
- 66 J. H. Lee, S. Fujii, R. Takahashi and K. Sakurai, *Chem. Commun.*, 2019, **55**, 1303–1305.
- 67 D. Elend, U. Pieles and P. Shahgaldian, *Chimia*, 2010, **64**, 45–48.
- 68 N. Moridi, O. Danylyuk, K. Suwinska and P. Shahgaldian, *J. Colloid Interface Sci.*, 2012, **377**, 450–455.
- 69 L. G. Tulli, N. Moridi, W. Wang, K. Helttunen, M. Neuburger, D. Vaknin, W. Meier and P. Shahgaldian, *Chem. Commun.*, 2014, **50**, 3938–3940.
- 70 L. G. Tulli, W. Wang, W. R. Lindemann, I. Kuzmenko, W. Meier, D. Vaknin and P. Shahgaldian, *Langmuir*, 2015, **31**, 2351–2359.
- 71 N. O. Mchedlov-Petrossyan, L. N. Vilkovala, N. A. Vodolazkaya, A. G. Yakubovskaya, R. V. Rodik, V. I. Boyko and V. I. Kalchenko, *Sensors*, 2006, **6**, 962–977.
- 72 R. V. Rodik, A. S. Klymchenko, N. Jain, S. I. Miroshnichenko, L. Richert, V. I. Kalchenko and Y. Mely, *Chem. – Eur. J.*, 2011, **17**, 5526–5538.
- 73 N. O. Mchedlov-Petrossyan, N. A. Vodolazkaya, R. V. Rodik, L. N. Bogdanova, T. A. Cheipesh, O. Y. Soboleva, A. P. Kryshtal, L. V. Kutuzova and V. I. Kalchenko, *J. Phys. Chem. C*, 2012, **116**, 10245–10259.
- 74 E. V. Ukhatskaya, S. V. Kurkov, M. A. Hjalmarsdottir, V. A. Karginov, S. E. Matthews, R. V. Rodik, V. I. Kalchenko and T. Loftsson, *Int. J. Pharm.*, 2013, **458**, 25–30.
- 75 E. V. Ukhatskaya, S. V. Kurkov, R. V. Rodik, V. I. Kalchenko, S. E. Matthews, P. Jansook and T. Loftsson, *J. Inclusion Phenom. Macrocyclic Chem.*, 2013, **79**, 473–483.
- 76 I. O. Melezhyk, R. V. Rodik, N. V. Ivorska, A. S. Klymchenko, Y. Mely, V. V. Shepelevych, L. M. Skivka and V. I. Kalchenko, *Anti-Infect. Agents*, 2015, **13**, 87–94.

- 77 R. V. Rodik, A.-S. Anthony, V. I. Kalchenko, Y. Mély and A. S. Klymchenko, *New J. Chem.*, 2015, **39**, 1654–1664.
- 78 C. Weeden, K. J. Hartlieb and L. Y. Lim, *J. Pharm. Pharmacol.*, 2012, **64**, 1403–1411.
- 79 T. Arimura, H. Kawabata, T. Matsuda, T. Muramatsu, H. Satoh, K. Fujio, O. Manabe and S. Shinkai, *J. Org. Chem.*, 1991, **56**, 301–306.
- 80 D. Hardy, R. M. Bill, A. Jawhari and A. J. Rothnie, *Biochem. Soc. Trans.*, 2016, **44**, 838–844.
- 81 T. Sun, L.-R. Qi, W.-W. Li, Y. Li, X.-M. Shuai, Z.-Q. Cai, H.-P. Chen, X.-G. Qiao and L.-F. Ma, *J. Chromatogr. A*, 2019, **1601**, 310–318.
- 82 H.-Y. Tian, H.-J. Li, Y.-J. Chen, D. Wang and C.-J. Li, *Ind. Eng. Chem. Res.*, 2002, **41**, 4523–4527.
- 83 T. Jin, F. Fujii, H. Sakata, M. Tamura and M. Kinjo, *Chem. Commun.*, 2005, 4300–4302.
- 84 N. Basilio, L. Garcia-Rio and M. Martin-Pastor, *J. Phys. Chem. B*, 2010, **114**, 4816–4820.
- 85 M.-X. Chen, T. Li, S. Peng and D. Tao, *New J. Chem.*, 2016, **40**, 9923–9929.
- 86 H.-W. Tian, Y.-C. Pan and D.-S. Guo, *Supramol. Chem.*, 2017, **30**, 562–567.
- 87 A. Fraix, D. Afonso, G. M. L. Consoli and S. Sortino, *Photochem. Photobiol. Sci.*, 2019, **18**, 2216–2224.
- 88 X.-Y. Hu, Y. Chen and Y. Liu, *Chin. Chem. Lett.*, 2015, **26**, 862–866.
- 89 Y.-X. Wang, D.-S. Guo, Y.-C. Duan, Y.-J. Wang and Y. Liu, *Sci. Rep.*, 2015, **5**, 9019.
- 90 S. Song, J.-H. Wang, H.-T. Feng, Z.-H. Zhu and Y.-S. Zheng, *RSC Adv.*, 2014, **4**, 24909–24913.
- 91 M. S. Becherer, B. Schade, C. Bottcher and A. Hirsch, *Chem. – Eur. J.*, 2009, **15**, 1637–1648.
- 92 F. Rodler, B. Schade, C. M. Jager, S. Backes, F. Hampel, C. Bottcher, T. Clark and A. Hirsch, *J. Am. Chem. Soc.*, 2015, **137**, 3308–3317.
- 93 P. Shahgaldian, M. A. Scloiti and U. Piele, *Langmuir*, 2008, **24**, 8522–8526.
- 94 L. G. Tulli, W.-J. Wang, V. Rullaud, W. R. Lindemann, I. Kuzmenko, D. Vaknin and P. Shahgaldian, *RSC Adv.*, 2016, **6**, 9278–9285.
- 95 J. H. Lee, S. Fujii, R. Takahashi and K. Sakurai, *Langmuir*, 2018, **34**, 12109–12115.
- 96 M. Fricke, D. Volkmer, C. E. Krill, M. Kellermann and A. Hirsch, *Cryst. Growth Des.*, 2006, **6**, 1120–1123.
- 97 M. Kellermann, W. Bauer, A. Hirsch, B. Schade, K. Ludwig and C. Bottcher, *Angew. Chem., Int. Ed.*, 2004, **43**, 2959–2962.
- 98 C. Yihwa, M. Kellermann, M. Becherer, A. Hirsch and C. Bohne, *Photochem. Photobiol. Sci.*, 2007, **6**, 525–531.
- 99 C. M. Jager, A. Hirsch, B. Schade, C. Bottcher and T. Clark, *Chem. – Eur. J.*, 2009, **15**, 8586–8592.
- 100 I. Di Bari, A. Fraix, R. Picciotto, A. R. Blanco, S. Petralia, S. Conoci, G. Granata, G. M. L. Consoli and S. Sortino, *RSC Adv.*, 2016, **6**, 105573.
- 101 I. Di Bari, R. Picciotto, G. Granata, A. R. Blanco, G. M. Consoli and S. Sortino, *Org. Biomol. Chem.*, 2016, **14**, 8047–8052.
- 102 G. Granata, I. Paterniti, C. Geraci, F. Cunsolo, E. Esposito, M. Cordaro, A. R. Blanco, S. Cuzzocrea and G. M. L. Consoli, *Mol. Pharmaceutics*, 2017, **14**, 1610–1622.
- 103 I. Di Bari, G. Granata, G. M. L. Consoli and S. Sortino, *New J. Chem.*, 2018, 18096–18101.
- 104 S. Friedman, S. Kulusheva, R. Volinsky, L. Zeiri, T. Schrader and R. Jelinek, *Anal. Chem.*, 2008, **80**, 7804–7811.
- 105 R. Zadnarm and T. Schrader, *J. Am. Chem. Soc.*, 2005, **127**, 904–915.
- 106 Y.-L. Liu, L. Liu, Y.-L. Wang, Y.-C. Han, D. Wong and Y.-J. Chen, *Green Chem.*, 2008, **10**, 635–640.
- 107 Z. Zheng, W.-C. Geng, J. Gao, Y.-J. Mu and D.-S. Guo, *Org. Chem. Front.*, 2018, **5**, 2685–2691.
- 108 L. Gallego-Yerga, M. Lomazzi, V. Franceschi, F. Sansone, C. Ortiz Mellet, G. Donofrio, A. Casnati and J. M. Garcia Fernandez, *Org. Biomol. Chem.*, 2015, **13**, 1708–1723.
- 109 K.-P. Wang, Y. Chen and Y. Liu, *Chem. Commun.*, 2015, **51**, 1647–1649.
- 110 X.-M. Chen, Y. Chen, Q. Yu, B.-H. Gu and Y. Liu, *Angew. Chem., Int. Ed.*, 2018, **57**, 12519–12523.
- 111 G. Granata, G. M. L. Consoli, R. Lo Nigro, G. Malandrino and C. Geraci, *Supramol. Chem.*, 2016, **28**, 377–383.
- 112 F. Sansone, M. Dudic, G. Donofrio, C. Rivetti, L. Baldini, A. Casnati, S. Cellai and R. Ungaro, *J. Am. Chem. Soc.*, 2006, **128**, 14528–14536.
- 113 T. Takeuchi, V. Bagnacani, F. Sansone and S. Matile, *ChemBioChem*, 2009, **10**, 2793–2799.
- 114 A. D. Martin, E. Houlihan, N. Morellini, P. K. Eggers, E. James, K. A. Stubbs, A. R. Harvey, M. Fitzgerald, C. L. Raston and S. A. Dunlop, *ChemPlusChem*, 2012, **77**, 308–313.
- 115 G. M. L. Consoli, G. Granata, R. Picciotto, A. R. Blanco, C. Geraci, A. Marino and A. Nostro, *MedChemComm*, 2018, **9**, 160–164.
- 116 E. James, P. K. Eggers, A. R. Harvey, S. A. Dunlop, M. Fitzgerald, K. A. Stubbs and C. L. Raston, *Org. Biomol. Chem.*, 2013, **11**, 6108–6112.
- 117 V. Rullaud, M. Siragusa, A. Cumbo, D. Gygax and P. Shahgaldian, *Chem. Commun.*, 2012, **48**, 12186–12188.
- 118 N. Moridi, C. Wackerlin, V. Rullaud, R. Schelldorfer, T. A. Jung and P. Shahgaldian, *Chem. Commun.*, 2013, **49**, 367–369.
- 119 V. Rullaud, N. Moridi and P. Shahgaldian, *Langmuir*, 2014, **30**, 8675–8679.
- 120 A. Galukhin, A. Erokhin, I. Imatdinov and Y. Osin, *RSC Adv.*, 2015, **5**, 33351–33355.
- 121 W.-C. Geng, Y.-C. Liu, Y.-Y. Wang, Z. Xu, Z. Zheng, C.-B. Yang and D.-S. Guo, *Chem. Commun.*, 2016, **53**, 392–395.
- 122 S. Fujii, Y. Sanada, T. Nishimura, I. Akiba, K. Sakurai, N. Yagi and E. Mylonas, *Langmuir*, 2012, **28**, 3092–3101.
- 123 S. Sakamoto, S. Fujii, K. Yoshida and K. Sakurai, *Langmuir*, 2016, **32**, 12434–12441.
- 124 M. Araki, S. Fujii, J. H. Lee, R. Takahashi and K. Sakurai, *Soft Matter*, 2019, 3515–3519.
- 125 E. Mylonas, N. Yagi, S. Fujii, K. Ikesue, T. Ueda, H. Moriyama, Y. Sanada, K. Uezu, K. Sakurai and T. Okobira, *Sci. Rep.*, 2019, **9**, 1982.



- 126 E. Houel, A. Lazar, E. Da Silva, A. W. Coleman, A. Solovyov, S. Cherenok and V. I. Kalchenko, *Langmuir*, 2002, **18**, 1374–1379.
- 127 M. Rehm, M. Frank and J. Schatz, *Tetrahedron Lett.*, 2009, **50**, 93–96.
- 128 J. Gasparello, A. Manicardi, A. Casnati, R. Corradini, R. Gambari, A. Finotti and F. Sansone, *Sci. Rep.*, 2019, **9**, 3036.
- 129 A. D. Martin, R. A. Boulos, K. A. Stubbs and C. L. Raston, *Chem. Commun.*, 2011, **47**, 7329–7331.
- 130 J. Mo, L. Wang, X. Huang, B. Lu, C. Zou, L. Wei, J. Chu, P. K. Eggers, S. Chen, C. L. Raston, J. Wu, L. Y. Lim and W. Zhao, *Nanoscale*, 2017, **9**, 13142–13152.
- 131 K. Samanta, D. S. Ranade, A. Upadhyay, P. P. Kulkarni and C. P. Rao, *ACS Appl. Mater. Interfaces*, 2017, **9**, 5109–5117.
- 132 S. Arimori, T. Nagasaki and S. Shinkai, *J. Chem. Soc., Perkin Trans. 1*, 1993, 887–889.
- 133 R. Takahashi, S. Matsumoto, S. Fujii, T. Narayanan and K. Sakurai, *Angew. Chem., Int. Ed.*, 2017, **56**, 6734–6738.
- 134 E. V. Ukhatskaya, S. V. Kurkov, S. E. Matthews, A. El Fagui, C. Amiel, F. Dalmas and T. Loftsson, *Int. J. Pharm.*, 2010, **402**, 10–19.
- 135 E. V. Ukhatskaya, S. V. Kurkov, S. E. Matthews and T. Loftsson, *J. Inclusion Phenom. Macrocyclic Chem.*, 2013, **79**, 47–55.
- 136 V. A. Burirov, G. A. Fatikhova, M. N. Dokuchaeva, R. I. Nugmanov, D. A. Mironova, P. V. Dorovatovskii, V. N. Khrustalev, S. E. Solovieva and I. S. Antipin, *Beilstein J. Org. Chem.*, 2018, **14**, 1980–1993.
- 137 R. Zadnarm, M. Arendt and T. Schrader, *J. Am. Chem. Soc.*, 2004, **126**, 7752–7753.
- 138 Y.-X. Wang, D.-S. Guo, Y. Cao and Y. Liu, *RSC Adv.*, 2013, **3**, 8058–8063.
- 139 S. Fujii, K. Sakurai, T. Okobira, N. Ohta and A. Takahara, *Langmuir*, 2013, **29**, 13666–13675.
- 140 S. Fujii, R. Takahashi and K. Sakurai, *Langmuir*, 2017, **33**, 4019–4027.
- 141 E.-H. Ryu, J. Yan, Z. Zhong and Y. Zhao, *J. Org. Chem.*, 2006, **71**, 7205–7213.
- 142 K. Khan, H. Huang and Y.-S. Zheng, *Curr. Org. Chem.*, 2012, **16**, 2745–2751.
- 143 K. Khan, S. L. Badshah, N. Ahmad, H. U. Rashid and Y. Mabkhot, *Molecules*, 2017, **22**, 783.
- 144 T. Mecca, G. M. Messina, G. Marletta and F. Cunsolo, *Chem. Commun.*, 2013, **49**, 2530–2532.
- 145 E.-H. Ryu and Y. Zhao, *Org. Lett.*, 2004, **6**, 3187–3189.
- 146 H. Huang, D.-M. Li, W. Wang, Y.-C. Chen, K. Khan, S. Song and Y.-S. Zheng, *Org. Biomol. Chem.*, 2012, **10**, 729–735.
- 147 H. Matsuoka, M. Tsurumi and N. Ise, *Phys. Rev. B: Condens. Matter Mater. Phys.*, 1988, **38**, 6279–6286.
- 148 H.-Y. Tian, Y.-J. Chen, D. Wang, C. C. Zeng and C. J. Li, *Tetrahedron Lett.*, 2000, **41**, 2529–2532.
- 149 S. Avvakumova, P. Fezzardi, L. Pandolfi, M. Colombo, F. Sansone, A. Casnati and D. Prospero, *Chem. Commun.*, 2014, **50**, 11029–11032.
- 150 K. Yoshida, S. Fujii, R. Takahashi, S. Matsumoto and K. Sakurai, *Langmuir*, 2017, **33**, 9122–9128.
- 151 S. Shinkai, H. Koreishi, H. Mori, T. Sone and O. Manabe, *Chem. Lett.*, 1985, 1033–1036.
- 152 L.-T. Zhang, L. A. Godinez, T.-B. Lu, G. W. Gokel and A. E. Kaifer, *Angew. Chem., Int. Ed. Engl.*, 1995, **34**, 235–237.
- 153 Y.-J. Zhang and W.-X. Cao, *New J. Chem.*, 2001, **25**, 483–486.
- 154 I. S. Ryzhkina, Y. V. Kiseleva, L. I. Murtazina, S. E. Solovieva, N. G. Manin and A. I. Konovalov, *Macrocyclics*, 2017, **10**, 190–195.
- 155 S. Houmadi, D. Coquiere, L. Legrand, M. C. Faure, M. Goldmann, O. Reinaud and S. Remita, *Langmuir*, 2007, **23**, 4849–4855.
- 156 N. Micali, V. Villari, G. M. Consoli, F. Cunsolo and C. Geraci, *Phys. Rev. E: Stat., Nonlinear, Soft Matter Phys.*, 2006, **73**, 051904.
- 157 R. Miyake, S. Fujii, J. H. Lee, R. Takahashi and K. Sakurai, *J. Colloid Interface Sci.*, 2019, **535**, 8–15.
- 158 Y. Tokunaga, H. Sakon, H. Kanefusa, Y. Shimomura and K. Suzuki, *ARKIVOC*, 2003, 135–143.
- 159 J. Dauvergne, E. M. Desuzinges, C. Faugier, S. Igonet, M. Soulié, E. Grousson, D. Cornut, F. Bonneté, G. Durand, E. Dejean and A. Jawhari, *ChemistrySelect*, 2019, **4**, 5535–5539.
- 160 S. Shinkai, Y. Shirahama, T. Tsubaki and O. Manabe, *J. Chem. Soc., Perkin Trans. 1*, 1989, 1859–1860.
- 161 J. Zhang, D.-S. Guo, L.-H. Wang, Z. Wang and Y. Liu, *Soft Matter*, 2011, **7**, 1756–1762.
- 162 Z. Wang, D.-S. Guo, J. Zhang and Y. Liu, *Acta Chim. Sin.*, 2012, **70**, 1709.
- 163 L. Gallego-Yerga, M. Lomazzi, F. Sansone, C. Ortiz Mellet, A. Casnati and J. M. Garcia Fernandez, *Chem. Commun.*, 2014, **50**, 7440–7443.
- 164 L. Gallego-Yerga, I. Posadas, C. de la Torre, J. Ruiz-Almansa, F. Sansone, C. Ortiz Mellet, A. Casnati, J. M. Garcia Fernandez and V. Cena, *Front. Pharmacol.*, 2017, **8**, 249.
- 165 X. Yan, V. Janout, J. T. Hsu and S. L. Regen, *J. Am. Chem. Soc.*, 2003, **125**, 8094–8095.
- 166 D. H. McCullough, V. Janout, J. W. Li, J. T. Hsu, Q. Truong, E. Wilusz and S. L. Regen, *J. Am. Chem. Soc.*, 2004, **126**, 9916–9917.
- 167 S. Fujii, K. Nishina, S. Yamada, S. Mochizuki, N. Ohta, A. Takahara and K. Sakurai, *Soft Matter*, 2014, **10**, 8216–8223.
- 168 P. Shahgaldian, A. W. Coleman, S. S. Kuduva and M. J. Zaworotko, *Chem. Commun.*, 2005, 1968–1970.
- 169 J. Bugler, N. A. J. M. Sommerdijk, A. J. W. G. Visser, A. van Hoek, R. J. M. Nolte, J. F. J. Engbersen and D. N. Reinhoudt, *J. Am. Chem. Soc.*, 1999, **121**, 28–33.
- 170 N. Bono, C. Pennetta, A. Sganappa, E. Giupponi, F. Sansone, A. Volonterio and G. Candiani, *Int. J. Pharm.*, 2018, **549**, 436–445.
- 171 D. Coquiere, J. Marrot and O. Reinaud, *Org. Lett.*, 2007, **9**, 3271–3274.
- 172 A. V. Solovyov, S. O. Cherenok, O. I. Kalchenko, L. I. Atamas, Z. I. Kazantseva, I. A. Koshets, I. F. Tsybmal and V. I. Kalchenko, *J. Mol. Liq.*, 2011, **159**, 117–123.
- 173 R. Bussolati, P. Carrieri, A. Secchi, A. Arduini, A. Credi, M. Semeraro, M. Venturi, S. Silvi, D. Velluto, R. Zappacosta and A. Fontana, *Org. Biomol. Chem.*, 2013, **11**, 5944–5953.

- 174 D. Vollhardt, J. Gloede, G. Weidemann and R. Rudert, *Langmuir*, 2003, **19**, 4228–4234.
- 175 F. Mayer, S. Tiruvadi Krishnan, D. T. Schuhle, S. V. Eliseeva, S. Petoud, E. Toth and K. Djanashvili, *Front. Chem.*, 2018, **6**, 1.
- 176 Y. Cakmak, T. Nalbantoglu, T. Durgut and E. U. Akkaya, *Tetrahedron Lett.*, 2014, **55**, 538–540.
- 177 O. Kasyan, E. R. Healey, A. Drapailo, M. Zaworotko, S. Cecillon, A. W. Coleman and V. Kalchenko, *J. Inclusion Phenom. Macrocyclic Chem.*, 2006, **58**, 127–132.
- 178 N. Moridi, D. Elend, O. Danylyuk, K. Suwinska and P. Shahgaldian, *Langmuir*, 2011, **27**, 9116–9121.
- 179 Z. Xu, S. Jia, W. Wang, Z. Yuan, B. Jan Ravoo and D.-S. Guo, *Nat. Chem.*, 2019, **11**, 86–93.
- 180 J. Gao, J. Li, W.-C. Geng, F.-Y. Chen, X.-C. Duan, Z. Zheng, D. Ding and D.-S. Guo, *J. Am. Chem. Soc.*, 2018, **140**, 4945–4953.
- 181 J. Gao, Z. Zheng, L. Shi, S.-Q. Wu, H. Sun and D.-S. Guo, *Beilstein J. Org. Chem.*, 2018, **14**, 1840–1845.
- 182 Y. Zhao and E.-H. Ryu, *J. Org. Chem.*, 2005, **70**, 7585–7591.
- 183 E.-H. Ryu and Y. Zhao, *J. Org. Chem.*, 2006, **71**, 9491–9494.
- 184 E.-H. Ryu, H. Cho and Y. Zhao, *Org. Lett.*, 2007, **9**, 5147–5150.
- 185 M. Lee, S.-J. Lee and L.-H. Jiang, *J. Am. Chem. Soc.*, 2004, **126**, 12724–12725.
- 186 Y.-Y. Xie, L.-F. Mao and L.-H. Li, *J. Chem. Res.*, 2013, 476–479.
- 187 M. Mori, A. Hirayama, H. Tsue and S. Tanaka, *Acta Chromatogr.*, 2007, **19**, 73–80.
- 188 L. S. Yakimova, L. H. Gilmanova, V. G. Evtugyn, Y. N. Osin and I. I. Stoikov, *J. Nanopart. Res.*, 2017, **19**, 173.
- 189 F. Liu, G.-Y. Lu, W.-J. He, M.-H. Liu and L.-G. Zhu, *Thin Solid Films*, 2004, **468**, 244–249.
- 190 P. Shahgaldian, E. Da Silva and A. W. Coleman, *J. Inclusion Phenom. Macrocyclic Chem.*, 2003, **46**, 175–177.
- 191 D. Momekova, D. Budurova, E. Drakalska, S. Shenkov, G. Momekov, B. Trzebiecka, N. Lambov, E. Tashev and S. Rangelov, *Int. J. Pharm.*, 2012, **436**, 410–417.
- 192 G. Sautrey, I. Clarot, E. Rogalska and J.-B. Regnouf-de-Vains, *New J. Chem.*, 2012, **36**, 2060.
- 193 J. Gualbert, P. Shahgaldian and A. W. Coleman, *Int. J. Pharm.*, 2003, **257**, 69–73.
- 194 G. M. L. Consoli, G. Granata, E. Galante, I. Di Silvestro, L. Salafia and C. Geraci, *Tetrahedron*, 2007, **63**, 10758–10763.
- 195 J.-H. Yim, J. Kim, D. W. Gidley, R. S. Vallery, H.-G. Peng, D. K. An, B.-K. Choi, Y.-K. Park and J.-K. Jeon, *Macromol. Mater. Eng.*, 2006, **291**, 369–376.
- 196 G. Sautrey, I. Clarot, A. B. Salem, E. Rogalska and J.-B. Regnouf de Vains, *New J. Chem.*, 2012, **36**, 78–85.
- 197 P. Shahgaldian, A. W. Coleman and V. I. Kalchenko, *Tetrahedron Lett.*, 2001, **42**, 577–579.
- 198 V. Bagnacani, V. Franceschi, L. Fantuzzi, A. Casnati, G. Donofrio, F. Sansone and R. Ungaro, *Bioconjugate Chem.*, 2012, **23**, 993–1002.
- 199 D. Volkmer, M. Fricke, M. Gleiche and L.-F. Chi, *Mater. Sci. Eng., C*, 2005, **25**, 161–167.
- 200 L. Y. Zakharova, Y. R. Kudryashova, N. M. Selivanova, M. A. Voronin, A. R. Ibragimova, S. E. Solovieva, A. T. Gubaidullin, A. I. Litvinov, I. R. Nizameev, M. K. Kadirov, Y. G. Galyametdinov, I. S. Antipin and A. I. Konovalov, *J. Membr. Sci.*, 2010, **364**, 90–101.
- 201 P. Shahgaldian and A. W. Coleman, *Langmuir*, 2003, **19**, 5261–5265.
- 202 O. M. Martin and S. Mecozzi, *Supramol. Chem.*, 2005, **17**, 9–15.
- 203 O. M. Martin and S. Mecozzi, *Tetrahedron*, 2007, **63**, 5539–5547.
- 204 A. B. Mirgorodskaya, E. I. Yatskevich, Y. R. Kudryashova, S. E. Solov'eva, I. S. Antipin, L. Y. Zakharova and A. I. Konovalov, *Kinet. Catal.*, 2011, **52**, 529–535.
- 205 Y. R. Kudryashova, F. G. Valeeva, L. Y. Zakharova, S. E. Solovieva, I. S. Antipin, A. T. Gubaidullin and A. I. Konovalov, *Colloid J.*, 2012, **74**, 67–77.
- 206 B. Korchowiec, A. Ben Salem, Y. Corvis, J. B. R. de Vains, J. Korchowiec and E. Rogalska, *J. Phys. Chem. B*, 2007, **111**, 13231–13242.
- 207 M. Pojarova, G. S. Ananchenko, K. A. Udachin, F. Perret, A. W. Coleman and J. A. Ripmeester, *New J. Chem.*, 2007, **31**, 871–878.
- 208 A. Mustafina, L. Zakharova, J. Elistratova, J. Kudryashova, S. Soloveva, A. Garusov, I. Antipin and A. Konovalov, *J. Colloid Interface Sci.*, 2010, **346**, 405–413.
- 209 A. V. Ten'kovstev, A. B. Razina and M. M. Dudkina, *Polym. Sci., Ser. B*, 2014, **56**, 274–281.
- 210 D. Volkmer and M. Fricke, *Z. Anorg. Allg. Chem.*, 2003, **629**, 2381–2390.
- 211 X. Yu, C.-L. Tu, L. He, R.-B. Wang, G.-M. Sun, D.-Y. Yan and X.-Y. Zhu, *J. Macromol. Sci., Part A: Pure Appl. Chem.*, 2009, **46**, 360–367.
- 212 D. Volkmer, M. Fricke, D. Vollhardt and S. Siegel, *J. Chem. Soc., Dalton Trans.*, 2002, 4547.
- 213 P.-F. Gou, W.-P. Zhu and Z.-Q. Shen, *J. Polym. Sci., Part A: Polym. Chem.*, 2010, **48**, 5643–5651.
- 214 R. Roy and J. M. Kim, *Angew. Chem., Int. Ed.*, 1999, **38**, 369–372.
- 215 P. Shahgaldian, M. Cesario, P. Goreloff and A. W. Coleman, *Chem. Commun.*, 2002, 326–327.
- 216 A. Dubes, I. L. Moudrakovski, P. Shahgaldian, A. W. Coleman, C. I. Ratcliffe and J. A. Ripmeester, *J. Am. Chem. Soc.*, 2004, **126**, 6236–6237.
- 217 A. Dubes, K. A. Udachin, P. Shahgaldian, A. N. Lazar, A. W. Coleman and J. A. Ripmeester, *New J. Chem.*, 2005, **29**, 1141.
- 218 G. S. Ananchenko, M. Pojarova, K. A. Udachin, D. M. Leek, A. W. Coleman and J. A. Ripmeester, *Chem. Commun.*, 2006, 386–388.
- 219 G. S. Ananchenko, K. A. Udachin, M. Pojarova, A. Dubes, J. A. Ripmeester, S. Jebors and A. W. Coleman, *Cryst. Growth Des.*, 2006, **6**, 2141–2148.
- 220 D. N. Polovyanenko, E. G. Bagryanskaya, A. Schnegg, K. Mobius, A. W. Coleman, G. S. Ananchenko, K. A. Udachin and J. A. Ripmeester, *Phys. Chem. Chem. Phys.*, 2008, **10**, 5299–5307.

- 221 P. Shahgaldian, A. W. Coleman, B. Rather and M. J. Zaworotko, *J. Inclusion Phenom. Macrocyclic Chem.*, 2005, **52**, 241–245.
- 222 X.-L. Lou, F. Cheng, P.-F. Cao, Q. Tang, H.-J. Liu and Y. Chen, *Chem. – Eur. J.*, 2009, **15**, 11566–11572.
- 223 A. I. Litvinov, F. G. Valeeva, L. Y. Zakharova, S. E. Solovieva, I. S. Antipin and M. K. Kadirov, *Russ. Chem. Bull.*, 2013, **62**, 1350–1353.
- 224 L. Li, H.-Y. Zhang and Y. Liu, *Sci. China: Chem.*, 2012, **55**, 1092–1096.
- 225 P. Shahgaldian, *Eur. J. Pharm. Biopharm.*, 2003, **55**, 107–113.
- 226 P. Shahgaldian, E. Da Silva, A. W. Coleman, B. Rather and M. J. Zaworotko, *Int. J. Pharm.*, 2003, **253**, 23–38.
- 227 L. Zakharova, Y. Kudryashova, A. Ibragimova, E. Vasilieva, F. Valeeva, E. Popova, S. Solovieva, I. Antipin, Y. Ganeeva, T. Yusupova and A. Kononov, *Chem. Eng. J.*, 2012, **185–186**, 285–293.
- 228 N. Maulucci, F. De Riccardis, C. B. Botta, A. Casapullo, E. Cressina, M. Fregonese, P. Tecilla and I. Izzo, *Chem. Commun.*, 2005, 1354–1356.
- 229 G. M. L. Consoli, G. Granata, R. Lo Nigro, G. Malandrino and C. Geraci, *Langmuir*, 2008, **24**, 6194–6200.
- 230 M. Mourer, R. E. Duval, P. Constant, M. Daffe and J.-B. Regnouf-de-Vains, *ChemBioChem*, 2019, **20**, 911–921.
- 231 X. Guo, L. Zhang, G.-Y. Lu, M.-F. Yin, F. Liu and M.-H. Liu, *Chin. Chem. Lett.*, 2005, **16**, 1543–1546.
- 232 L. Yakimova, P. Padnya, D. Tereshina, A. Kunafina, A. Nugmanova, Y. Osin, V. Evtugyn and I. Stoikov, *J. Mol. Liq.*, 2019, **279**, 9–17.
- 233 O. M. Martin, L. Yu and S. Mecozzi, *Chem. Commun.*, 2005, 4964–4966.
- 234 Z.-S. Wang, G.-Y. Lu, X. Guo and H.-M. Wu, *Supramol. Chem.*, 2003, **15**, 327–334.
- 235 E. A. Andreyko, P. L. Padnya and I. I. Stoikov, *Colloids Surf., A*, 2014, **454**, 74–83.
- 236 E. A. Andreyko, P. L. Padnya and I. I. Stoikov, *J. Phys. Org. Chem.*, 2015, **28**, 527–535.
- 237 E. A. Andreyko, P. L. Padnya, R. R. Daminova and I. I. Stoikov, *RSC Adv.*, 2014, **4**, 3556–3565.
- 238 F. Liu, Y.-H. Wang and G.-Y. Lu, *Chem. Lett.*, 2005, **34**, 1450–1451.
- 239 A. R. Esker, L.-H. Zhang, C. E. Olsen, K. No and H. Yu, *Langmuir*, 1999, **15**, 1716–1724.
- 240 L. H. Zhang, A. R. Esker, K. No and H. Yu, *Langmuir*, 1999, **15**, 1725–1730.
- 241 X. Guo, G.-Y. Lu and Y. Li, *Thin Solid Films*, 2004, **460**, 264–268.
- 242 B. Guan, M. Jiang, X.-G. Yang, Q. Liang and Y.-Y. Chen, *Soft Matter*, 2008, **4**, 1393.
- 243 S. Jebors, G. S. Ananchenko, A. W. Coleman and J. A. Ripmeester, *Tetrahedron Lett.*, 2007, **48**, 5503–5506.
- 244 S. Jebors, F. Fache, S. Balme, F. Devoige, M. Monachino, S. Cecillon and A. W. Coleman, *Org. Biomol. Chem.*, 2008, **6**, 319–329.
- 245 F. A. Loiseau, A. M. Hill and K. K. Hii, *Tetrahedron*, 2007, **63**, 9947–9959.
- 246 S. Jebors, B. Lesniewska, O. Shkurenko, K. Suwinska and A. W. Coleman, *J. Inclusion Phenom. Macrocyclic Chem.*, 2010, **68**, 207–217.
- 247 P. L. Padnya, E. A. Andreyko, O. A. Mostovaya, I. K. Rizvanov and I. I. Stoikov, *Org. Biomol. Chem.*, 2015, **13**, 5894–5904.
- 248 D. Volkmer, M. Fricke, C. Agena and J. Mattay, *J. Mater. Chem.*, 2004, **14**, 2249.
- 249 C. Tu, G. Li, Y. Shi, X. Yu, Y. Jiang, Q. Zhu, J. Liang, Y. Gao, D. Yan, J. Sun and X. Zhu, *Chem. Commun.*, 2009, 3211–3213.
- 250 L. S. Yakimova, P. L. Padnya, A. F. Kunafina, A. R. Nugmanova and I. I. Stoikov, *Mendeleev Commun.*, 2019, **29**, 86–88.
- 251 G. Gattuso, A. Notti, A. Pappalardo, S. Pappalardo, M. F. Parisi and F. Puntoriero, *Tetrahedron Lett.*, 2013, **54**, 188–191.
- 252 G. Gattuso, A. Notti, S. Pappalardo, M. F. Parisi, I. Pisagatti and S. Patanè, *New J. Chem.*, 2014, **38**, 5983–5990.
- 253 G. Arena, A. Pappalardo, S. Pappalardo, G. Gattuso, A. Notti, M. F. Parisi, I. Pisagatti and C. Sgarlata, *J. Therm. Anal. Calorim.*, 2015, **121**, 1073–1079.
- 254 L. Barbera, G. Gattuso, F. H. Kohnke, A. Notti, S. Pappalardo, M. F. Parisi, I. Pisagatti, S. Patane, N. Micali and V. Villari, *Org. Biomol. Chem.*, 2015, **13**, 6468–6473.
- 255 W.-P. Zhu, J. Ling and Z.-Q. Shen, *Macromol. Chem. Phys.*, 2006, **207**, 844–849.
- 256 A. V. Ten'kovtsev and A. B. Razina, *Russ. J. Appl. Chem.*, 2009, **82**, 1615–1619.
- 257 I. Pisagatti, L. Barbera, G. Gattuso, S. Patanè, M. F. Parisi and A. Notti, *Supramol. Chem.*, 2018, **30**, 658–663.
- 258 A. V. Tenkovtsev, M. M. Dudkina, L. I. Scherbinskaya, V. Aseyev and H. Tenhu, *Polymer*, 2010, **51**, 3108–3115.
- 259 Z.-M. Zhao, Y. Wang, J. Han, H.-D. Zhu and L. An, *Chem. Pharm. Bull.*, 2015, **63**, 180–186.
- 260 G. de Miguel, M. T. Martin-Romero, J. M. Pedrosa, E. Munoz, M. Perez-Morales, T. H. Richardson and L. Camacho, *Phys. Chem. Chem. Phys.*, 2008, **10**, 1569–1576.
- 261 G. de Miguel, M. T. Martin-Romero, M. Perez-Morales, E. Munoz and L. Camacho, *J. Porphyrins Phthalocyanines*, 2009, **13**, 597–605.
- 262 S. Jebors, A. Leydier, Q. Wu, B. Bertino Ghera, M. Malbouyre and A. W. Coleman, *J. Microencapsulation*, 2010, **27**, 561–571.
- 263 A. M. Gonzalez-Delgado, J. J. Giner-Casares, G. Brezesinski, J. B. Regnouf-de-Vains and L. Camacho, *Langmuir*, 2012, **28**, 12114–12121.
- 264 U. Darbost, M. Giorgi, N. Hucher, I. Jabin and O. Reinaud, *Supramol. Chem.*, 2005, **17**, 243–250.
- 265 Z. Rafiee, A. Kakanejadifard, R. Hosseinzadeh, M. Nemati and M. Adeli, *RSC Adv.*, 2016, **6**, 17470–17473.
- 266 V. A. Burirov, D. A. Mironova, R. R. Ibragimova, R. I. Nugmanov, S. E. Solovieva and I. S. Antipin, *Colloids Surf., A*, 2017, **515**, 41–49.
- 267 R. R. Ibragimova, V. A. Burirov, A. R. Aimetdinov, D. A. Mironova, V. G. Evtugyn, Y. N. Osin, S. E. Solovieva and I. S. Antipin, *Macroheterocycles*, 2016, **9**, 433–441.
- 268 V. Burirov, A. Valiyakhmetova, D. Mironova, E. Sultanova, V. Evtugyn, Y. Osin, S. Katsyuba, T. Burganov, S. Solovieva and I. Antipin, *New J. Chem.*, 2018, **42**, 2942–2951.

- 269 V. A. Burilov, R. I. Nugmanov, R. R. Ibragimova, S. E. Solovieva and I. S. Antipin, *Mendeleev Commun.*, 2015, **25**, 177–179.
- 270 A. A. Vavilova, V. V. Gorbachuk, D. N. Shurpik, A. V. Gerasimov, L. S. Yakimova, P. L. Padnya and I. I. Stoikov, *J. Mol. Liq.*, 2019, **281**, 243–251.
- 271 V. A. Burilov, R. R. Ibragimova, B. H. Gafiatullin, R. I. Nugmanov, S. E. Solovieva and I. S. Antipin, *Macromolecules*, 2017, **10**, 215–220.
- 272 V. A. Burilov, D. A. Mironova, R. R. Ibragimova, S. E. Solovieva, B. König and I. S. Antipin, *RSC Adv.*, 2015, **5**, 101177.
- 273 Q. Liang, G.-S. Chen, B. Guan and M. Jiang, *J. Mater. Chem.*, 2011, **21**, 13262.
- 274 S. Aleandri, A. Casnati, L. Fantuzzi, G. Mancini, G. Rispoli and F. Sansone, *Org. Biomol. Chem.*, 2013, **11**, 4811–4817.
- 275 B. Guan, Q. Liang, Y. Zhu, M.-H. Qiao, J. Zou and M. Jiang, *J. Mater. Chem.*, 2009, **19**, 7610–7613.
- 276 Q. Liang, B. Guan and M. Jiang, *J. Mater. Chem.*, 2010, **20**, 8236.
- 277 Q. Liang, C. Li, G. Chen and M. Jiang, *J. Colloid Interface Sci.*, 2012, **383**, 82–88.
- 278 D. T. Schuhle, J. Schatz, S. Laurent, L. Vander Elst, R. N. Muller, M. C. Stuart and J. A. Peters, *Chem. – Eur. J.*, 2009, **15**, 3290–3296.
- 279 J. W. Steed, D. R. Turner and K. J. Wallace, *Core concepts in supramolecular chemistry and nanochemistry*, Wiley, Chichester, West Sussex, England, 2007.
- 280 C. Lau, R. Bitton, H. Bianco-Peled, D. G. Schultz, D. J. Cookson, S. T. Grosser and J. W. Schneider, *J. Phys. Chem. B*, 2006, **110**, 9027–9033.
- 281 M. Miyake, K. Yamada and N. Oyama, *Langmuir*, 2008, **24**, 8527.
- 282 J. N. Israelachvili, D. J. Mitchell and B. W. Ninham, *J. Chem. Soc., Faraday Trans. 2*, 1976, **72**, 1525–1568.
- 283 Q. Liang, B. Guan and M. Jiang, *Prog. Chem.*, 2010, **22**, 388–399.
- 284 H.-T. Cui, Y.-M. Feng, W.-Z. Ren, T. Zeng, H.-Y. Lv and Y.-F. Pan, *Recent Pat. Nanotechnol.*, 2009, **3**, 32–41.
- 285 N.-M. Hwang, J.-S. Jung and D.-K. Lee, *Thermodynamics – Fundamentals and its application in science*, InTech, Rijeka, Croatia, 2012.
- 286 E. Mattia and S. Otto, *Nat. Nanotechnol.*, 2015, **10**, 111–119.
- 287 C. Wang, Z.-Q. Wang and X. Zhang, *Acc. Chem. Res.*, 2012, **45**, 608–618.
- 288 Y. Kang, K. Liu and X. Zhang, *Langmuir*, 2014, **30**, 5989–6001.
- 289 P. Xing, T. Sun and A. Hao, *RSC Adv.*, 2013, **3**, 24776–24793.
- 290 C. Wang, Z. Wang and X. Zhang, *Small*, 2011, **7**, 1379–1383.
- 291 Y. Kang, X. Tang, Z. Cai and X. Zhang, *Adv. Funct. Mater.*, 2016, **26**, 8920–8931.
- 292 X. Zhang, *Supramolecular amphiphiles*, The Royal Society of Chemistry, London, UK, 2017.
- 293 O. Varga, M. Kubinyi, T. Vidóczy, P. Baranyai, I. Bitter and M. Kállay, *J. Photochem. Photobiol., A*, 2009, **207**, 167–172.
- 294 V. Francisco, N. Basilio, L. Garcia-Rio, J. R. Leis, E. F. Marques and C. Vazquez-Vazquez, *Chem. Commun.*, 2010, **46**, 6551–6553.
- 295 V. Lau and B. Heyne, *Chem. Commun.*, 2010, **46**, 3595–3597.
- 296 M. Megyesi and L. Biczok, *J. Phys. Chem. B*, 2010, **114**, 2814–2819.
- 297 K. Wang, D.-S. Guo, X. Wang and Y. Liu, *ACS Nano*, 2011, **5**, 2880–2894.
- 298 D.-S. Guo, B.-P. Jiang, X. Wang and Y. Liu, *Org. Biomol. Chem.*, 2012, **10**, 720–723.
- 299 D.-S. Guo, K. Wang, Y.-X. Wang and Y. Liu, *J. Am. Chem. Soc.*, 2012, **134**, 10244–10250.
- 300 Z.-Q. Li, C.-X. Hu, Y.-Q. Cheng, H. Xu, X.-L. Cao, X.-W. Song, H.-Y. Zhang and Y. Liu, *Sci. China: Chem.*, 2012, **55**, 2063–2068.
- 301 N. Basilio, A. Pineiro, J. P. Da Silva and L. Garcia-Rio, *J. Org. Chem.*, 2013, **78**, 9113–9119.
- 302 Y. Cao, Y.-X. Wang, D.-S. Guo and Y. Liu, *Sci. China: Chem.*, 2013, **57**, 371–378.
- 303 B.-P. Jiang, D.-S. Guo, Y.-C. Liu, K.-P. Wang and Y. Liu, *ACS Nano*, 2014, **8**, 1609–1618.
- 304 Z.-B. Qin, D.-S. Guo, X.-N. Gao and Y. Liu, *Soft Matter*, 2014, **10**, 2253–2263.
- 305 C. Costa, V. Francisco, S. G. Silva, M. L. C. do Vale, L. Garcia-Rio and E. F. Marques, *Colloids Surf., A*, 2015, **480**, 71–78.
- 306 Y.-X. Wang, Y.-M. Zhang and Y. Liu, *J. Am. Chem. Soc.*, 2015, **137**, 4543–4549.
- 307 J. G. Harangozo, V. Wintgens, Z. Miskolczy, J. M. Guigner, C. Amiel and L. Biczok, *Langmuir*, 2016, **32**, 10651–10658.
- 308 Y.-C. Liu, Y.-Y. Wang, H.-W. Tian, Y. Liu and D.-S. Guo, *Org. Chem. Front.*, 2016, **3**, 53–61.
- 309 D.-S. Guo, K. Chen, H.-Q. Zhang and Y. Liu, *Chem. – Asian J.*, 2009, **4**, 436–445.
- 310 K. Wang, D.-S. Guo and Y. Liu, *Chem. – Eur. J.*, 2010, **16**, 8006–8011.
- 311 N. Basilio and L. Garcia-Rio, *Chem. – Eur. J.*, 2009, **15**, 9315–9319.
- 312 N. Basilio, M. Martin-Pastor and L. Garcia-Rio, *Langmuir*, 2012, **28**, 6561–6568.
- 313 N. Basilio, B. Gomez, L. Garcia-Rio and V. Francisco, *Chem. – Eur. J.*, 2013, **19**, 4570–4576.
- 314 N. Basilio, D. A. Spudeit, J. Bastos, L. Scorsin, H. D. Fiedler, F. Nome and L. Garcia-Rio, *Phys. Chem. Chem. Phys.*, 2015, **17**, 26378–26385.
- 315 N. Basilio, B. Gomez and L. Garcia-Rio, *Langmuir*, 2017, **33**, 13008–13013.
- 316 C. Bize, J. C. Garrigues, M. Blanzat, I. Rico-Lattes, O. Bistri, B. Colasson and O. Reinaud, *Chem. Commun.*, 2010, **46**, 586–588.
- 317 V. Wintgens, C. Le Coeur, C. Amiel, J. M. Guigner, J. G. Harangozo, Z. Miskolczy and L. Biczok, *Langmuir*, 2013, **29**, 7682–7688.
- 318 V. Wintgens, Z. Miskolczy, J. M. Guigner, C. Amiel, J. G. Harangozo and L. Biczok, *Langmuir*, 2015, **31**, 6655–6662.
- 319 V. Wintgens, J. G. Harangozo, Z. Miskolczy, J. M. Guigner, C. Amiel and L. Biczok, *Langmuir*, 2017, **33**, 8052–8061.
- 320 X. Yao, X. Wang, T. Jiang, X. Ma and H. Tian, *Langmuir*, 2015, **31**, 13647–13654.

- 321 L. Di Costanzo, S. Geremia, L. Randaccio, R. Purrello, R. Lauceri, D. Sciotto, F. G. Gulino and V. Pavone, *Angew. Chem., Int. Ed.*, 2001, **40**, 4245–4247.
- 322 H. Huang, D.-M. Li, W. Wang, Y.-C. Chen, K. Khan, S. Song and Y.-S. Zheng, *Org. Biomol. Chem.*, 2012, **10**, 729–735.
- 323 D.-S. Guo and Y. Liu, *Acc. Chem. Res.*, 2014, **47**, 1925–1934.
- 324 I. S. Ryzhkina, Y. V. Kiseleva, L. I. Murtazina, Y. N. Valitova, S. E. Solov'eva, L. M. Pilishkina and A. I. Konovalov, *Russ. Chem. Bull.*, 2010, **59**, 1327–1335.
- 325 C.-L. Tu, L.-J. Zhu, P.-P. Li, Y. Chen, Y. Su, D.-Y. Yan, X.-Y. Zhu and G.-Y. Zhou, *Chem. Commun.*, 2011, **47**, 6063–6065.
- 326 B. C. M. A. Ashwin, C. Saravanan, M. Senthilkumaran, R. Sumathi, P. Suresh and P. M. Mareeswaran, *Supramol. Chem.*, 2017, **30**, 32–41.
- 327 R. V. Rodik, A. S. Klymchenko, N. Jain, S. I. Miroshnichenko, L. Richert, V. I. Kalchenko and Y. Mely, *Chem. – Eur. J.*, 2011, **17**, 5526–5538.
- 328 S. Peng, K. Wang, D.-S. Guo and Y. Liu, *Soft Matter*, 2015, **11**, 290–296.
- 329 J. G. Harangozó, V. Wintgens, Z. Miskolczy, C. Amiel and L. Biczók, *Colloid Polym. Sci.*, 2016, **294**, 1807–1814.
- 330 K. Wang, D.-S. Guo, M.-Y. Zhao and Y. Liu, *Chem. – Eur. J.*, 2016, **22**, 1475–1483.
- 331 S. Peng, J. Gao, Y. Liu and D.-S. Guo, *Chem. Commun.*, 2015, **51**, 16557–16560.